REPORT DOCUMENTATION PAGE

Form Approved OMB No. 0704-0188

1. AGENCY USE ONLY (Leave blank)	2. REPORT DATE	3. REPORT TYPE AND DATES COVERED
	1995	Final Report

4. TITLE AND SUBTITLE

Development of Algorithms and Programs for the Diffraction and Statistical Radiotomography of the Ionosphere

5. FUNDING NUMBERS

F6170893W0893

6. AUTHOR(S)

Dr. Vyatcheslav Kunitsyn

7. PERFORMING ORGANIZATION NAME(S) AND ADDRESS(ES)

Moscow University
Department of Physics
119899 Moscow, Russia

8. PERFORMING ORGANIZATION REPORT NUMBER

SPC-93-4063

9. SPONSORING/MONITORING AGENCY NAME(S) AND ADDRESS(ES)

EOARD
PSC 802 BOX 14
FPO 09499-0200

10. SPONSORING/MONITORING AGENCY REPORT NUMBER

SPC-93-4063

11. SUPPLEMENTARY NOTES

12a. DISTRIBUTION/AVAILABILITY STATEMENT

Approved for public release; distribution is unlimited.

12b. DISTRIBUTION CODE

A

13. ABSTRACT (Maximum 200 words)

The aim of this work was to develop efficient algorithms and programs for the solutions of the ionospheric diffraction and statistical radiotomography (RT) problems. The purpose of this paper is to describe shortly the RT methods and program developed for reconstruction ionospheric irregularities structures together with some results of computer simulation.

14. SUBJECT TERMS

15. NUMBER OF PAGES

81

16. PRICE CODE

17. SECURITY CLASSIFICATION OF REPORT	18. SECURITY CLASSIFICATION OF THIS PAGE	19. SECURITY CLASSIFICATION OF ABSTRACT	20. LIMITATION OF ABSTRACT
UNCLASSIFIED	UNCLASSIFIED	UNCLASSIFIED	UL

Development of Algorithms and Programs for the Diffraction and Statistical Radiotomography of the Ionosphere.

Final (12-month) report (EOARD Contract SPC 93-4063)

CONTENT pp.

Principal investigator

Professor V.Kunitsyn

1. Introduction

The aim of this work was to develop efficient algorithms and programs for the solutions of the ionospheric diffraction and statistical radiotomography (RT) problems. The diffraction and statistical RT problems are related with reconstruction of the scattering ionospheric irregularities structure. The use of tomographic methods is perhaps an unavoidable stage in evolution of nearly all diagnostic systems. At a sufficiently high level of development of remote sensing technology and data processing resources, it become possible to reconstruct the spatial structure of a medium on the basis of tomography. Tomographic approaches have already transformed sensing methods in many fields and provided fundamentally new results. The major achievements of tomography in medicine and molecular biology are widely known. Tomographic methods have made it possible to detect previously unknown phenomena in geophysics (seismotomography of the Earth and acoustic tomography of the ocean). At the present stage, radio sounding technology makes it possible to use satellite resources to perform ionospheric sounding in a wide range of different positions of the transmitting and receiving systems and to use tomographic methods. In connection with this, work on RT of the ionosphere has began actively in recent years.

The purpose of this paper is to describe shortly the RT methods [1-8] and program developed for reconstruction ionospheric irregularities structures together with some results of computer simulation. We are dealing with reconstruction of the irregularities of the electron density and of the effective collision frequency by scattered radio waves field. Mathematicians used very often designations the inverse problem (IP) or the

inverse scattering problem (ISP) for such problems of structure reconstruction owing to the scattered field. Here we used the terms IP or ISP and diffraction tomography as synonims. The ionosphere has a rather complex structure; local irregulariries of various scales, including turbulent regions, are present in addition to a quasi-stratified background with large scales. Therefore, problems of satellite RT of the ionosphere should be divided into statistical RT and deterministic RT problems. The latter, in turn, are divided into problems of diffraction RT and ray RT of large structures, where diffraction effects are not significant.

There is no special reason to provide a strict classification of any field of science developing, but certain delimitations and explanations of the terminology must be provided so that we will not later be reproached for "inventing" new terms unnecessarily. In the cases where any projections or "cross sections" of an inhomogeneous object (or a certain transformation of the object, such as Fourier transform) are known from remote sensing data and the problem is to reconstruct the structure of the object, the problem should be considered as a tomographic problem. At present, the mathematical foundation for tomography is related to integral geometry, where it is necessary to reconstruct an object using data on it in the form of integrals with respect to small-dimension manifolds. Therefore, the term tomography is understood not in narrow initial sense, as layer-by-layer study of the structure of the inhomogeneous objects, but ruther in the wider sense, as recording of projections or cross-sections of an object and subsequent reconstruction of the structure of the object from them. The projections of an object are various integrals with respect to small-dimension manifolds. The range of

problems of radio remote sensing of the ionosphere using satellites examined in this paper includes reconstruction of the structure of ionospheric irregularities from files of various tomographic-type data (projections, cross sections), which provides the basis for using the term RT of the ionosphere.

Problems of satellite RT should be divided into deterministic and statistical problems. In the case of a deterministic RT problem, it is necessary to reconstruct the structure of certain large irregularities or a group of irregularities. If a large number of irregularities occupies a certain region in space, it is unadvised to reconstruct the structure of all realizations (generations) of irregularities every moment of time. Here, it makes sense to pose the problem of reconstruction of the characteristics of full ensemble of irregularities, the structure of the statistical characteristics of the irregularities such as the correlation function of the electron density, etc.

We will single out a number of fundamental features of problems of RT of the ionosphere or the IP of reconstruction of the structure of the inhomogeneous ionosphere. The dimensions of the transmitting and receiving systems feasible in practice are much less than the distances from them to the irregularities to be reconstructed, which are hundreds of kilometers, i.e., the aperture angles are small. Since it is extremely difficult and expensive to create transmitting and receiving systems with a large number of receivers, the necessity for aperture synthesis in one coordinate becomes clear. Synthesis apertures can be realized, for example, using a moving transmitter on a satellite. We will emphase that satellite radio sounding makes it possible in practice to obtain files of various tomographic data and to actually realize RT of the inhomogeneous ionosphere. In view of

the small aperture angles, it is advisable to pose the problem of reconstruction of the structure of irregularities with dimensions singficantly exceeding the wavelength. Therefore, the IP of reconstruction of the structure of scatterers which are large in compasion with the wavelength will be examined here, but the dimensions of the irregularities may be both greater than or less than Fresnel zone, and diffraction effects must be considered in a number of cases.

2. Physical and mathematical formulation of the radio tomographic sounding problem.

Radio wave propagation in near-earth space and scattering in plasma irregularities in the ionosphere are discribed by a system of Maxwell equations with the corresponding material equations [9]. In the general case, the dielectric permittivity of the plasma is a tensor value due to spatial dispersion, even in the absence of a magnetic field. However, the spatial dispersion can be disregarded for ionospheric irregularities of both natural and artificial origin, since the thermal velocities of the electrons in the plasma are significantly less then than the speed of light, i.e., the approximation of a "cold" plasma is valid. Likewise, the velocities of diffusion, mixing and other transport processes, as well as the velocity of the transmitting and receiving systems, does not exceed 10 km/s ($v/c < 3 \cdot 10^{-4}$), therefore , the quasistationary approximation is valid; within the framework of it, the "slow" time dependence of the characteristics of the medium and fields can be considered as a dependence on the parameter.

In place of the equations for the field $\vec{\mathcal{E}}(\vec{r},t)$ of a radio wave, it is convenient to use equations for the complex amplitudes $\vec{E}$ of the corresponding monochromatic components, i.e., it is advisable to introduce

$$\vec{\mathcal{E}}(\vec{r},t) = \vec{E}(\vec{r},t)e^{-i\omega t} + \vec{E}^*(\vec{r},t)e^{i\omega t}.$$

For brevity, the complex amplitudes $\vec{E}(\vec{r},t)$ with a "slow" time will be called the field hereafter. Subject to the observations made above, within the framework of the quasistationary approximation and a "cold" plasma, from the Maxwell equations we have the equation for the field

$$\Delta\vec{E} + \frac{\omega^2}{c^2}\hat{\varepsilon}\vec{E} - \text{grad div}\,\vec{E} = 0, \qquad (1)$$

where $\hat{\varepsilon}$ is the complex dielectric permittivity tensor, $f = \omega/2\pi$ is the frequency. Analysis of radio wave propagation in an inhomogeneous magnetoactive plasma with a tensor dependence of $\hat{\varepsilon}$ is a difficult problem. There are no algorithms for calculating the parameters of radio signals and the characteristics of the scattered fields in the general case of an arbitrary dependense of $\hat{\varepsilon}(\vec{r})$ on the coordinates. Therefore, the statement of the ISP of reconstruction of the structure of the tensor characterizing an ionospheric irregularity using data on the measured field is unrealistic at present, and hardly advisable in general. The non-diagonal elements of the tensor can be disregarded at high frequencies, since they do not exceed the square of the ratio of the plasma frequency f_N to the sounding frequency, i.e., $\sim (f_N/f)^2(f_H/f)$ (f_H is the gyrofrequency) [9]. For example, the typical maximum concentration in the ionosphere is $N_0 \sim 10^6$ cm^{-3}. For it and where $f > 50$ Mhz, $(f_N/f)^2(f_H/f) \leqslant 0{,}001$. Likewise, the

last, "depolarization" term of equation (1), the order of which is determined by the ratio of the emission wavelength to the characteristic scale of variation of the concentration, can also be disregarded at high frequencies.

Thus, in the case of high sounding frequencies vector equation (1) decomposes into three scalar equations, and it is sufficient to examine the equation for one field component

$$\Delta E + k^2\hat{\varepsilon}(\vec{r},k)\, E = 0, \qquad (2)$$

where $\varepsilon(\vec{r},\omega) = 1 - \dfrac{4\pi r_e N(\vec{r})}{k^2(1 + i\nu(\vec{r})/\omega)}$, $k = 2\pi f/c = \omega/c$ is the wave number, r_e is the classical electron radius, $\nu(\vec{r})$ is effective collision frequency, $N(\vec{r})$ is the electron concentration; "ion" contribution to the dielectric permittivity can be disregarded [3]. The relation for ε has the same form in both the International System of Units (SI) and CGS system; only the expression for r_e changes.

Then, it will be convinient to introduce the complex function $q(\vec{r},\omega) = k^2(1-\varepsilon) = 4\pi r_e N(\vec{r})/(1 + i\nu(\vec{r})/\omega)$ and divide it into two parts: $q \to q_0(z,\omega) + q(\vec{r},\omega)$, one of which corresponds to the regular stratified ionosphere with the dependencies $N_0(z)$ and $\nu_0(z)$, and the other of which is related to the three-dimension (3D) irregularities on the background of the stratified medium $N(\vec{r})$ and $\nu(\vec{r})$. The specific and concrete form of relations for $\nu_0(z)$ and $\nu(\vec{r})$ depends on the specifics of the problem [1]. By reconstructing the structure of the complex function $q(\vec{r},\omega)$, it is also possible to reconstruct the structure of these 3D disturbances with known information on the regular large scale ionosphere. Therefore we will deal with the two problems: first, the problem of reconstruction of the regular large scale

ionosphere $q_0(z,\omega)$ - ray RT problem; second, the problem of reconstruction the 2D or 3D irregularities structure - diffractional and (or) statistical RT problem. The introduction of q is also justified by the fact that the quantity $q \sim (1 - \varepsilon)$ applies to the generalized susceptibilities [10] characterizing the response of the medium to the field. Furthermore, the scalar Helmholtz eguation assumes the form of stationary Schrodinger equation, where q is the complex potential:

$$\Delta E + k^2 E - q_0(z,\omega)E - q(\vec{r},\omega)E = \delta(\vec{r} - \vec{r}_0) \qquad (3)$$

The delta function in the right side of (3) corresponds to the point sounding source in the majority of satellite radio sounding experiments, since the wave can be assumed to be spherical within the major lobe of the directional pattern of an arbitrary source. The dimensional constant A_0 in front of the δ-function in equation (3) is omitted so that it need not be rewritten in all subsequent formulas. The constant is expressed by means of the total power of a point source [1]. Here, A_0 corresponds to the amplitude value of the field of a point source, i.e.,

$$E_0(\vec{r}) = - A_0 \exp(ikr)/(4\pi r).$$

Hereafter, we can always return to the dimensional field $E \to A_0 E$ when necessary.

The ISP for equation (3) can be formulated in the following manner: it is necessary to reconstruct the structure of the irregularities from measurements of the field in a certain limited region of a fixed surface in a limited range of frequencies and positions of the sounding source. Knowledge of the complex function $q(\vec{r},\omega)$ makes it possible to reconstruct the structure of both $N(\vec{r})$ and $\nu(\vec{r})$. Here $q(\vec{r},\omega)$ is a finite function, since the

irregularities of $N(\vec{r})$ are confined in space. The regular stratified ionosphere is assumed to be known here, i.e., the IP of reconstruction of the regular ionosphere is solved by other, sufficiently well-developed methods, or its influence can be disregarded, for example, as in the UHF/VHF waveband.

The sheme of the experiments on diffraction and statistical RT is presented in Fig.1. The satellite, with a transmitter on board moves at altitude $z = z_0$; the receiving system is located in the plane $z = z_R$ (on the ground). The receiving system can be a transverse array of receivers for diffraction RT or statistical RT (or a collection of transverse arrays). Receivers of array arranged along (the y-axis) a line transverse to the satellite path (the x-axis), arrays being separated by distances of hundreds of kilometers. The scatterer (a group of irregularities) is located near the altitude $z = z_s$.

3. The solution of the diffraction radiotomography problem (inverse scattering problem).

Rigorous results of solution of IP (3) for the complex potential do not exist. We will emphasize that in the case of propagation of waves of various nature in the actual physical media the complex nature of the potential q has a fundamental character and the corresponding dispersion relations relating the real and imaginary parts of the potential can be derived [10]. The fundamental results on solution of the 3D inverse problem for the Schrodinger equation with the real potential $q(\vec{r})$ not depend on the frequency (where $q_0(\vec{r},\omega) = 0$) obtained in [11,12] should be noted here. As to the complex nature of the potentials, there no rigorous results for the 1D IP, i.e the extension of the familiar Gelfand-Levitan-Marchenko algorithm to this case is unknown, even more so for a arbitrary dependence of the potential from the energy (frequency ω) [13].

Approximate approaches to solution of the 3D ISP are therefore of undoubted interest. The approximate approach to solution of inverse RT problem is justified by the properties of the regular ionosphere, the typical scales of essential disturbances of which significantly exceed the radio sounding wavelength. Therefore, the geometrical optics approximation is applicable to description of wave propagation on the background of the regular ionosphere. The scattering in weak irregularities is described within the framework of such familiar approximations as the Born approximation and Rytov approximation (BA and RA). More specialized methods have been used to calculate the scattering in strong-scattering irregularities.

There are many papers connected with the approximate

approaches to ISP [14-18]. The scattering by weak irregularities was described within the BA and RA. The iterative methods were used for strong-scattering irregularities. But there are some specific features of the ionosphere problems, namely: the size of irregularities is very big (it can exceed the probing wavelength in 10^3- 10^4 times), the ionosphere irregularities can be either weak-scattering or strong-scattering. It is very difficult to use iterative methods for big size strong-scattering irregularities directly. However it is sufficient to use the small-angle approximation according to the big size of irregularities or their detailes. In what follows we consider the methods of ISP solutions only, based on the asymptotic approximation for the forward small-angle scattering. It should be noted it is particularly interesting for tomographic methods to consider such cases of small-angle scattering, when a wavelength of sounding radiation is much less compared with the scales of object specific detailes. This is necessary condition to reconstruct the complicated internal structure of the object.

In the beginning it is useful to consider the ISP in the high-frequency limit i.e. the source field freguency is essentially higher than the critical frequency of the regular ionosphere. In this case the refraction index is close to unity, and the influence of the regular ionosphere may be neglected. Then, instead of (1), the following equation should be used:

$$\Delta E + k^2 E - q(\vec{r},\omega)E = \delta(\vec{r}-\vec{r}_0) \qquad (4)$$

This differential equation is equivalent to the Lippmann-Schwinger integral equation

$$E(\vec{r}) = E_0(\vec{r}) + \int G(\vec{r}-\vec{r}')\, E(\vec{r}')\, q(\vec{r}',\omega)\, d^3r' \qquad (5)$$

where $G(r)=-(4\pi r)^{-1}\exp(ikr)$ is the Green's function for a vacuum and $E_0(\vec{r})=G(\vec{r}-\vec{r}_0)$ is the source field.

It is necessary to bear in mind that the potential q depends on N and ν as follows (the usual condition for ionospheric radioprobing $\nu << \omega$ is taken into account) [1]

$$q = 4\pi r_e N(\vec{r})/(1 + i\nu(\vec{r})/\omega) \simeq 4\pi r_e N(\vec{r})(1 - i\nu(\vec{r})/\omega) \qquad (6)$$

For the case of small-angle scattering the transmitter, a scattering object and the receiver are situated along a straight line approximately. Assuming that the direction of this straight line is closed to the direction of z-axis one can obtain an approximate equation, describing the forward small-angle scattering, instead of (5) [1,7]

$$U(\vec{r}) = 1 + \int F(\vec{r},\vec{r}')\, U(\vec{r}')\, q(\vec{r}',\omega)\, d^3r' \equiv 1 + \hat{F}Uq \qquad (7)$$

Here $U=E/E_0$ is the normalized field. Under the derivation (7) the Fresnel's approximation was used for the Green function G either as for the sounding wave field. After some transformations we come from (5) to the formula (7), where the kernel F of the equation (7) contains coordinates of the transmitter z_0, the finite scatterer z_s and the receiver z_R

$$F(\vec{r},\vec{r}') = -\frac{1}{4\pi\zeta}\exp\left(i\frac{k}{2\zeta}(\vec{\rho}' - \vec{s})^2\right), \qquad (8)$$

$$\vec{s} = \vec{\rho}_R(z_0 - z_s)/(z_0 - z_R) + \vec{\rho}_0(z_s - z_R)/(z_0 - z_R),$$

$$\zeta = (z_0 - z_s)(z_s - z_R)/(z_0 - z_R).$$

In general case the formulae for s and ζ have to include the integration variable z' instead of z_s. But if the object scale is less than longitudinal Fresnel resolution the varriable z' can be

changed on the constant z_s.

There is another form of the equation (7), using the complex phase $\Phi = \ln E$, $\Phi - \Phi_0 = \ln U$

$$\Phi - \Phi_0 = \ln (1 + \hat{F}q \exp(\Phi - \Phi_0)) \qquad (9)$$

which includes the RA (the first iteration of the non-linear equation (9))

$$\Phi - \Phi_0 = \ln (1 + \hat{F}q) \simeq \hat{F}q \quad \text{or} \quad U = \exp(\hat{F}q) \qquad (10)$$

Taking into account (7,10) and making use of the Fresnel's transformation we have the algorithm for reconstruction of 2D cross-section of potential q [1,2]

$$q_z(\vec{\rho}, \omega) \equiv \int q(\vec{r},\omega)\, dz = (k/2\pi\zeta)^2 \int V(\vec{s}) \exp(-ik(\vec{s}-\vec{\rho})^2/2\zeta) d^2s. \qquad (11)$$

The integral projection $q_z(\vec{\rho})$ can be obtained after transformation of field data. For case of the BA we have $V=-4\pi\zeta(E-E_0)/E_0$ and for the case of the RA $V = -4\pi\zeta(\Phi-\Phi_0)$ [1,2]. Changing the direction of the sounding wave incident ("turning" the z-axis) one can obtain a set of 2D-projections, which makes it possible the tomography reconstruction of the 3D structure.

Determination of the linear potentials $q_z(\vec{\rho},\omega)$ (11) from complex potential $q(\vec{r},\omega)$ in the case of forward scattering reduces the ISP to a problem of tomographic reconstruction - the problem of reconstruction an object from projections. The intensive development in the past decade of tomographic methods for studying the structure of objects is to a significant extent the result of advances in x-ray tomography. The reconstruction algorithms used in practical x-ray tomography are based on a linear approximation of the ray trajectories. In mathematical respects, such problems

reduce to reconstruction of the attenuation function or refractive index from group of linear integrals and to reconstruction of an object from its small-dimensional projections. In addition to x-rays, practically all known types of emissions and waves are now used for tomographic purposes. The linear approximation frequently does not provide good results in tomographic investigations using optical and ultrasonic waves, microwaves and other waves. Therefore, methods for reconstruction with consideration of reflection and diffraction effects have been developed intensively in recent years, and a special term - diffraction tomography - has appeared [8-12,4].

The solutions of the IP of reconstruction of the structure of a scatterer with diffraction considered in the case of "forward" scattering obtained above can also be applied to the field of diffraction tomography. ISP reduces to the tomographic problem of reconstructing a 3D object from 2D projections $q_z(\vec{\rho},\omega)$ (11). By rotating the object or rotating the transmitting and receiving system in relation to the object (axis z), it is possible to obtain a series of linear integrals of $q_z(\vec{\rho},\omega)$, which can be used for tomographic reconstruction of the refractive index. However, the problem of reconstructing the 2D structure from a set of 1D "cross sections", i.e., functions measured by one receiver as the transmitter on a satellite moves, is also a tomographic problem. Furthermore, the physical meaning of the quantities measured by one receiver is of integrals over the cross section of the spectrum of the irregularity. A set of such integrals makes it possible to reconstruct the 2D cross section of spectrum, which is equivalent to reconstruction of 2D integrated projection of $q_z(\vec{\rho},\omega)$. The set of 2D projections makes it possible to perform tomographic reconstruction of the 3D structure.

The influence of diffraction reduces to the fact that the linear integral (11) is dependent not only on the field "on the ray", bur also on the field in vicinity of the intersection point of the ray and recording plane ($z = z_R$). If the emission frequency is high, then at the limit $\omega \to \infty$ the integral (11) should only be dependent on the field on the ray (the eikonal approximation with a stright line trajectory).

Let a plane sounding wave ($\vec{\rho}_0=0$, $z_0 \to \infty$) strike the object. Then, by calculating the integral (11) at the of high k ($kr_m^2/2\zeta \gg 1$) by the saddlepoint method (assuming that $V(\vec{s},\omega) = -4\pi\zeta\Phi_1$ in accordance with smooth perturbation method approximation), we obtain

$$q_z(\vec{\rho},k) \equiv \int q(\vec{r},k)dz \simeq (k/2\pi\zeta)^2\, V(\vec{\rho}_R)(2\zeta/k)(-i\pi) = 2ik\Phi_1(\vec{\rho}_R). \tag{12}$$

To demonstrate, the advance of the complex phase Φ at the object in the geometrical optics approximation with a linear ray is equal to the integral of complex refractive index $n(\vec{r},\omega) = v\,\overline{1-q/k^2}$

$$\Phi = \Phi_0 + \Phi + \ldots = ik \int n(\vec{r},\omega)\, dz =$$

$$= ik \int v\,\overline{1-q/k^2}\, dz \simeq ik \int (1-q/2k^2)\, dz$$

From this, for the first approximation of the complex phase of the field we have $\Phi_1 \simeq -iq_z/2k$, which agrees with (12), i.e., at the high-frequency limit linear integrals of type (11) are only dependent on the field on the ray. This means that the approximation used here also contains the geometrical optics approximation with linear trajections at the high-frequency limit. The result of the limitation on $\vec{s}$ of the region where the field is recorded is that the function $q_z(\vec{\rho},\omega)$ reconstructed from limited

data on $\Phi_1(\vec{s})$ will be smoothed. The null space of the equation is determined by the parameters of the recording system and defines the Rayleigh resolution limit [1]; then $q_z(\vec{\rho},\omega)$ is an integral over a ray of finite "thickness".

To reconstruct the 2D structure of ionospheric irregularities according to the transformation (11) we need the information about the approximate coordinate of the scatterer z_s. Let us discuss briefly a method for determination of a distance to the scatterer, which is essential for irregularities reconstruction by integral transformations. If only an approximate value of the distance is known then there appear errors in $\vec{s}$ and ζ, and hence, the reconstructed function is destorted. Let us consider an example where a source is placed on board of a satellite and the corresponding distortions arising in this case. The distance between the satellite and the receivers $(z_0 - z_R)$ is known quite precisely, but in determination the distances "source - scatterer" $(z_0 - z_s)$ and "scatterer - receivers" $(z_s - z_R)$ a systematic error Δ is present: $z_s' = z_s - \Delta$. It may be shown that reconstruction errors are small for such values of Δ, which correspond to the longitudinal resolution of the measuring system. This conclusion is also confirmed by numerical simulations [1].

It easy to show that when the error Δ is less than the longitudinal resolution, $\Delta \ll \lambda\, 2\zeta^2/(\max\ s)^2$, the reconstructed function is

$$\tilde{q}_z(\vec{\rho}) \simeq q_z(x/u_x,\ y/u_y)\ \exp\left(i\frac{k}{2\zeta u_x u_y}\ (y^2 - x^2)\right), \qquad (13)$$

where $u_x = 1 - \Delta/(z_s - z_R)$, $u_y = 1 + \Delta/(z_0 - z_s)$. This equation makes it possible to determine the distance to the scatterer by performing reconstruction with different values of Δ. At the true location of the scatterer (Δ=0) the "phase front" curvature of the

function $\tilde{q}_z$ under reconstruction changes to the opposite with respect to each coordinate. These problems are considered in detail in [1] and partly in [6]. There one can find the generalization of the method for the ionosphere with the stratified background; the method for determination of inhomogeneities parameters ("mass", space coordinates, size and other moments of potential q) by means of a small number of receivers and solutions of IP due to data of back- scattering.

It is possible to consider the more general case, namely, the strong scattering case. For this case in accordance with (7,10) we reconstruct the projection Q_z of the product of the potential and the normalized field Q=qU, namely,

$$\int qU\, dz = Q_z(\vec{\rho}) \qquad (14)$$

It should be stressed that in general the normalized field U[q] depends on the potential and on the direction of the sounding wave incident. So it is impossible to solve the problem of the product qU reconstruction by means of the direct transformation of a set of projections (14). It is possible to suggest iteration procedures of the ISP solution to the equation (14) directly. But, if the scale of ionospheric inhomogeneities more than sounding wavelength in 10^3- 10^4 times, it is even complicated to solve the direct scattering problem. So for such cases it is necessary to use asymptotic methods. The special asymptotic methods of the solution of the ISP for the case of strong and large scatterers were developed in [1,18]. For example the following asymptotic representation of normalized field was obtained

$$U(\vec{\rho},z) = \exp\Big[-\frac{i}{2k}\int_{-\infty}^{z} q(\vec{\rho}+z')dz + \frac{1}{4k^2}\int_{-\infty}^{z}(z-z')\frac{\partial^2 q(\vec{\rho}+z)}{\partial\vec{\rho}^2}dz' + O(k^{-3})\Big] \qquad (15)$$

This formula is correct for infinitly smooth potential. The corresponding additional terms in the sum (15) will appear in the presence of derivatives discontinuities. The formula (15) permits us to construct the simple iteration procedure of the ISP solution, when it is not necessary to solve numerically neither the direct scattering problem, or the ISP. The given first guess of the potential q_1 (a priori information or transformation under the condition of weak-scattering) defines the approximation of the normalized field functional $U[q_1]$ according to (15). Using this approach it is possible to solve the usual tomographic problem of the reconstruction $q(\vec{r})$ (14) with known "weight" U due to $Q_z(\vec{\rho})$ under the different directions of the sounding wave incident. Later on the iteration procedure with the potential approximations obtained is repeated.

The formula representation (15) permits us to formulate the conditions of applicatability of the weak-scattering approximations. According to this condition the first term ($\sim k^{-1}$) and all successive terms of the expansion (15) have to be small. The restriction on the first term gives us the well-known condition of the BA applicatability.

$$qr_m/2k \ll 1 \qquad (16)$$

Here q is the typical (mean) value of the potential, r_m is the maximum size of the inhomogeneity. In the case when the wavelength of the sounding radiation λ=2m and the value of disturbances of the ionosphere electron density $N \sim 10^{11}$el/m^3 the condition (16) leads to the inequality $r_m \ll$ 2 km. The disturbances of the electron density, scattering radiowaves, have to be measured relative to the background of the regular stratified ionosphere. So, if the background value $N \approx 10^{11}$el/m^3 and the disturbances are

sufficiently strong (10%), the BA is valid up to the sizes of dozens km. But for the case of the main ionosphere maximum ($N \sim 10^{12}$ m^{-3}) the scale restriction is significant and it is necessary to take into consideration the first term of (15). The second term of (15) for simple scatterers without internal structure is less ($kr_m \gg 1$) than the first one. In the case when there are some internal details inside the scatterer with the scale $a \gg \lambda$ and the typical value of the potential q', the second term can be more than the first. Hence the other necessary condition of the BA is the condition that the second term with the transverce derivative is small

$$q' r_m / (4k^2 a) \ll 1. \qquad (17)$$

In many practical cases it is sufficient to take into account the first term of (15) only, but the scatterer is not the Born's scatterer according to (16) and the inequality (17) is valid. Such conditions allows us to get the simple analytic formula [1,14], which connects the function Q_z reconstructed due to the experimental data and the projection of the scattering potential q_z (15).

$$Q_z(\vec{\rho}) = 2ik\,[\exp(-iq_z(\vec{\rho})/2k) - 1] \qquad (18)$$

This formula is the basis of the tomography reconstruction for the most of ionospheric applications. Really, the inhomogeneities with the scale about ten or more kilometers, the deviations of which are about 10% with respect to the background, are the strong inhomogeneities (the left hand side of (16) is more or approximately equal to 6, when $\lambda = 2$ m), but the inequality (17) is valid for the internal details with the scale more than hundreds of meters and with the electron density disturbances about 100% compared with the background.

The uniqueness of solutions of the similar ISP was considered many times earlier [1-3]. Some exact results are known. For the problems in question the uniqueness of the transformation q_z (11) and the following reconstruction (14,18) of projections can be easily proved for the finite volume.

The results described above allow us to get 2D projections of localised ionospheric inhomogeneities with the help of the moving satellite transmitter and the transverse arrow of Earth receivers. If there are some arrows of receivers separated by distances about hundreds kilometers along the line of the satellite flight, it is possible to obtain some 2D projections. Having a set of 2D projections one can reconstruct the 3D structure also. Such experiment (with some arrows of receivers) is rather complicated and it was not realized yet. Nowadays experiments connected with the reconstruction of the 2D localized inhomogeneities were carried out [1,5]. This is the tomography problem also because it is possible to reconstruct the 2D inhomogeneity projection or the 2D cross-section of its spectrum after the corresponding transformations by means of a set of 1D field records in each receiver.

We will consider the examples of numerical calculations by means of eleborated programs.

Using the first numerical example, we will illustrate the necessity for considering diffraction effects in RT reconstruction of objects with dimensions r_m comparable to the dimensions of the Fresnel zone $\sqrt{\lambda\zeta}$. As was demonstrated above (12), diffraction effects are insignificant where $kr_m^2/2\zeta \gg 1$ and can significantly distort the results where $kr_m^2/2\zeta \leqslant 1$. Fig. 2a shows $q_z(\vec{\rho})$, consisting of two irregularities - two Gaussians ($\sim \exp(-\rho^2/r_i^2)$

with parameters ($r_1/\sqrt{\lambda\zeta}$ = 5, $r_2/\sqrt{\lambda\zeta}$ = 1/3, for the λ=2m, ζ=200km, $2r_1$ = 6.3km, $2r_2$ = 420m). If we reconstruct the complex phase after the emission passes through one large irregularity, then according to (12) Im Φ_1 is proportional with a high accuracy to the function $q_z(\rho)$ from a large irregularity. However, the imaginary part of the complex phase Φ_1 (Fig. 2b) from a pair of irregularities bears little resemblance to Fig. 2a due to diffraction effects in small irregularity. Fig. 3 shows the similar picture for the two irregularities with parameters ($r_1/\sqrt{\lambda\zeta}$ = 5, $r_2/\sqrt{\lambda\zeta}$ = 1/8). The pair of irregularities is reconstructed very accurately in the case where the Fresnel inversion (11) is used.

For reconstruction of the structure of ionospheric irregularities the questions about sampling data and reconstruction procedure are significant. The sounding radio signals are always recorded by point receivers. The signal from each receiver recording the emission of the moving transmitter on the satellite is also sampled by an electronic circuit with a fixed interrogation frequency. Moreover, the integral transformations as a result of which the structure of the scattering irregularities is reconstructed can be realized numerically on a computer only after the appropriate digitization. Therefore, both the form of the data recorded and the nature of the numerical processing and the reconstruction of the objects lead to the necessity for performing purely discrete operations. However, in theoretical examination of the solution of the inverse scattering problem the immediate switch to discrete formulas is hardly advisable in the majority of cases. Usually, the discrete analogues to the reconstruction formulas are significantly more

cumbersome, and besides the discrete form hinders analysis of the results obtained. On the other hand, the switch from continual relations to their discrete analogues does not cause difficultes in the majority of cases and is performed in a unique manner. So, continual formulas can be considered a compact notation of their discrete analogues for further practical reconstruction.

Let us consider the switch to discrete analysis of the reconstruction procedure and the questions associated with this switch using the transformations (8), (11). It should be noted that, the methods for digital processing of signals and fields have been developed rather well and covered in the literature [19,20].

First, we switch in (8, (11) to the dimensionless variables $\vec{P} = \vec{\rho}/\sqrt{v\lambda\zeta}$; $\vec{S} = \vec{s}/\sqrt{v\lambda\zeta}$, normalized to the radius of the Fresnal zone. Intriducing the quantities

$$F_q(\vec{P}) \equiv \frac{q_z(\vec{\rho})\lambda}{4\pi} e^{i\pi P^2} \quad \text{и} \quad F_v(\vec{S}) \equiv \frac{V(\vec{s})}{4\pi\zeta} e^{-i\pi S^2} \tag{19}$$

from (11) we obtain the pair of integral Fourier transforms for them [1]

$$\begin{aligned} F_q(\vec{P}) &= \int F_v(\vec{S})\, e^{-2i\pi\vec{S}\vec{P}}\, d^2S \\ F_v(\vec{S}) &= \int F_q(\vec{P})\, e^{+2i\pi\vec{S}\vec{P}}\, d^2P \end{aligned} \tag{20}$$

By virtue of the definition $F_q(\vec{P})$ is a finite function due to the finiteness of $q_z(\rho)$. Let the dimensions of the object not exceed the limits of the segment $[-P_{Ox}, P_{Ox}]$ in axis x and $[-P_{Oy}, P_{Oy}]$ in axis y, i.e., the carrier of the function $F_q(\vec{P})$ is contained in a fixed rectangle. Then, $F_v(\vec{S})$ will be an infinite

and analytical function with a finite spectrum $F_q(\vec{P})$. According to the Kotel'nikov theorem $F_v(\vec{S})$ can be represented in the form of an infinite series in terms of sample functions with the sampling intervals $\Delta S_x = P_{0x}/2$, $\Delta S_y = P_{0y}/2$:mm

$$F_v(S_x,S_y) = \sum_{m_x m_y} F_v\left(\frac{x}{2P_{0x}}, \frac{y}{2P_{0y}}\right) \operatorname{sinc}(2\pi P_{0x}S_x - \pi m_x) \operatorname{sinc}(2\pi P_{0y}S_y - \pi m_y)$$

Substituting this representation in (20) and integrating with respect to S_x, S_y, we obtain the relation

(21)

$$F_q(\vec{P}) = \sum_{m_x\ m_y} F_v\left(\frac{m_x}{2P_{0x}}, \frac{m_y}{2P_{0y}}\right) e^{-2i\pi[P_x\Delta S_x m_x + P_y\Delta S_y m_y]} (2P_{0x}\ 2P_{0y})^{-1}.$$

Using the concept of signals which are really indistinguishable at the level ε [21], it is advisable to introduce a finite function which is really indistinguishable at a fixed level from $F_v(\vec{S})$. Let the carrier of this function be contained in the rectangle $[-S_{0x},S_{0x}]$ x $[-S_{0y},S_{0y}]$. Then, according to the Landau-Pollack theorem [21,22] the approximate dimension of the set of all functions $F_v(\vec{S})$ finite at a fixed level with a carrier in the rectangle $[-S_{0x},S_{0x}]$ x $[-S_{0y},S_{0y}]$ and with a finite spectrum supp $F_q(\vec{P}) \in [-P_{0x}, P_{0x}] \times [-P_{0y}, P_{0y}]$ is close to $N_xN_y = (2S_{0x}\times 2P_{0x})$ x $(2S_{0y}\times 2P_{0y})$. In other words, due to the finite accuracy in measurement of the signals it can assumed that both the signal and its spectrum are finite. The limitation on the carrier of the spectrum leads to a finite sampling frequency and

$$F_q(\vec{P}),\ \Delta P_x = 1/2S_{0x},\ \Delta P_y = 1/2S_{0y},$$

here, the number of sampling intervals on the Cartesian axes is equal to $N_x = = 2S_{0x}/\Delta S_x = 2P_{0x}/\Delta P_x$, $N_y = 2S_{0y}/\Delta S_y = 2P_{0y}/\Delta P_y$. From this, assuming $P_x = n_x\Delta P_x$, $P_y = n_y\Delta P_y$, it is simple to switch

from (19), (20) to a pair of discrete transformations for $\tilde{F}_v = F_v/(\Delta P_x \Delta P_y)$ и $\tilde{F}_q = F_q$

$$\tilde{F}_q(n_x,n_y) = \frac{1}{N_x N_y} \sum_{m_x=-N_x/2}^{N_x/2-1} \sum_{m_y=-N_y/2}^{N_y/2-1} \tilde{F}_v(m_x,m_y)\, e^{-2i\pi\left(\frac{m_x n_x}{N_x} + \frac{m_y n_y}{N_y}\right)}, \tag{22}$$

$$\tilde{F}_v(m_x,m_y) = \sum_{n_x=-N_x/2}^{N_x/2-1} \sum_{n_y=-N_y/2}^{N_y/2-1} \tilde{F}_q(n_x,n_y)\, e^{-2i\pi\left(\frac{m_x n_x}{N_x} + \frac{m_y n_y}{N_y}\right)}.$$

Later on, the fast Fourier transformation algorithms are used in the numerical modeling and the numbering of the sums over m_x, n_x is shifted from 0 to $N_x - 1$, and likewise for m_y, n_y.

The dimensions of the reception region S_{0x}, S_{0y} and, consequently, the sampling intervals ΔP_x, ΔP_y also determine the resolutions. To demonstrate, the minimum resolvable interval δ_x in x is equal to $\delta_x = \sqrt{\lambda\zeta}$, $\Delta P_x = \sqrt{\lambda\zeta}/2S_{0x} = = \lambda\zeta/2S_m$. A limitation of the reception region always limits the resolution or the sampling interval and the function with a finite spectrum. Therefore, generally speaking, with a limited reception region it is possible to switch immediately from (21) to the finite, discrete Fourier transform (22).

The switch from other continual reconstruction formulas containing the Fourier and Fresnel transforms to their discrete forms is also made according to this scheme.

The practical realization of reconstruction of the structure is governed to a great extent by the resistance of the reconstruction procedure to the various types of noises and distortions which unavoidably appear in measurements and processing of experimental data. Let us illustrate the influence

of noises and distortions on reconstruction of the structure on the examples of numerical simulation. Briefly discribe a modeling scheme using the example of two-dimensional Fresnel reconstruction.

The modeling scheme

$$q_z(\vec{\rho}) \Rightarrow F_q(\vec{P}) \Rightarrow F_v(\vec{S}) \Rightarrow V(\vec{S}) \Rightarrow \underset{\uparrow}{\ldots\ldots} \Rightarrow \tilde{q}_z(\vec{\rho})$$

noises, distortions

The function $q_z(\vec{\rho})$ characterizing the two-dimensional structure of the electron concentration irregularities and the effective collision frequency is defined. Then, the quantity $F_q(\vec{P})$ is calculated using formula (19). After performing the discrete Fourier transform (22) corresponding to (20), $F_v(\vec{S})$ is obtained and, thus, the field $V(\vec{S})$ in a discrete grid. This stage of modeling is related to the direct scattering problem, where it is assumed that the scattering is calculated well within the framework of the corresponding approximations. Further, the noise can be added to the data on the field obtained, after which the inverse discrete Fourier transform (22) corresponding (20) is performed, and the result of reconstruction $\tilde{q}_z(\vec{\rho})$ is obtained as a result. The influence of distortions is modeled in asimilar manner: in the inverse transformation stage, the parameters of the transformation are changed or "distorted".

The results of numerical modeling of the influence of noises have demonstrated the stability of the reconstruction procedure. Fig.4 shows two actual irregularities of $q_z(\vec{\rho})$ - two Gaussians with various dimensions on a 64x64 grid. The total size of the image frame in units of the scale of the Fresnel zone $\sqrt{\lambda\zeta}$ is

equal 5x5. After calculating the complex phase of the field scattered by these irregularities, the data on V were disturbed by noise. Then, reconstruction was performed; the quality of it was sufficient even with comparatively large errors in the measured field [23]. For example, Fig.5 shows the result of reconstruction of these irregularities according to data on Φ_1 with additive complex Gaussian noise having a variance of 0.05 of maximum amplitude of the change in the real and imaginary parts of complex phase of the field. Fig.6. illustrates reconstruction with double the noise (a variance level of 0.1). Another numerical example: actual irregularities - "cylinder" and "parabola" are represented in Fig.7. The result of reconstruction of this model structure with additive noise (a variance level of 0.05) is shown in Fig.8. Fig.9 illustrates the reconstruction with double noise (0.1). If we perform preliminary processing of the data, then even higher noise levels will not noticeably influence the results of reconstructions.

Numerical estimation of the level of influence of the noises is of interest for practical applications. It is advisable to characterize the level of influence of the noises in the metric C and L^2. In a discrete reconstruction procedure, it is better to use their discrete, normalized analogues, i.e. we will estimate the difference between the function $\tilde{f}$ reconstructed from noisy data and real function f by the numbers

$$\rho_C(f,\tilde{f}) = \frac{\max\limits_i |f_i - \tilde{f}_i|}{\max\limits_i |f_i|}; \quad \rho_{L^2}(f,\tilde{f}) = \left[\frac{\sum\limits_i (f_i - \tilde{f}_i)^2}{\sum\limits_i f_i^2} \right]^{1/2}, \quad (23)$$

where summation and selection of maximum are performed for all increments of recorded function.

The dependence of the normalized disturbance of the reconstructed two-dimensional structures (i.e., the difference between the true real $q_z(\vec{\rho})$ and reconstructed $\tilde{q}_z$ in the metrics ρ_c and ρ_{L^2}) on the amplitude Δ of normalized (to the maximum amplitude of the change in the field) complex Gaussian noise is shown in Tabl.1 for the irregularities in Fig.7. It is clear that the normalized deviations of the reconstructed two-dimensional structures are comparable to the noise level. The absolute disturbances of the real part, although the true function is real.

Distortions of irregularities reconstructed by radio tomographic methods appear due to imprecise determination of the distance to the irregularities and, as a result, incorrect knowledge of the given parameters of the integral transformations. The influence of distortions was modeled by the scheme described above. The model in Fig.10 (two irregularities: "cos" and "cos^2" ellipse) is the object of reconstruction. The imprecisely determined coordinate of the scatterer $z_s' = z_s - \Delta$ with an error Δ was substituted in the parameters of the Fresnel transformation. Numerical values $z_0 - z_s = 700$ km, $z_s - z_R = 300$ km, $\lambda = 2$ m typical for satellite sounding were used in the calculations. The dimension of the Fresnel zone here $\sqrt{\lambda\zeta} \approx 0{,}65$ km, the frame dimension was 6,4x6,4 km and the transverse resolution δ was of the order of a hundred meters. Fig.11-15 provide reconstructed two-dimensional structures with various values of the error in determination of the coordinates Δ measured in kilometers; Δ is successively equal to -10, +20, -20, +30, +40 km. It is clear that an error of 10 km has little influence on the reconstruction. Errors Δ of the order of 20 km distort the object, but the characteristic details of the object are reconstructed fairly.

Only errors exceeding 30-40 km noticeably distort the reconstructed irregularity and may lead to incorrect conclusions on the structure of the object. The values of the errors in reconstruction in normalized metrics are shown in Tabl.2. The modeling was performed for two Gaussians. The analogy dependence of error reconstruction on the Δ is shown in the graphs in [1]. The reconstruction errors have a clearly pronounced minimum and are minor ($\leqslant 0{,}1 \div 0{,}2$) within $\pm$ (5 - 10)km. We will note that dimension of this minimum agrees in order of magnitude with the longitudinal resolution δ_z of the system; here, the transverse resolution $\delta \sim \lambda/\theta \sim 100$ m, the aperture angle $\theta \sim 0{,}02$ и $\delta_z \sim \lambda/\theta^2 \sim 5$ km. Therefore, determination of the distance to scatterer with accuracy of the order of the longitudinal resolution of the recording system is sufficient for high-quality reconstruction. The method for determining the distance according to the change in the curvature of the "phase" of the reconstructed function makes it possible to achieve this accuracy in insignificant noises [1].

On reconstruction of q_z using the formula (18) the main obstacle is that Qq_z is a periodical function of q_z, therefore, a real part of q_z is not unambigiously defined by Q_z, which we get from experimental data. Since that, making use the formula (18) one cannot immediately reconstruct scatterers that exceed $4\pi k$. It should be noted here that it's much more than BA-based reconstruction procedures are applicable to. Namely, we have found using numerical simulations that BA holds for scatterers satisfying the inequality

$$q_z/2k < 0.1.$$

In principle, one can reconstruct more intensive scatterers, assuming that Q_z is zero if q_z crosses πk level, or if any additional information about the scaterer structure is available.

We have derived an algorithmic procedure for finite scatterers, which allows one to reconstruct scatterers exceeding $4\pi k$. We have seen that the main obstacle which restricts this procedure capabilities is the finite number of receivers which register the scattered field. From the formal mathematical point of view, that simply means we get only finite number of Fourier expansion terms , i.e. we deal with the truncated Fourier series of Q_z.

Thus to obtain q_z we have to derive it from a truncated Fourier expansion of Q_z, which in turn is a nonlinear transcendent function of q_z. This makes us use the numerical simulations to investigate the domain of applicability of this procedure, because immediate analysis of that algorithm is extremely difficult.

We have performed such an investigation of this procedure applying it to various scatterers. The examples of such numerical simulations of reconstruction of 1D projections of 2D scatterers are presented on Fig.16-18. The scatterer - receiver distance was assumed to be 300 km, the sounding wavelength was 2m. Thick curves correspond to initial projections q_z which had to be reconstructed, thin curves are the reconstructed images of q_z using the procedure described above. Just for checking, the Q_z patterns are also shown (small amplitude fast oscillating curves of normal thickness). On the Figure 16, the scatterer is not too strong, so two curves simply coincide (the projection is exactly reconstructed). On the Fig.17-18, where stronger patterns are given, one can see the discrepancy between exact image and

reconstruction. One can see very easy that mistakes in the procedure work arise mostly on those fragments of scatterers where the transverse derivative $|dq_z/dx| = |dQ_z/dx|$ is big enough, so the oscillations of Q_z become so fast that Q_z is no longer approximated by the truncated Fourier expansion well enough. They may cause the loss of zeros of Q_z, which correspond to increments or decrements of $4\pi k$. The numerical simulations using wide variety of scatterers have confirmed this conclusion. Moreover, they have shown that only the transverse derivative absolute value $|dq_z/dx|$ is critical for the correct reconstruction. Of course, it causes the limitation on the maximal intensity of the scatterer, since for continuous function $q_z(x)$ $|q_z| < a\ |dq_z/dx|$. For this reason, the problem to calculate this boundary value for $|dq_z/dx|$ had also been posed. The value which we get estimating the supremum of the truncated Fourier expansion derivative (it is bounded as a derivative of polynom) is much more than actual value. Fig.19 shows the normalized derivative value times $2\pi N$ plotted versus N, where N is the number of terms retained in the Fourier series. We assumed that well-approximating reconstruction it that one which has the maximal normalized discrepancy between exact and reconstructed images less than 0.1.

The description of Fortran Programs

System Requirements

- Computer: IBM AT or compatible (with coprocessor)
- Operating System: MS-DOS or PC-DOS version 3.0 and later
- Memory: at least Extended memory 4 Mbytes (depends on geometry and type of approximation reconstructed function)
- Hard Disk Space: 4 Mbytes
- Software: compiler 1.4e and linker 2.2d NDP-FORTRAN-386(c) MicroWay or later

1. Program <DT_DIR.for>

This program solves direct problem, namely, determines complex field $V(\vec{S})$ by means of Fast Fourier Transformation (FFT) based on the model structure of irregularities.

Input parameters and files:

(the determination of the irregularities parameters)
file <mod_par.tsk> contains the following parameters:

```
<< line 1 in file
      'wave length (km):'                    0.002    (DLV in program)
   line 2
   'distance to satellite (km):'             1000.    (ZZ0 in program)
   line 3
   'distance to irregularities (km):'        300.>>   (Z in program)
```

These parameters you can change in the file.

NY - number of receivers
MNY - the degree of 2 for NY (namely, 2^MNY=NY)
NX - number of discrete intervals on the axis X
MNX - the degree of 2 for NX (namely, 2^MNX=NX)
RMN - the radius of the Fresnel zone.
PX,PY - the limits of segments [-PX/2, PX/2] in axis X and [-PY/2, PY/2] in axis Y; object (model structure not exceed these limits; variable $\vec{P}$)
SX,SY - the limits of rectangle [-SX/2, SX/2]x[-SY/2,SY/2] (variable $\vec{S}$)

YR - the size of the receiving system (km)
XO2 - the size of aperture "synthesized" by satellte (km)
DXX, DYY - the size of frame (km*km)
NMOD - number of model structure (1-10):
1 - the gaussians
2 - "homogeneous" ellipse
3 - "parabolic" ellipse
4 - " 2 + 3 "
5 - " 2 " with absorption 10%
6 - " 3 " with absorption 20%
7 - "cos" ellipse
8 - "cos^2" ellipse
9 - " 7 + 8 "
10 - arbitrary

Nmod is introduced from the screen
Const5=0.1 (namely,10%) - constant for NMOD=5
Const6=0.2 (20%) - constant for NMOD=6

Z1,Z2,Z3,UG ——————————————
A1,B1,A2,B2,XO,YO,Y1,A3,FPC,FPS | parameters for
AELP,BELP |
APAR,BPAR | models
AELP1,BELP1,APAR1,BPAR1 ——————

RN - complex field
Subroutine <SMAXMI> calculates min and max of array
Subroutine <FFT> calculates 1-D Fast Fourier Transformation

Output files:
<MODEL.GRD> - contains the model structure of irregularities and the number of the model (NMOD) and constans VMD and ZRD (for determination of reconstruction's errors)
<V_real.grd> - the array of real parts of the field RN
<V_imag.grd> - the array of imaginary parts of the field RN
Execution
f77 dt_dir.for
RUN
dt_dir.exp

2. Program <DT_INV.for>

This program solves inverse scattering problem for weak-scattering irregularities in the case when noise is present in the measurements of the field and calculates the errors of the reconstruction in metric C and L2 in dependence on level of noise.

Input parameters and files:

Parameters < NX, MNX, NY, MNY, PX, PY, SX, SY >are similar to same parameters of program <DT_DIR.FOR>.

FILES (from program <DT_DIR.for>):

<MODEL.GRD> - input file of model structure.

<V_real.grd> - the array of real parts of the field RN.

<V_imag.grd> - the array of imaginary parts of the field RN.

Parameter <Error> - the level of noise (0 < error < 1)

Error is introduced from the screen.

Const5, Const6 - are similar to same parameters of program <DT_DIR.for>

Subroutine <SMAXMI> calculates min and max of array

Subroutine <FFT> calculates 1-D Fast Fourier Transformation

Function <RAN> - determinates random values in [0,1].

K33 - the constant for function <RAN>

Output files:

REC_er.GRD - the reconstruction

er_r!er.dat - contains the errors of reconstruction in metric C and L2

Same errors are shown on the screen.

Execution

f77 dt_inv.for

RUN

dt_inv.exp

3. Program <DT_ERR.for>

This program solves inverse scattering problem for weak-scattering irregularities in the case when distortions are present in the measurements of the field and calculates the errors of the reconstruction in metric C and L2 in dependence on distortions.

Input parameters and files:

Parameters < NX, MNX, NY, MNY, PX, PY, SX, SY > are similar to same parameters of program <DT_DIR.FOR>.

FILES (from program <DT_DIR.for>):

<MODEL.GRD> - input file of model structure.

<V_real.grd> - the array of real parts of the field RN.

<V_imag.grd> - the array of imaginary parts of the field RN.

<mod_par.tsk> is similar the same file in program <DT_DIR.for>.

Parameter <DEL> - the error of irregularities coordinate in km DEL is introduced from the screen.

Subroutine <FFT> calculates 1-D Fast Fourier Transformation

Output files:

REC_cr.GRD - the reconstruction

er_r!cr.dat - contains the errors of reconstruction in metric C and L2

Same errors are shown on the screen.

Execution

f77 dt__err.for

RUN

dt_err.exp

4. The solution of the statistical radiotomography problem (statistical inverse scattering problem)

Rather frequently, the ionosphere contains entire regions filled with large numbers of irregularities of various dimensions. Such a state is typical for the equatorial and polar regions, especially at night. In this case it is advisable not to reconstruct individual realization of such disturbed ionosphere, but rather to pose the problem of reconstruction of the statistical characteristics of the turbulent random ionosphere such as correlation function or spectrum of fluctuations. So, such reconstruction of random ionosphere statistical properties by the measured field statistics it is reasonable to name the statistical ISP or the statistical RT problem [24,25].

We consider the reconstruction of ionosphere electron density fluctuations spectrum by means of satellite radioprobing data. Integral equations, which relate the measured field to the medium structure are probably the most convenient and adequate mathematical technique for the tomography. In this paper we shall show how to derive such equations. For simplicity it is reasonable to use two frames of reference. The first "global" frame of reference $\vec{r}=(x,y,z)=(\vec{\rho},z)$, its origin is related to the receiving system as in the previous section (Fig.1). The origin of the second frame of reference $\vec{\mathcal{R}}=(\mathcal{X},\mathcal{Y},\mathcal{Z})=(\vec{\mathcal{P}},\mathcal{Z})$ is reasonable to locate at one of the transmitter positions and the $\mathcal{Z}$ axis to direct to the center of the receiving system. As the transmitter moves it is convenient to use several such "local" frames with different orientations. Such frames are introduced to make derivations shorter, because the probing wave scattering in each local frame may be treated as "almost forward" small-angle scattering. The

lower boundary of the layer of irregularities is z_d, the upper - z_u in the global frame $\vec{r}$. After performing the Fresnel expansions of exponents in the (5) for small-angle scattering, we obtain the integral equation for U (7). This equation is written in the local reference frame, $\vec{S}(Z-Z_0) = (Z'-Z_0)\vec{R} + (Z-Z')\vec{R}$; $D(Z-Z_0) = (Z'-Z_0)(Z-Z')$. For making formulas shorter we assume, that the transmitter is located exactly at the local frame origin, i.e. $\vec{R}_0 = (\vec{P}_0,Z_0)=(0,0,0)$.

To reduce calculations and to use known results we transform (7) to the parabolic equation in new variables $\xi = 1/Z$, $\vec{\sigma} = \vec{P}/Z$, $\xi'= 1/Z'$. Then $(\vec{S}-\vec{P}')^2/D = (\vec{\sigma}-\xi'\vec{P}')^2/(\xi'-\xi)$ and U satisfies the differential equation

$$(-2ik\frac{\partial}{\partial\xi} + \Delta_\sigma - \xi^{-2}q)\ U(\xi,\vec{\sigma}) = 0 \qquad (24)$$

Equation (24) is derived from (7) by differentiating and making use of the following relation for the fundamental solution of the Schrodinger operator [24]. Having derived the parabolic equation we use the methods developed to obtain equations for the first and the second moments of U [26,27]. Let us assume also that the random field q to be Gaussian and δ-correlated along Z,

$$B(\vec{R}_1,\vec{R}_2)\equiv \langle q(\vec{P}_1,Z_1)\ q(\vec{P}_2,Z_2)\rangle = \delta(Z_2-Z_1)\ A_q(\vec{P}_2-\vec{P}_1) \qquad (25)$$

In the similar way in the variables $(\vec{\sigma},\xi)$ it is possible to derive from (24) equations for the second moments of the normalized field $\gamma(\vec{R}) = E(\vec{R})/\langle E(\vec{R})\rangle$,

$\Gamma_{1,0}(\vec{P},Z) = \langle\gamma(\vec{P}_2,Z)\ \gamma^*(\vec{P}_1,Z)\rangle$ - the first coherence function,

$\Gamma_{2,0}(\vec{P},Z) = \langle\gamma(\vec{P}_2,Z)\ \gamma(\vec{P}_1,Z)\rangle$ - the second coherence function of

the second order. As the calculations are described in the papers mentioned above, we present only the final result in the variables $\vec{\mathcal{P}}_+ = (\vec{\mathcal{P}}_1+\vec{\mathcal{P}}_2)/2$, $\vec{\mathcal{P}} = \vec{\mathcal{P}}_2-\vec{\mathcal{P}}_1$ and for statistically homogeneous layer, when the dependence on $\vec{\mathcal{P}}_+$ is absent.

$$\left[ik\left(\frac{\partial}{\partial \mathcal{Z}} + \frac{\vec{\mathcal{P}}}{\mathcal{Z}}\frac{\partial}{\partial \vec{\mathcal{P}}}\right) + \Delta_\perp + \frac{i}{4k} A_q(\vec{\mathcal{P}})\right] \Gamma_{2,0} = 0, \quad \Gamma_{2,0}(\vec{\mathcal{P}},\mathcal{Z}_u) = 1 \tag{26}$$

The integral equation, corresponding to (21), has the form

$$\Gamma_{2,0}(\vec{\mathcal{P}},\mathcal{Z}) = 1 + \frac{i}{16\pi k}\int d^3\mathcal{R}' \frac{A_q(\vec{\mathcal{P}}')}{\mathcal{D}} \Gamma_{2,0}(\vec{\mathcal{P}}',\mathcal{Z}') \exp\left(\frac{ik}{4\mathcal{D}}(\vec{\mathcal{S}}-\vec{\mathcal{P}}')^2\right) \tag{27}$$

The following formula for $\Gamma_{1,1}$ is well known [26,27].

$$\Gamma_{1,1}(\vec{\mathcal{P}},\mathcal{Z}) = \exp\left(\frac{1}{4k^2}\int_{\mathcal{Z}_u}^{\mathcal{Z}} A_q\left(\vec{\rho}\frac{\mathcal{Z}'}{\mathcal{Z}}\right) d\mathcal{Z}'\right) \tag{28}$$

Eguation (27) follows from (26). The resulting integral equation is valid also at $\vec{\mathcal{P}}_0 \neq 0$, $\mathcal{Z}_0 \neq 0$.

The integral equation (27) is the basis of the statistical RT. According to (20) $A_q(\vec{\mathcal{P}})$ is the correlation function projection, $\int B(\vec{\mathcal{P}},\mathcal{Z})\, d\mathcal{Z} = A_q(\vec{\mathcal{P}})$. Measured wave coherence functions allow us to determine projections of the complex potential q correlation function by the (27,28). To begin with, let's assume, that irregularities occupy a sufficiently extensive layer, oblique to the probing wave propagation direction. To reconstruct projection $A_q(\vec{\mathcal{P}})$ it's necessary to determine the layer coordinate $\mathcal{Z}_s$. It may be done by a single receiver. The special procedure for determination of the scattering layer $\mathcal{Z}$-coordinate by equation (22) was developed [1,24].

In many situations randomly inhomogeneous media represent

statistically quasi-homogeneous fields with slowly varying statistical properties, i.e. such fields, for which the correlation radius of the differential argument is essentially less than the scale of the variance σ. In other words, the correlation function is represented as a product $B(\vec{\mathcal{R}}_1,\vec{\mathcal{R}}_2) = \sigma^2(\vec{\mathcal{R}})\mathcal{K}(\Delta\vec{\mathcal{R}},\vec{\mathcal{R}})$, where $\vec{\mathcal{R}} = (\vec{\mathcal{R}}_1+\vec{\mathcal{R}}_2)/2$, $\Delta\vec{\mathcal{R}} = \vec{\mathcal{R}}_1-\vec{\mathcal{R}}_2$. A randomly inhomogeneous field with the costant correlation coefficient $\mathcal{K}(\Delta\vec{r})$ but with varying fluctuations variance $\sigma^2(\vec{\mathcal{R}})$ may be called an "additive" field, because the electron density changings influence only the fluctuations intensity, but the correlation coefficient dependence on the summarize argument $\vec{\mathcal{R}}$ is absent. Assuming the field q to be δ-correlated, as was done above, it is possible to obtain similar equations by the same technique. The correlation function projection $A_q(\vec{\mathcal{P}})$ in the integrands should be replaced by $\sigma^2(\mathcal{Z})\,K(\vec{\mathcal{P}})$. Here $K(\vec{\mathcal{P}}) = \int \mathcal{K}(\Delta\vec{\mathcal{R}})\,d(\Delta\mathcal{Z}')$ is the correlation function projection. Then formula for $\Gamma_{1,1}$ and the equation for $\Gamma_{2,0}$ have the form

$$\Gamma_{2,0}(\vec{\mathcal{P}},\mathcal{Z}) = 1 + \frac{i}{16\pi k}\int d^3\mathcal{R}'\,\frac{\sigma^2(\mathcal{Z}')K(\vec{\mathcal{P}}')}{\mathcal{D}}\,\Gamma_{2,0}(\vec{\mathcal{R}}')\,\exp\left(i\frac{k}{4\mathcal{D}}(\vec{\mathcal{S}}-\vec{\mathcal{P}}')^2\right) \tag{29}$$

$$\Gamma_{1,1}(\vec{\mathcal{P}},\mathcal{Z}) = \exp\left(\frac{1}{4k^2}\int_{\mathcal{Z}_u}^{\mathcal{Z}}\sigma^2(\mathcal{Z}')\,K\left(\vec{\rho}\,\frac{\mathcal{Z}'}{\mathcal{Z}}\right)d\mathcal{Z}'\right) \tag{30}$$

The equations (29,30) contain the unknown function $\sigma^2(\vec{\mathcal{R}})$. So, the problem of the correlation function reconstruction is divided into two ones: the problem of reconstruction of the fluctuations variance $\sigma^2(\vec{\mathcal{R}})$, and the problem of the $\mathcal{K}(\Delta\vec{\mathcal{R}})$ reconstruction given the measured projections $K(\vec{\mathcal{P}})$.

The formula (30) allows us to determine integrals of $\sigma^2(\mathcal{Z})$ along the direction ($\mathcal{Z}$ axis) of the probing wave propagation. If a

set of different integrals is given for a region filled with irregularities we arrive at a tomography problem. Usually in the experiments there exist a natural limit to the number of projections and angular range of probing waves propagation directions. Hence, the problem when data are known in the small angle range should be solved. A similar problem was solved in the ray RT. Information about the fluctuations intensity $\sigma^2(\vec{R})$ distribution is sufficient to reconstruct a set of correlation function projections given by measured coherence functions. Methods of the statistical RT problem solution are similar to the discussed above, with the substitution of the product $\sigma^2(\vec{R})K(\vec{P})$ of the known function $\sigma^2(\vec{R})$ and the correlation function projection $K(\vec{P})$ instead of A_q. A set of projections $K(\vec{P})$ allows us to perform tomography reconstruction of the correlation coefficient $\mathcal{K}(\Delta\vec{R})$ or its spectrum.

With the help of examples we want to illustrate the results of programs and numerical pattering. Reconstruction of electron concentration fluctuations spectra was made in two steps: pattering of environment fluctuation spectra and recovery of the power angle spectra of the dispersive environment.

I. Pattering of environment fluctuation spectra. In the given program <ST-DIR.FOR> the account of accidental realisations of electron concentration power fluctuation spectra is made. The pattering scheme is given of tabl.3.

1. The sum of three (of five) Gauss lines with defferent width and intensivity was taken as a pattern of spectra with a few maximums. The location of local maximums and their width depend on the dimentions of the area (32*32,64*64,etc.) and were given by the quantity of accounts from the beginning of the area.The intensivity of local maximums was given in the percent relativity

from the intensivity of the center maximum.

2. The computation of correlation function projections of dispersed field Γ_{11} is made in polar coordinates for the given reception angles in condition with equation (28). The projections of environment correlation functions $R(\rho,\phi_n)$ calculated with the help of fast Fourier transformation from the spectra $\Phi(\rho,\phi_n)$ for every given reception angle in area $[0,\pi/2]$.

3. The form of casual realisations of the dispersed field is made in two steps. At first, with the help of linear congruent method [28,29] statisticaly independent one-dimentional realisations of casual numbers with proportional spectra were obtained. Then, with the help of spectra method of reorganization [30] the prosess with given correlation function $\Gamma_{11}(\rho,\phi_n)$ was formed.

4. The selected (casual) correlation functions of the field $\tilde{\Gamma}_{11}(\rho,\phi_n)$ were calculated from alone realisations of the field.

5. The selected projections of correlation functions of the environment $\tilde{R}(\rho,\phi_n)$ were calculated by logariphmation of the function $\tilde{\Gamma}_{11}(\rho,\phi_n)$. The appropriate $\tilde{R}(\rho,\phi_n)$ casual power spectra of environment fluctuations $\tilde{\Phi}(\rho,\phi_n)$ are defined with the help of standard procedure fast Fourier transformation. The given model of environment spectra (in Decart coordinates) is given as the illustration on fig.20,a. Area dimentions are 64*64, width of central and local maximums on the level of 0.5 their intensivity is 1/8 from linear dimentions of the area. The local maximum intensivety is $I_l=0.3I_c$ (I_c means intensivity of central maximum). From the fig 20,b one can see casual spectra of environment fluctuations, formed from one field realisation for every given reception angle. It is easy to see, that for more calculations reconstraction of angle spectra) the same casual function need

smoothing, i.e. period of its oscilations is equal to the account step [29]. On fig.21 statistically middled (by 50(a) ond 100(b) realisations) angle spectra of the intensivity of environment fluctuations , took by the given below scheme, are given.

II. Recovery of the power angle spectra of the dispersive environment.

In program <ST-INV.FOR> the account of reconstructions of environment power angle spectra from the information in finit reception angle area. For solving the problem of recovery the method of function decomposition into Lejandr polynoms is used. The system of linear equations, made by this method, is solving by Gordon method [30]. On the last step of the account the linear interpolation of the function $\Phi(\rho,\phi_n)$ in Decart coordinates is made.

On fig.23 one can see reconstructions of power spectra of plasma fluctuations calculated from one realisation of dispersed field in each direction of the reciption of the signal. The account was made for three-racurs reception system (fig.22,b). It was supposed that angle areas makes $0\text{-}20^0$,$35\text{-}55^0$,$65\text{-}85^0$ from vertical. On fig.23 the model and reconstruction of its casual realisation (the width of central and local maximums is 1/8 and 1/10 from the linear dimentions of area (64*64),intensivity $I_l=0.3I_c$) is shown. On fig.24 the results of the same account for the dimentions of local and central maximums of 1/16 and 1/8 is shown. Analising the results, we can see that the best reconstructions are obtained for the models of sufficiently narrow spectra (fig.25-28). In this case (fig.28) the recovery of realisation of pattern from 5 local maximums (width is 1/20, relativity of intensivity is 1:0.3:0.2) is sufficiently good. On fig.29 the reconstruction of realisation of pattern from 5 local

maximums (width 1/16, relativity of intensivity is 1:0.3:0.2) is given.The results of the accounts also show that weak intensive local maximums (1:0.1) recover sufficiently good (fig. 30). But the essential part is played by the width of the spectra.On fig.31 the reconstruction of model, which appropriate to the experimental observations[24]. It is clear, that recovery of the spectra from one realisation allow to underline the particularities of its structure. Comparison analisys shows that in spectra reconstructions the locations of local maximums coincide with the original but the intensivities are differ. It future thes difference can be overcomed by using of correlative filters.

The quality of reconstruction very much depend on the quantity and width of reception areas. On fig.32,a reconstruction of model from fig.24, made by two-racurs scheme(fig.22), is given. Reception angles area - 0^0-30^0 and 50^0-80^0. The same reconstructions are made for the experimental model (fig.30). It is clear, that 3-racurs sceme is prefered. On fig.33 are given spectra reconstructions for three reception areas: 0^0-10^0, 40^0-50^0, 70^0-80^0, which are in connection with fig.32. It is clear that to give more quality to the reconstruction the width of reception area should have optimum value.

The description of Fortran Programs

System Requirements

- Computer: IBM AT or compatible (with coprocessor)
- Operating System: MS-DOS or PC-DOS version 3.0 and later
- Memory: at least Extended memory 4 Mbytes (depends on size of frame and number of rays)
- Hard Disk Space: 4 Mbytes
- Software: compiler 1.4e and linker 2.2d NDP-FORTRAN-386(c) MicroWay or later

1. Program <ST-DIR.**for**>

This program solves direct problem, namely, determines the model structure and calculates the random realizations of angle power spectrum.

Input parameters and files:

M - size of frame
NM - size of half frame
JMN - number of rays in [0;π/2] range
KR1 - local maximum size
KR - central maximum size
NOO - spectrum coordinate of local maximum
OTT - level of local maximum power
array HH - model of angle power spectrum in polar coordinates
array SPAD - correlation function model of scattering field
Subroutine SMAXMI calculates maximum and minimum of one-dimension function
Subroutine SMAXNI calculates maximum and minimum of two-dimension function
Subroutine SPGEN calculates balance multipliers
Subroutine RANFIL calculates random fields(complex)
Subroutine CORPAT calculates random correlation function
Subroutine FORT1 calculates one-dimension Fast Fourier Transformation
Function RAN1 calculates uniform random number

Output files:
<RANDSP.GRD> - contains random realization of angle
power spectrum,size(JMN:M)

Execution
f77 st-dir.for
RUN
st-dir.exp

3. Program <ST-INV.for>

This program solves inverse problem for statistical RT, namely, calculates reconstructions of power spectrum of electron density in Decart coordinates for varios namber of receivers.

Input parameters and files:
Parameters
M - size of frame
NM - half size of frame
NN - half size of frame +1
ITER - number of iterations
JPI - number of reseivers
JMN - numer of rays in [0,π/2] range
JT1, JT2, JT3, JT4,JT5,JT6 - boundaries of angle ranges
of reception in degrees
NU - number of rays in angle ranges of reception
NXX -number of Lejandr cofficient
FILE <RANDSP.GRD> contains realization of angle power spectrum
(OUTPUT file of progpam ST-DIR.for)
OUTPUT FILE:
< RECONS.GRD> contains the reconstraction of realizations
angle power spectrum in Decart
coordinates,size(M:M).

Execution
f77 st-inv.for
RUN
st-inv.exp

References.

1. V.E.Kunitsyn, E.D.Tereshchenko, *Tomography of the Ionosphere*, Moscow, Nauka, 1991 (in Russian).
2. V.E.Kunitsyn, "Inverse Scattering Problem in the Layered Medium", Moscow University Physics Bulletin, Vol.26, No 6, pp.33-40, 1985.
3. V.E.Kunitsyn, "Determination of the structure of ionospheric irregularities", Geomagnetizm and Aeronomy, Vol.26, pp.75-81, 1986.
4. V.E.Kunitsyn, "Diffraction Tomography in the Fresnel Zone", Moscow University Physics Bulletin, Vol.41, No 2, pp.43-48, 1986.
5. V.E.Kunitsyn, N.G.Preobrazhensky, E.D.Tereshchenko, "Reconstruction of ionospheric irregularities structure based on the radioprobing data", Dokl.Akad.Nauk USSR, Vol.306, pp.575-579, 1989.
6. V.E.Kunitsyn, E.D.Tereshchenko, *The reconstruction of the ionosphere irregularities structure*, Preprint Polar Geophys. Inst., № 90-01-69, pp.1-60, 1990.
7. V.E.Kunitsyn, "Diffraction Tomography based on small-angle scattering data", Transactions SPIE, Vol.1843, pp.172-182, 1992.
8. V.E.Kunitsyn, E.D.Tereshchenko, "Radio Tomography of the Ionosphere", Antennas Rropagation Magazine, Vol.34, pp.22-32, 1992.
9. V.L.Ginzburg, *Propagation of electromagnetic waves in plasma*, New York, Gordon and Breach Science Publishers, Inc., 1961.
10. L.D.Landau, E.M.Lifshits, *Statistical physics*, New York, Pergamon Press, 1980.
11. L.D.Faddeev, "Three-dimensional inverse scattering problem", J.Sov.Math., Vol 5, pp. 334-360, 1976.
12. R.G.Newton, "Inverse scattering II. Three dimentions" J.Math. Phys., Vol.21, pp.1698-1715, 1980.
13. K.Chadan, P.C.Sabatier, *Inverse problems in quantum theory*, New York, Springer-Verlag, 1977.
14. A.J.Devaney, "Geophys. diffraction tomography", IEEE Trans. Geosci. and Remote Sencing, Vol.22, pp.3-13, 1984.
15. R.K.Mueller, M.Kaveh, G.Wade, "Reconstructive tomography and applications to ultrasonics", Proc. IEEE, Vol.67, pp.567-587, 1979.
16. D.Lesselier, D.Vuillet-Laurent, F.Jouvie at al., "Iterative solutions of some direct and inverse problems in electromagnetics and acoustics", Electromagnetics, Vol.5, pp.147-189, 1985.

17. K.J.Langeberg, "Applied inverse problems for acoustic, electromagnetic and elastic wave scattering", in P.Sabatier (ed.), Basic methods of tomography and inverse problems, Bristol, Adam Hilger, pp.127-467, 1987.
18. W.Tabbara, B.Duchene, C.Pichot. et al, "Diffraction tomography: contribution to the analysis of some applications in microwaves and ultrasonics", Inverse Problems, Vol.4, pp.305-331,1988.
19. W.K.Pratt, Digital Image Processing, New York, A Wiley Interscience Publ., 1978.
20. D.E.Dadgeon, R.M.Mersereau, Multidimensional Digital Signal Processing, Prentice-Hall, Inc., 1984.
21. D.Slepian, "About bandwidth", Proc.IEEE, Vol.64, No.3, pp.292-300.
22. H.J.Landau, H.O.Pollak, "Prolate spheroidal wave functions, Fourier analysis and uncertainty", Bell Syst.Tech.J., Vol.40, pp. 65-84; Vol.41. pp.1295-1336, 1961.
23. E.S.Andreeva, V.E.Kunitsyn, "The reconstruction of the projections of scattered irregularities by inexact wavefield data", In: Waves propagation and diffraction in inhomogeneous media, Moscow, Moscow Inst. Physics and Technology, pp. 9-14, 1989.
24. V.E.Kunitsyn, E.D.Tereshchenko, "Determination of the turbulent spectrum in the ionosphere by a tomographic method", Journ.Atm.Terr.Phys., Vol.54, pp.1275-1282, 1992.
25. A.V.Galinov, V.E.Kunitsyn, E.D.Tereshchenko, "A tomographic approach to the investigation of a randomly nonuniform ionosphere", Geomagnetism and Aeronomy, Vol.31, No.3, pp.351-356, 1991
26. V.I.Tatarski, *Wave propagation in a turbulent medium*, New York, McGraw-Hill, 1961.
27. A.Ishimaru, *Wave propagation and scattering in random media*, Orlando (Florida), Academic Press, 1978.
28. I.M.Sobol, *Monte-Carlo method*, Moscow, Nauka, 1978 (in Russian).
29. S.Chakrabarti, S.K.Mitra, "Calculations of two dimensional digital filters by spectral convolution", Proc.IEEE, Vol.65, No.6, 1977.
30. R.Gordon, R.Bender, A.Lent, Journ.Theor.Biol., Vol.29, 1970.

σ	ρ_c	ρ_{L^2}
$1*10^{-2}$	0.034	0.033
$2*10^{-2}$	0.066	0.067
$3*10^{-2}$	0.100	0.101
$4*10^{-2}$	0.134	0.135
$5*10^{-2}$	0.165	0.167
$6*10^{-2}$	0.201	0.200
$7*10^{-2}$	0.229	0.232
$8*10^{-2}$	0.267	0.270
$9*10^{-2}$	0.302	0.327
10^{-1}	0.337	0.332

Tabl. 1

Δ(KM)	ρ_c	ρ_{L^2}
-10	0.154	0.183
-20	0.345	0.436
-30	0.439	0.675
-40	0.672	0.882
10	0.093	0.101
20	0.241	0.253
30	0.468	0.475
40	0.654	0.717

Tabl. 2

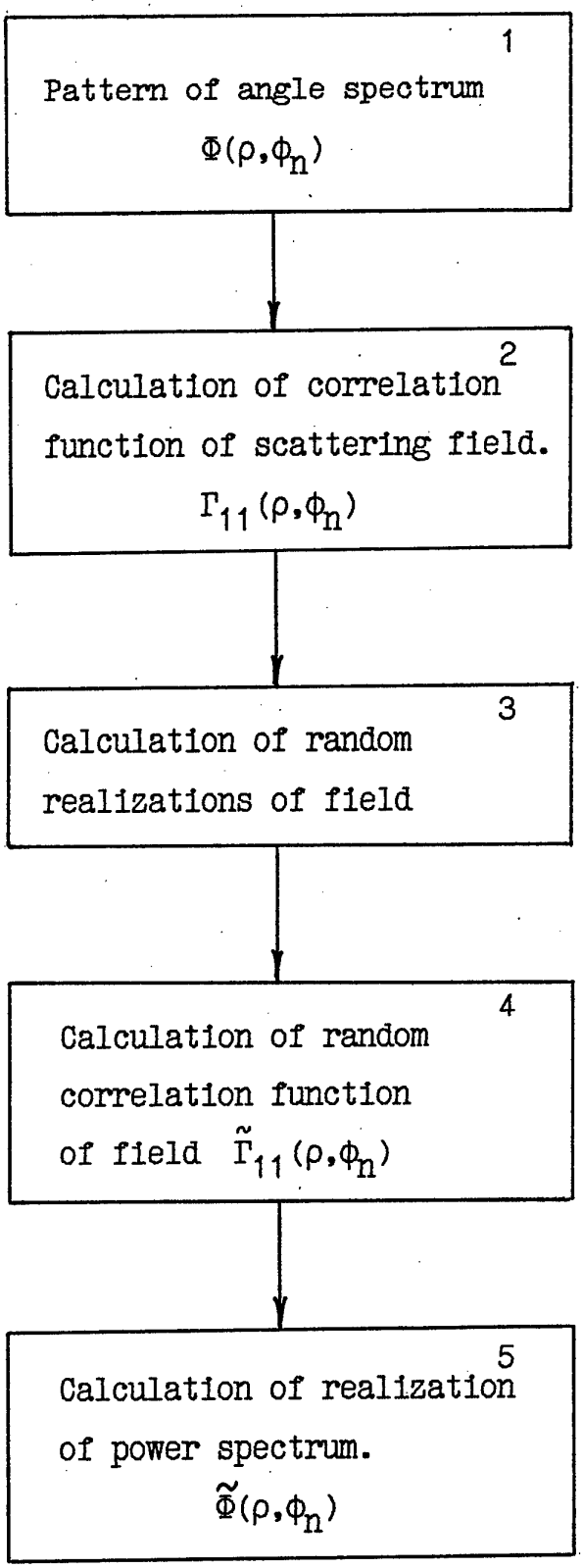
1
Pattern of angle spectrum
$\Phi(\rho,\phi_n)$
2
Calculation of correlation function of scattering field.
$\Gamma_{11}(\rho,\phi_n)$
3
Calculation of random realizations of field
4
Calculation of random correlation function of field $\tilde{\Gamma}_{11}(\rho,\phi_n)$
5
Calculation of realization of power spectrum.
$\tilde{\Phi}(\rho,\phi_n)$

Tabl. 3

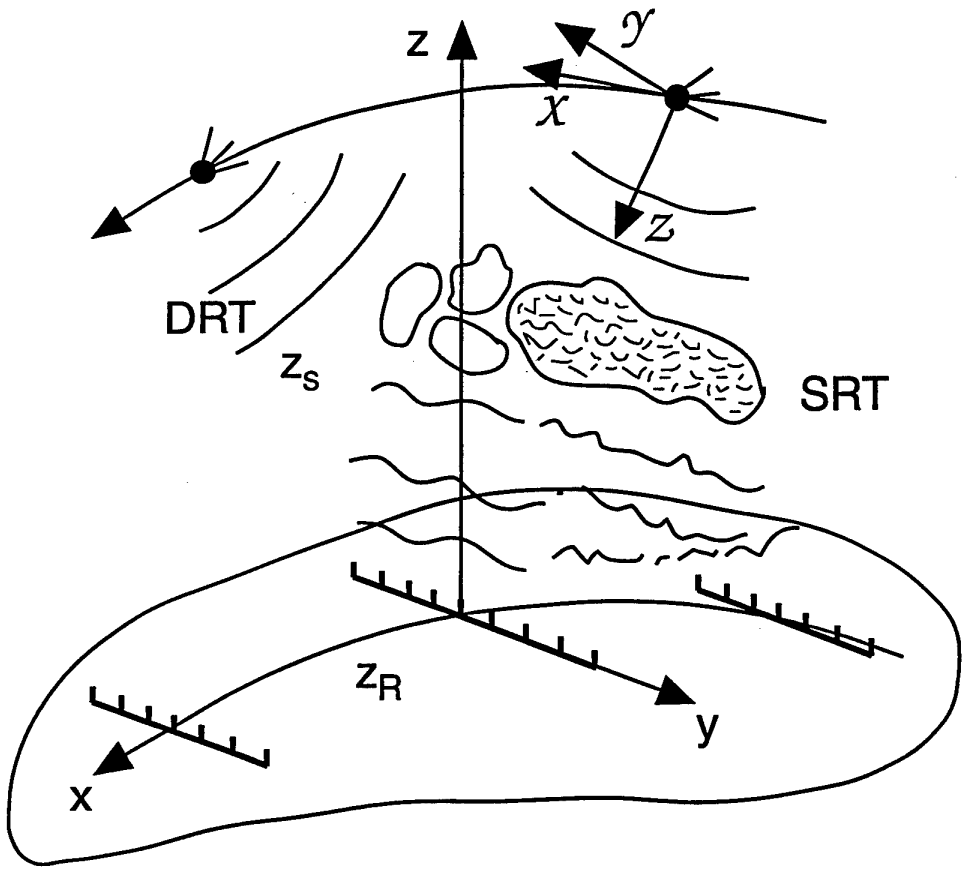

Figure 1.

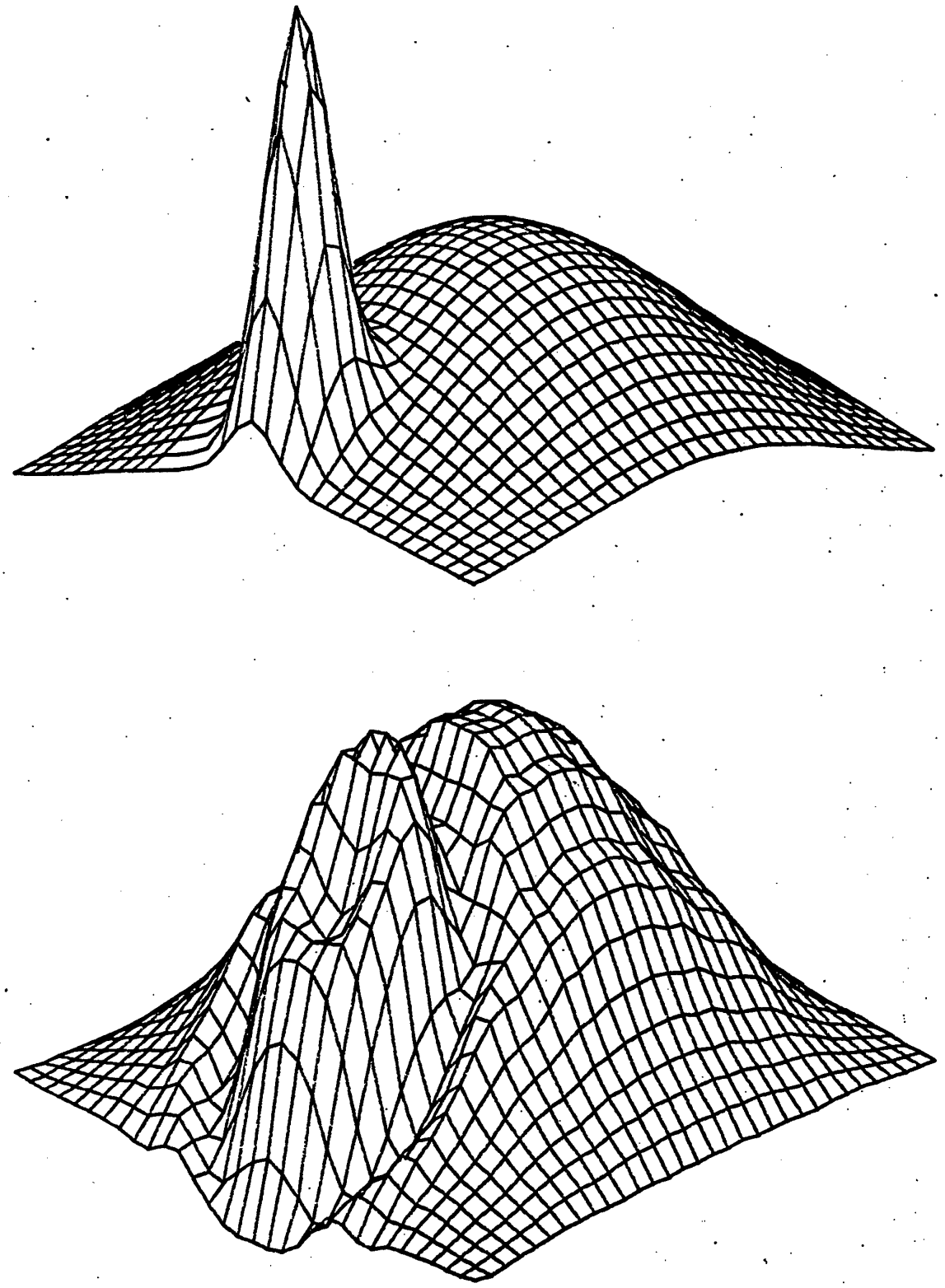

Fig. 2

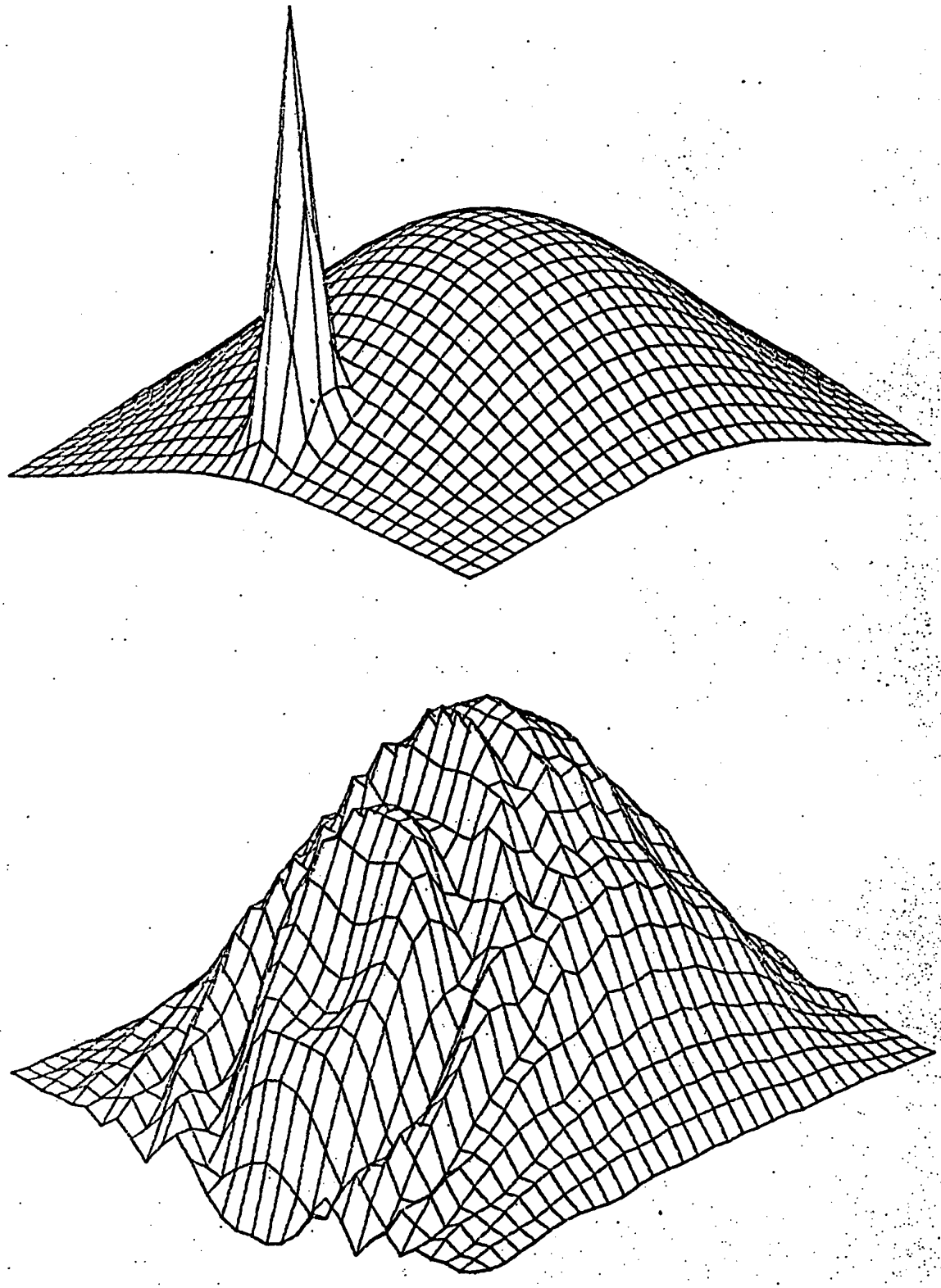

Fig.3

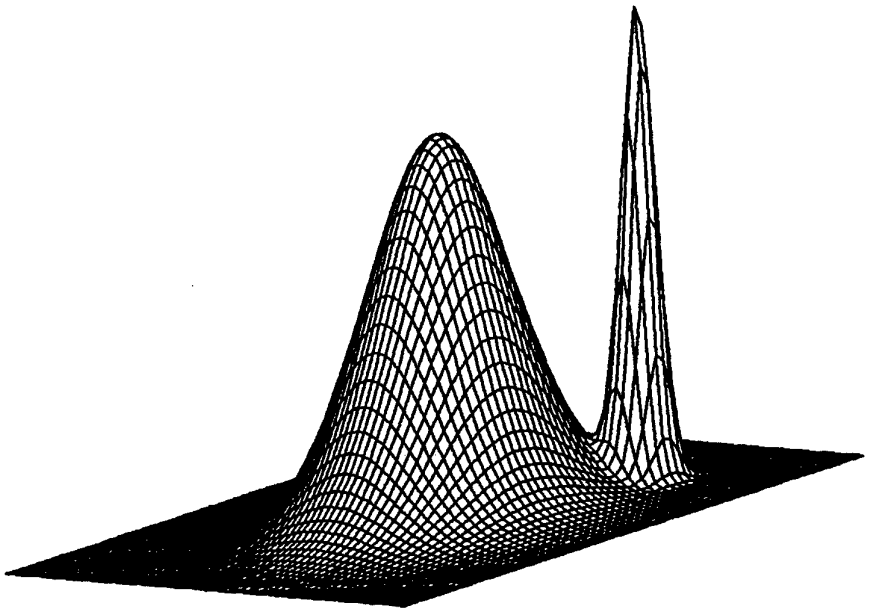

Fig 4.

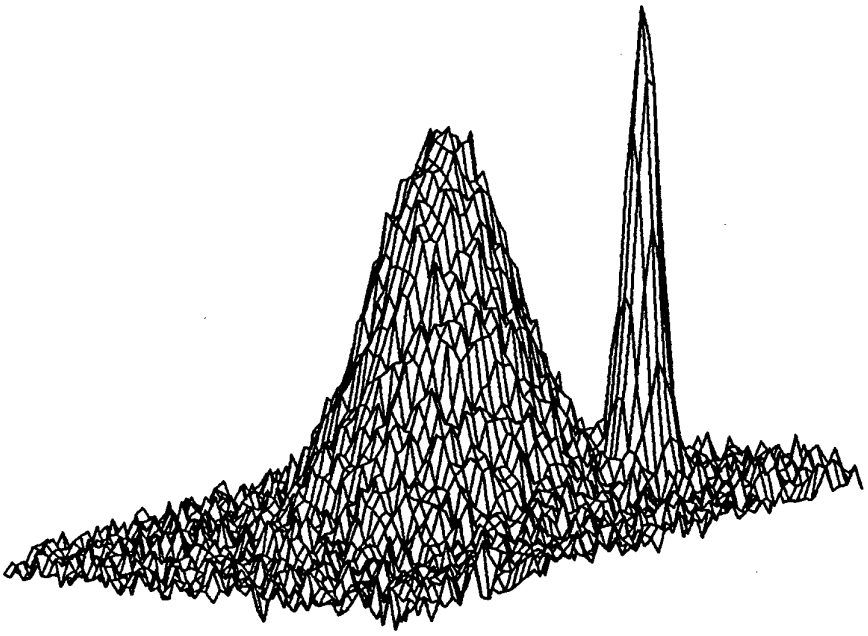

Fig.5

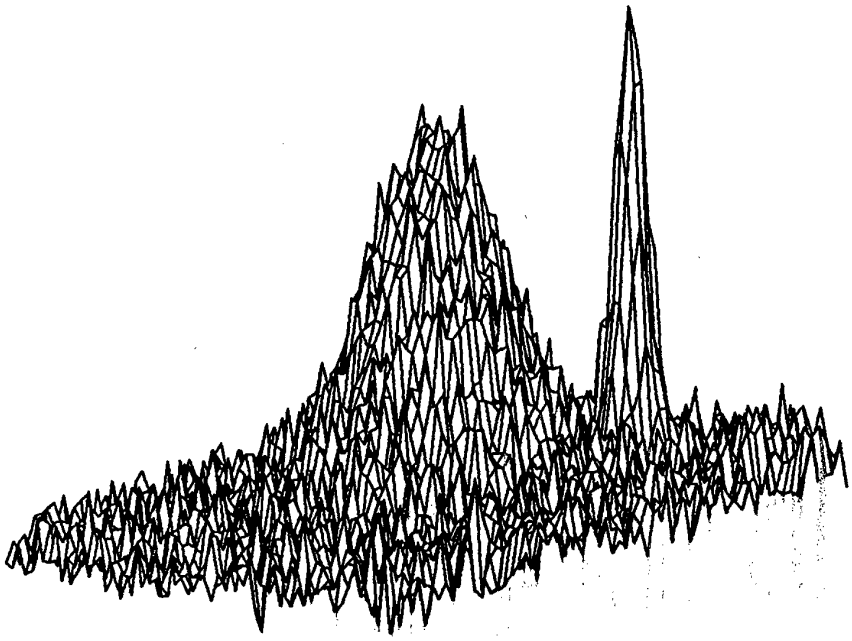

Fig 6.

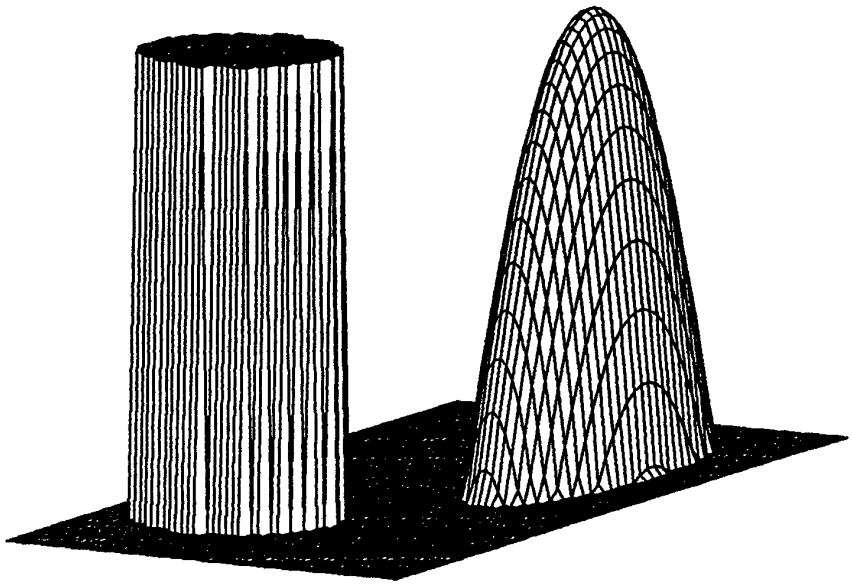

Fig. 7

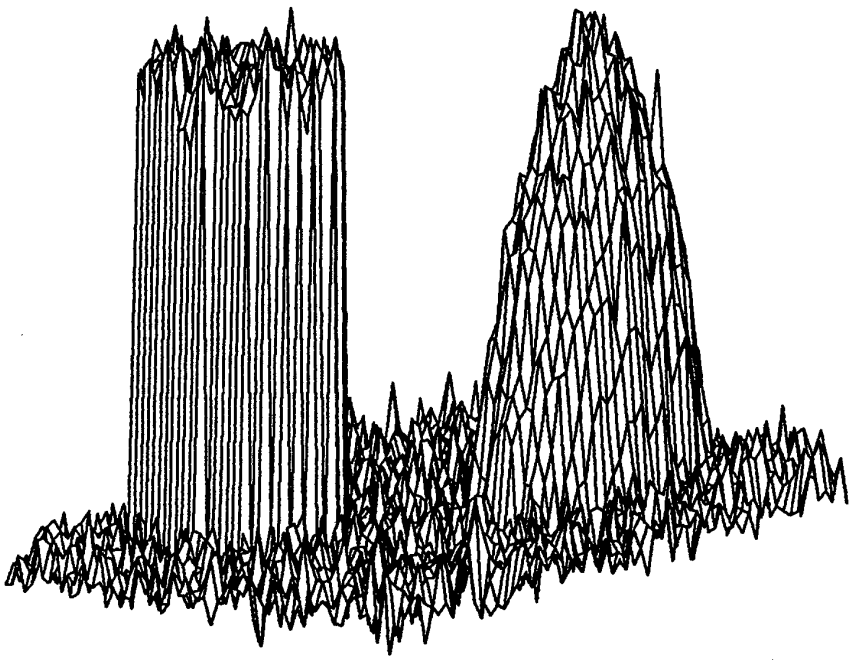

Fig.8

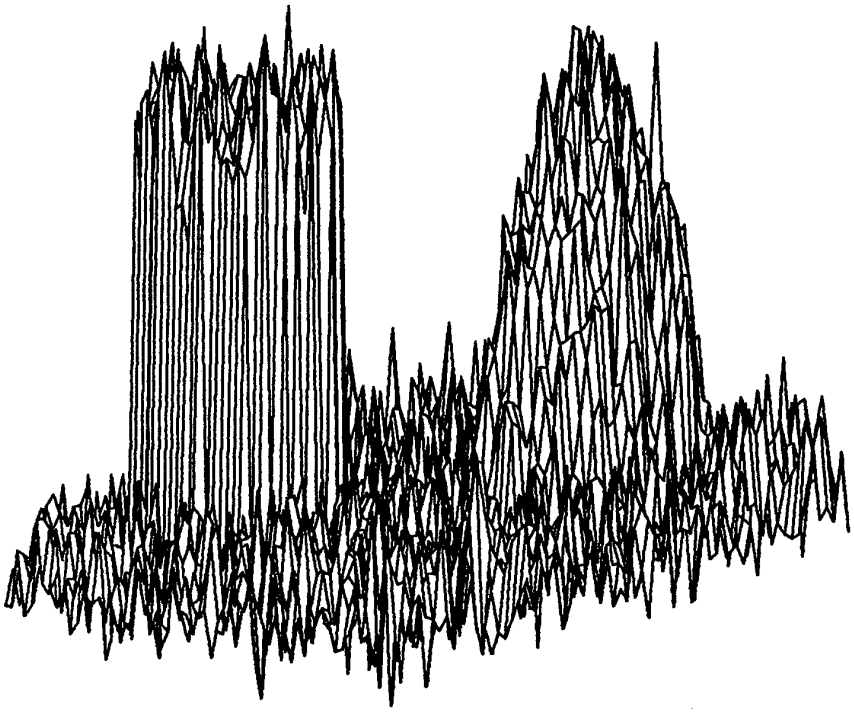

Fig. 9

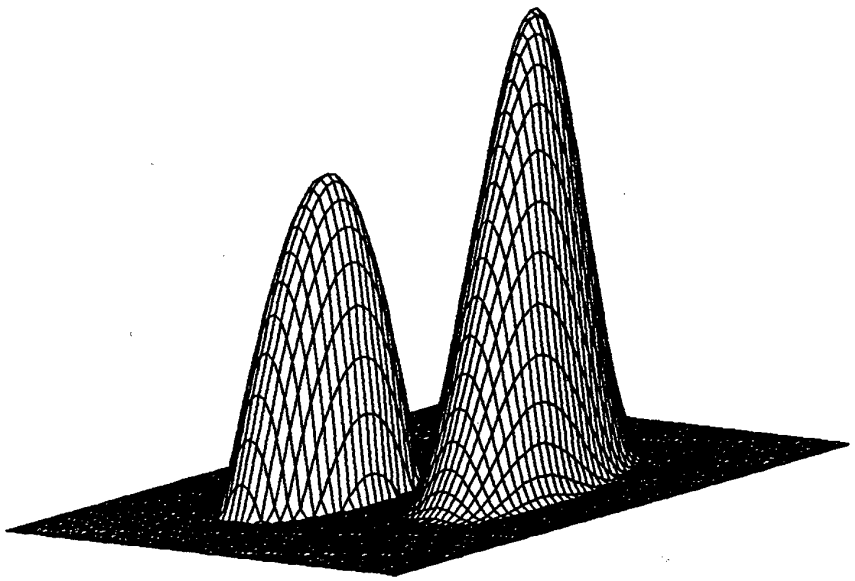

Fig. 10

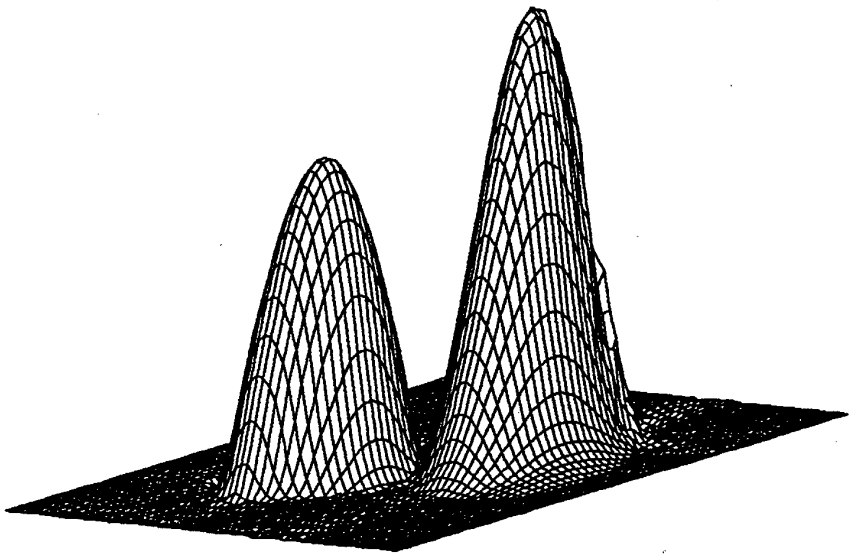

Fig. 11

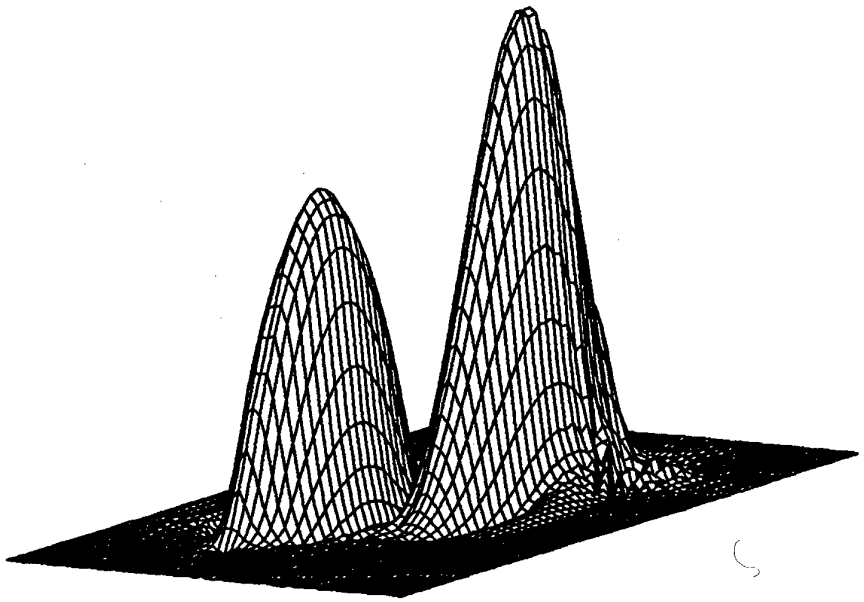

Fig. 12

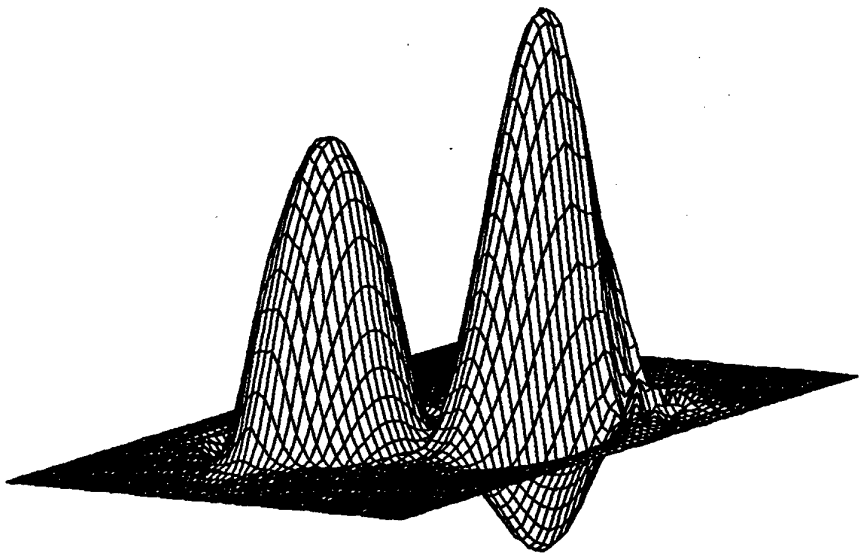

Fig. 13

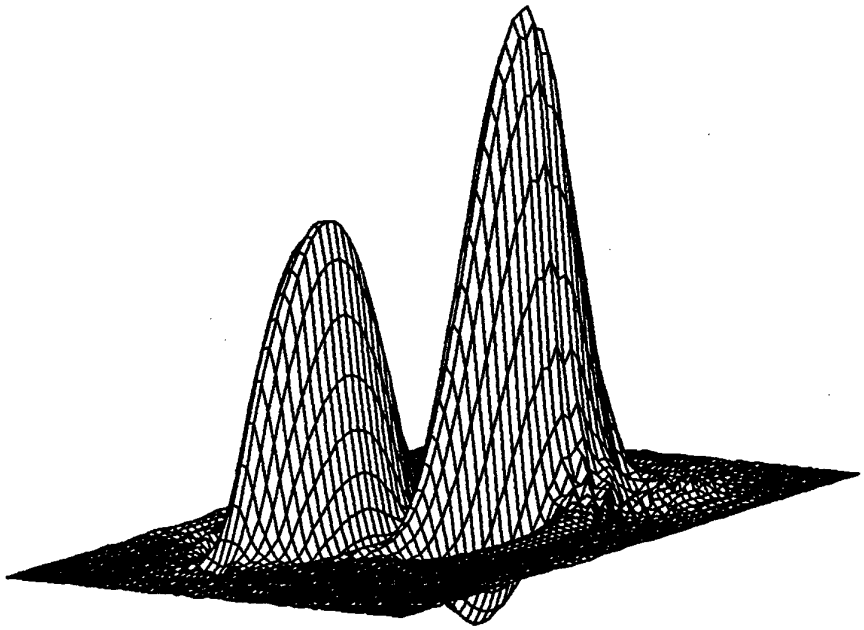

Fig. 14

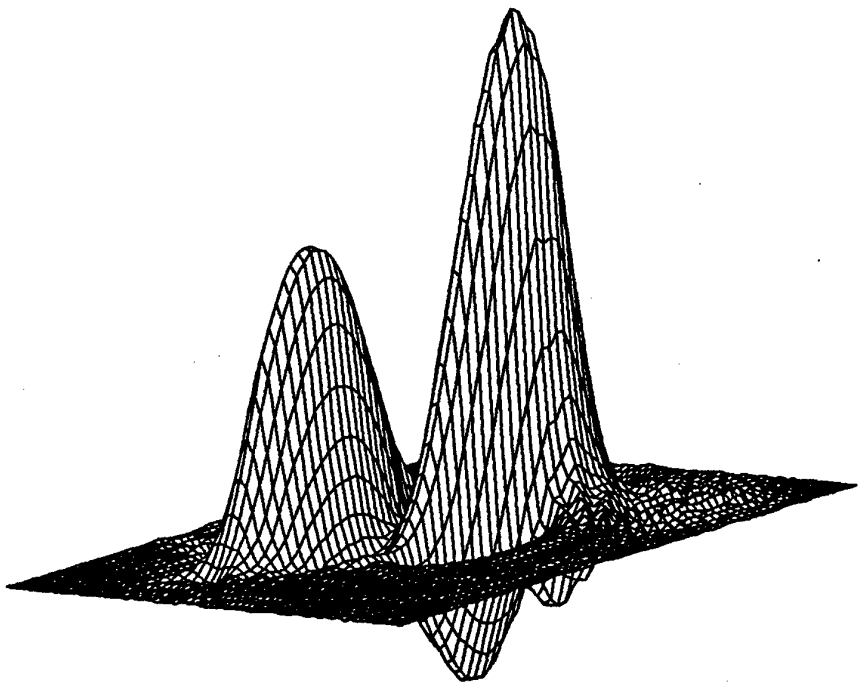

Fig. 15

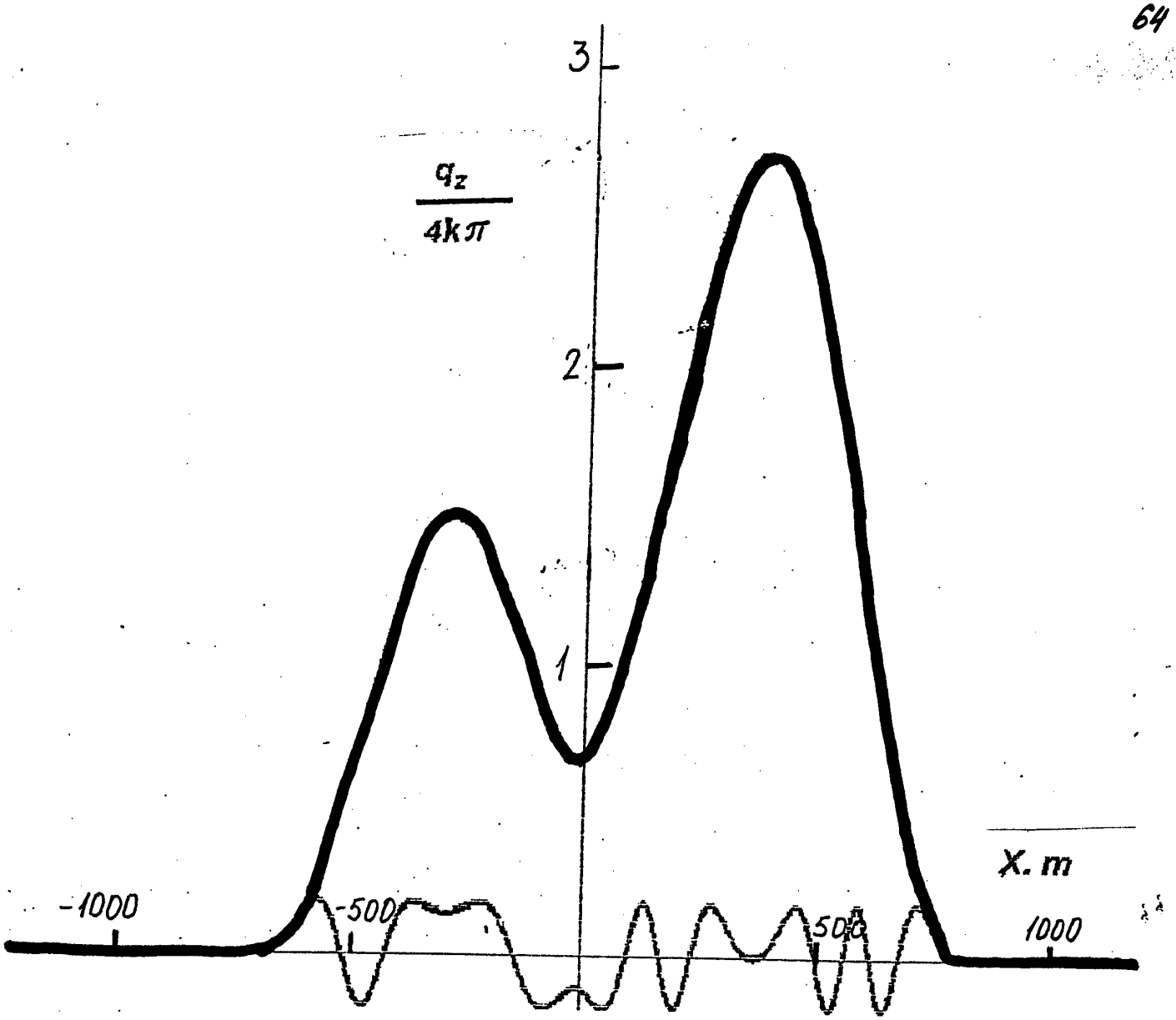

Fig. 16

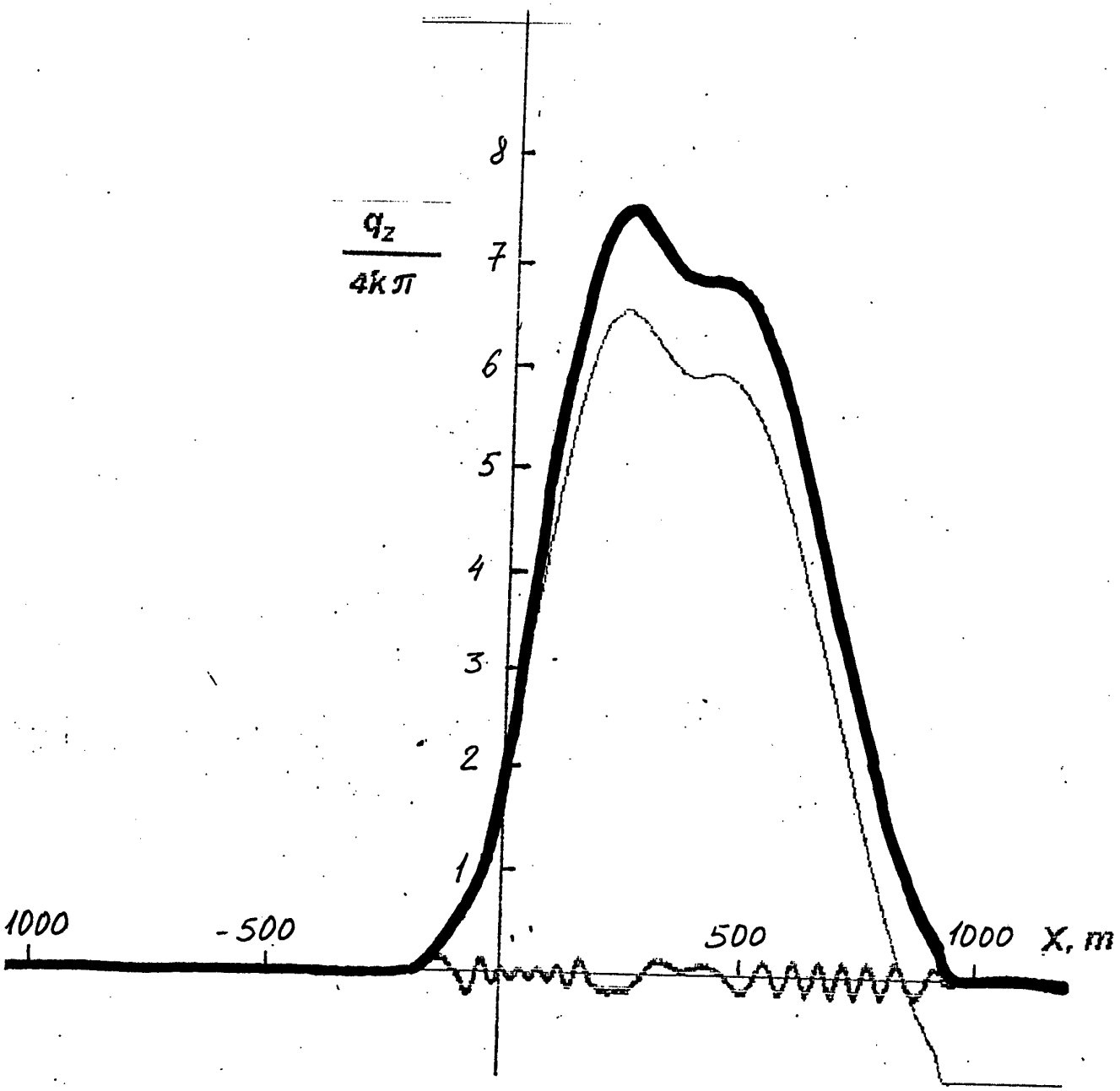

Fig. 17

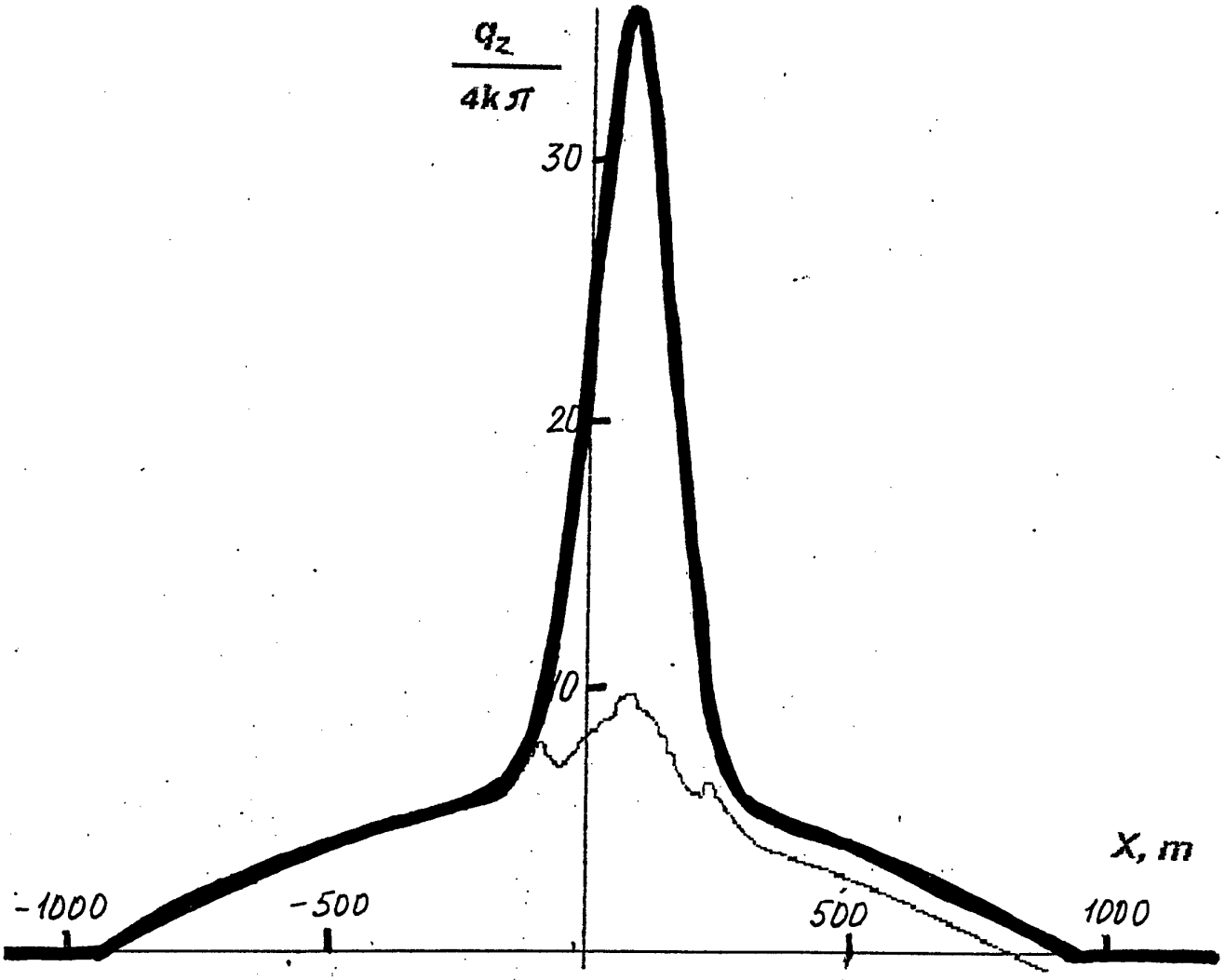

Fig. 18

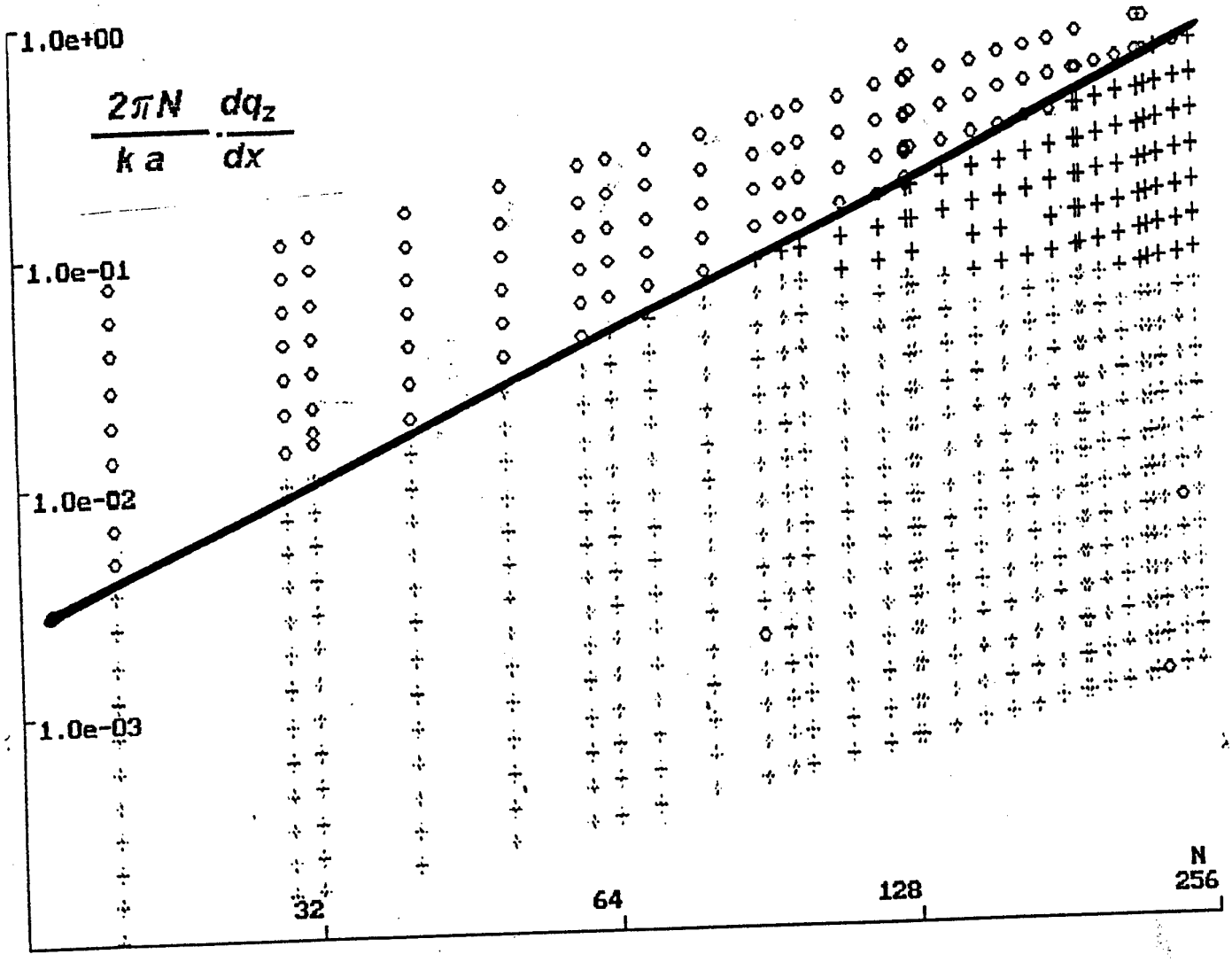
1.0e+00
$\frac{2\pi N}{k a} \cdot \frac{dq_z}{dx}$
1.0e-01
1.0e-02
1.0e-03
32
64
128
N
256

Fig. 19

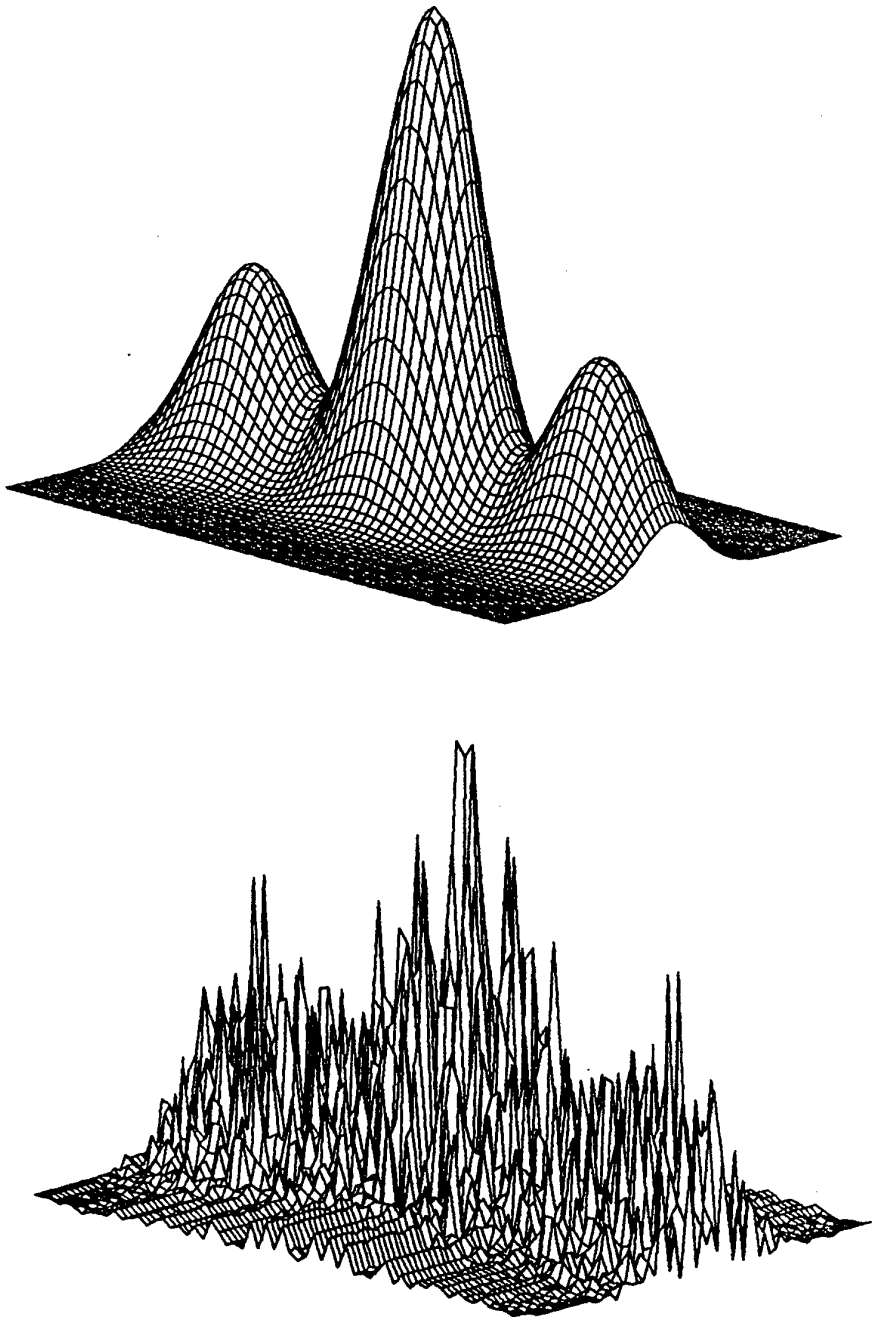

Fig. 20

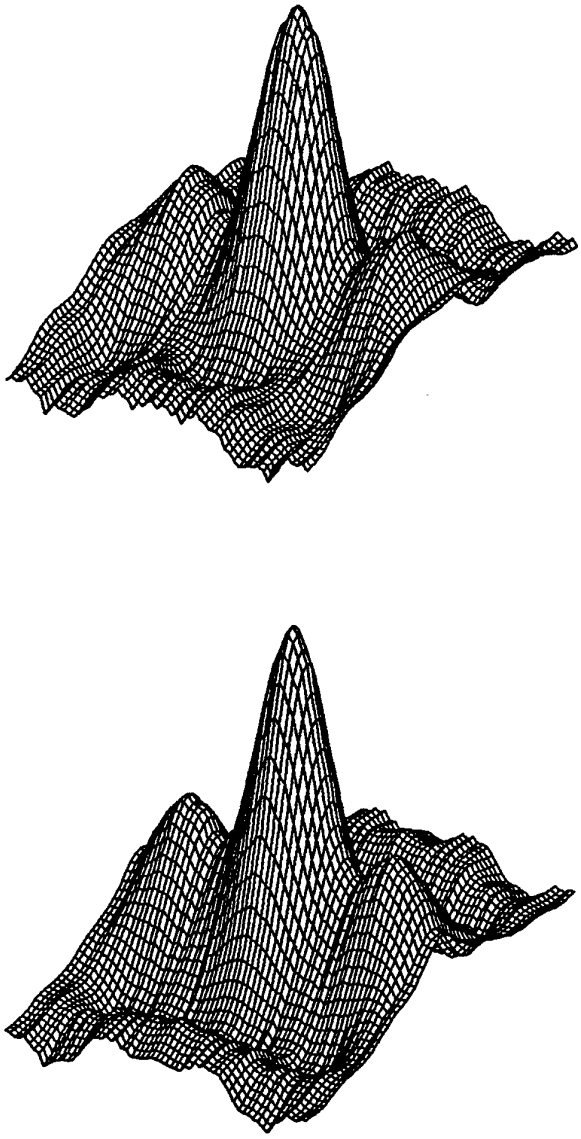

Fig 21

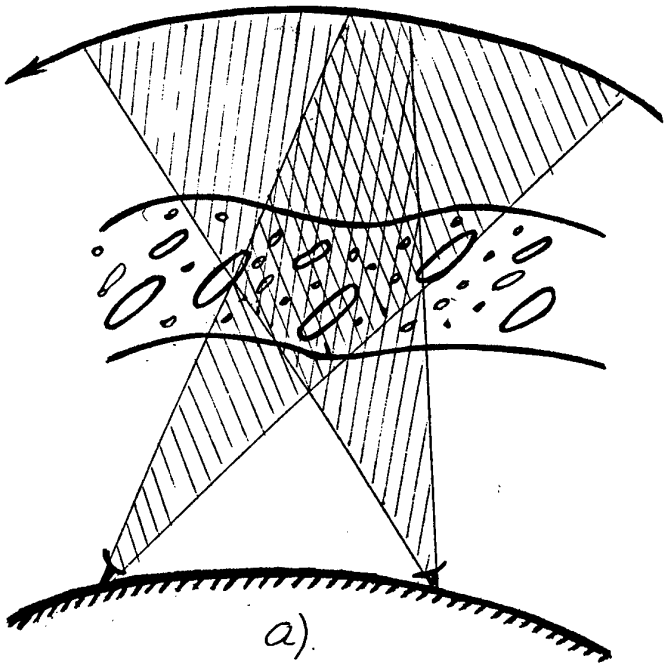

a)

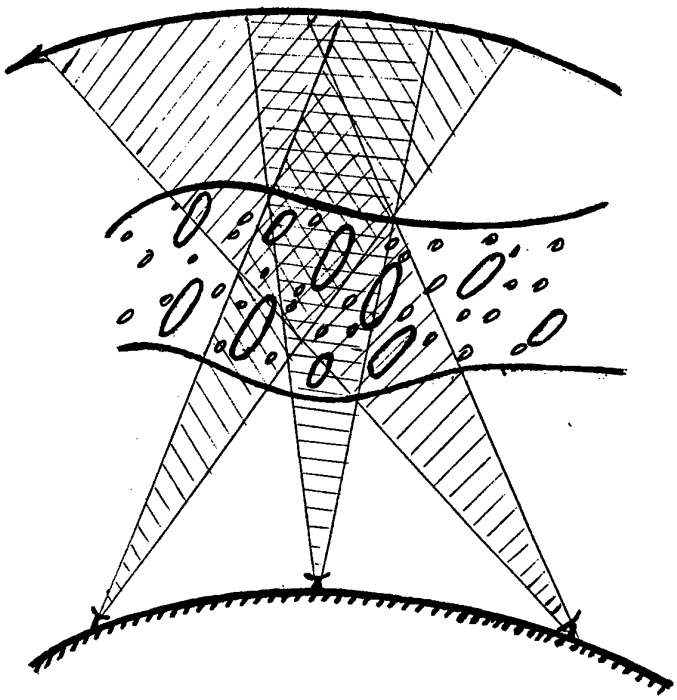

Fig. 22

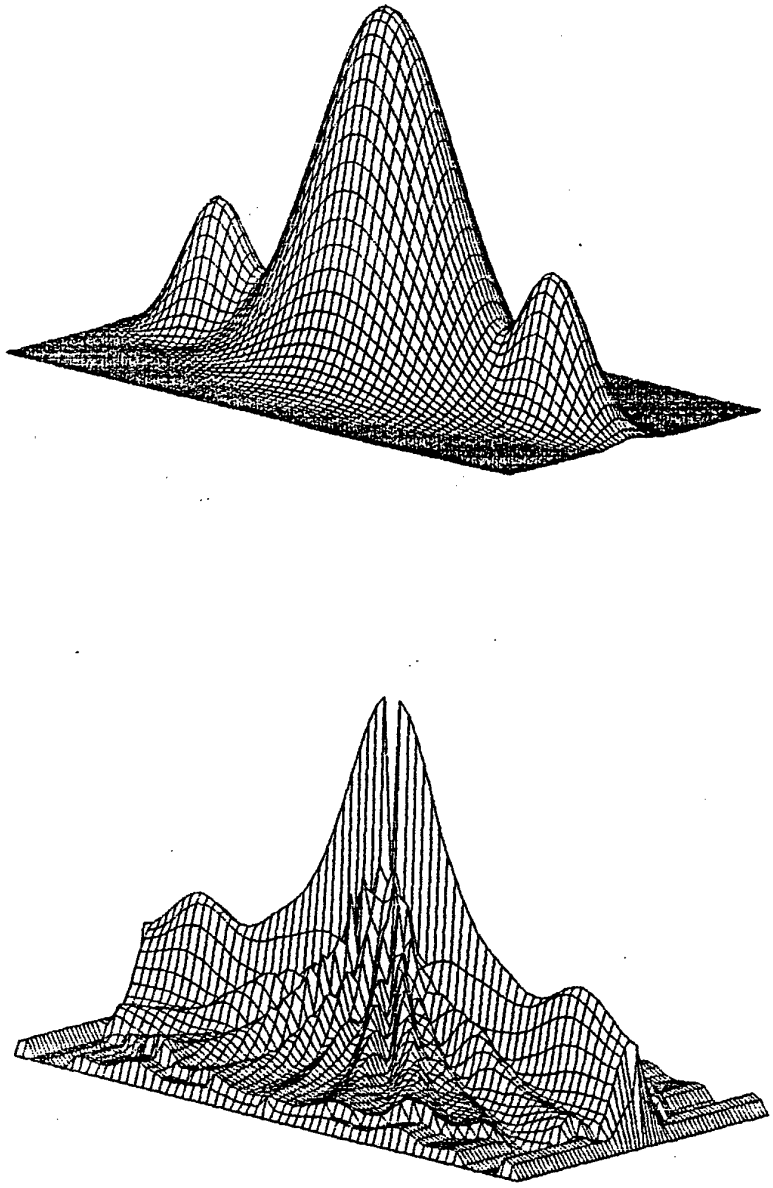

Fig. 23

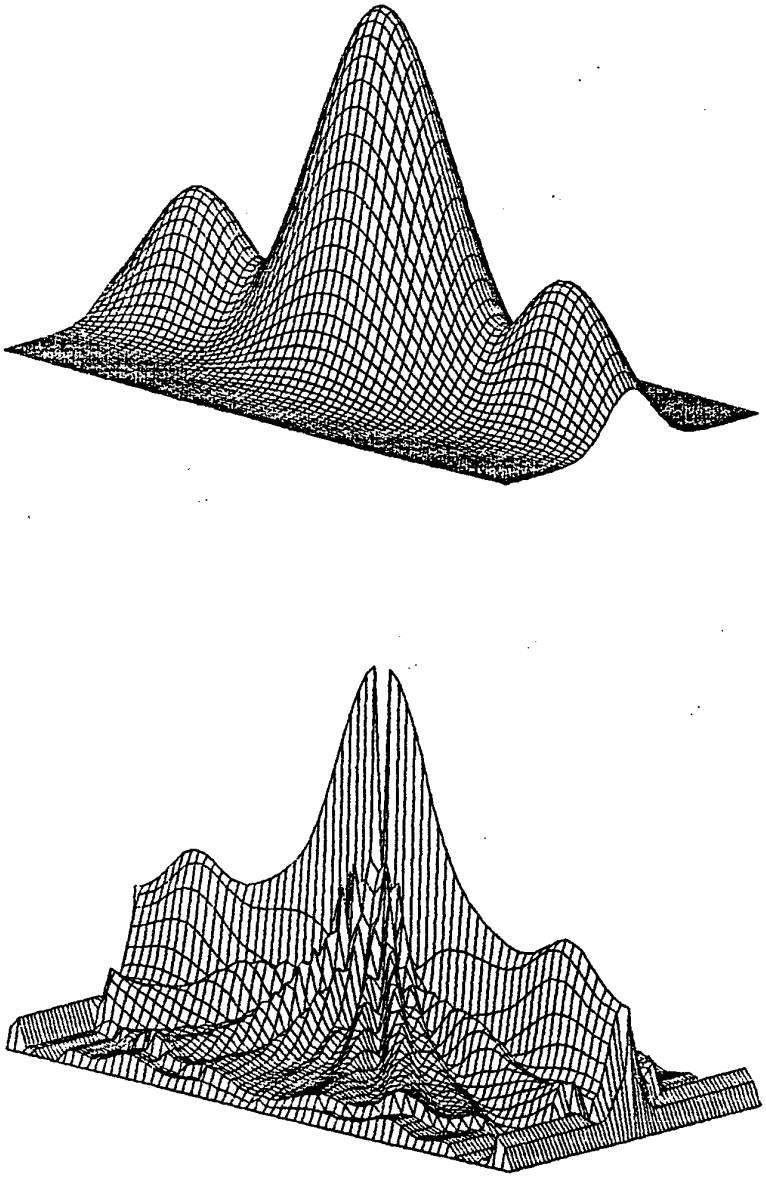

Fig. 24

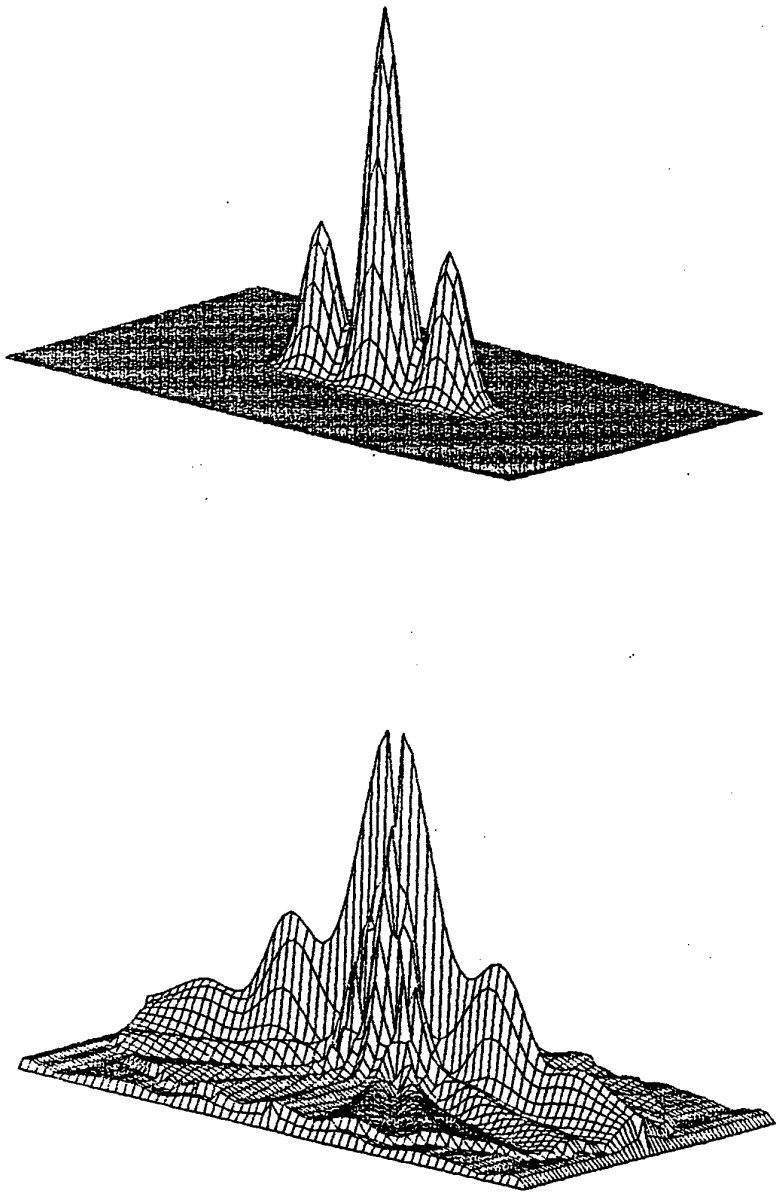

Fig. 25

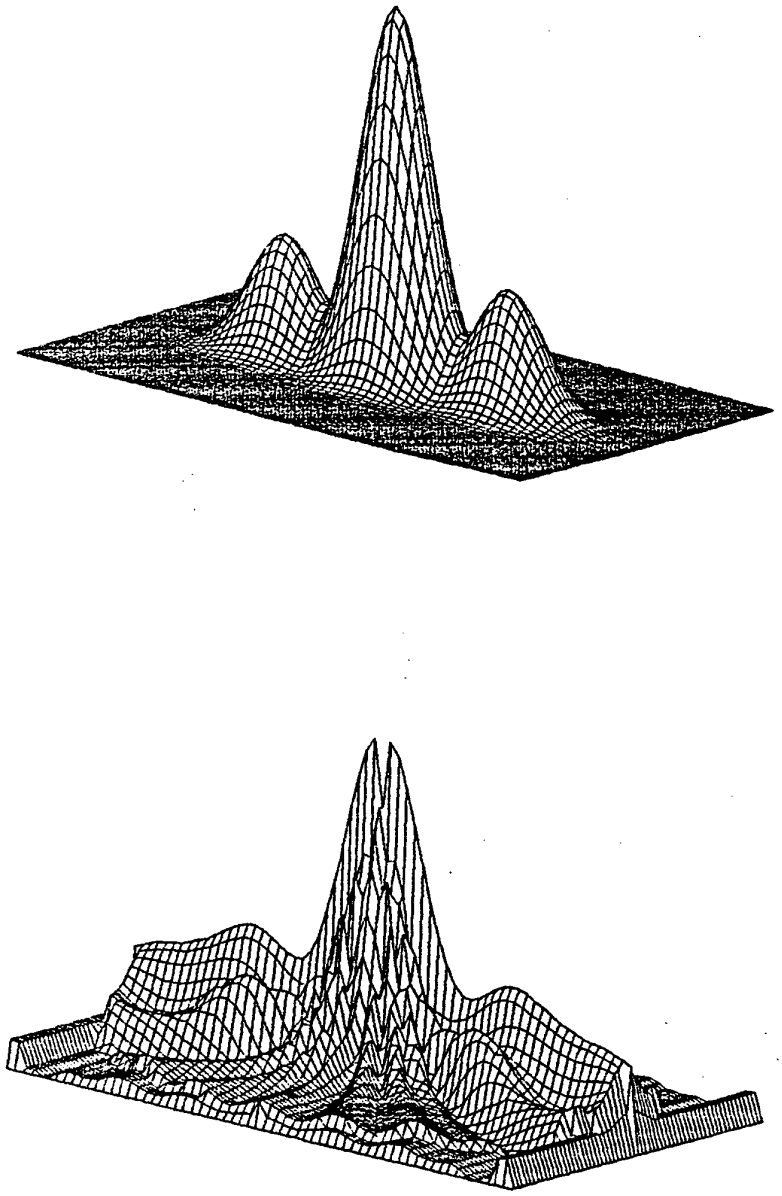

Fig. 26

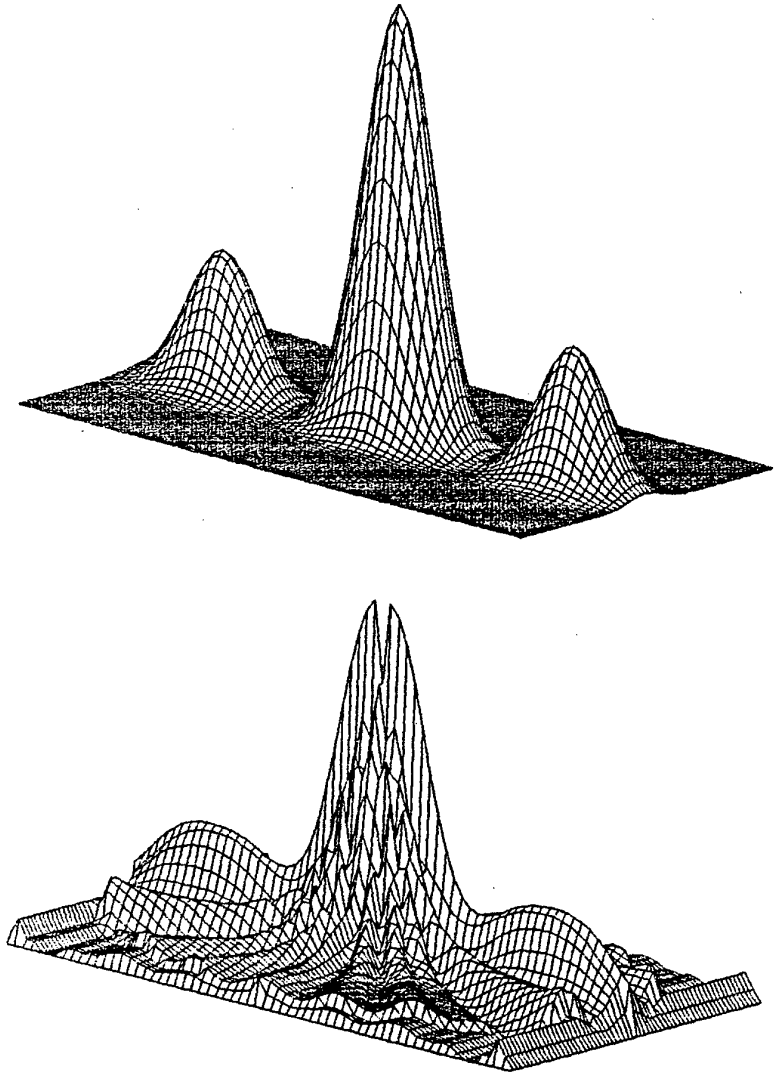

Fig. 27

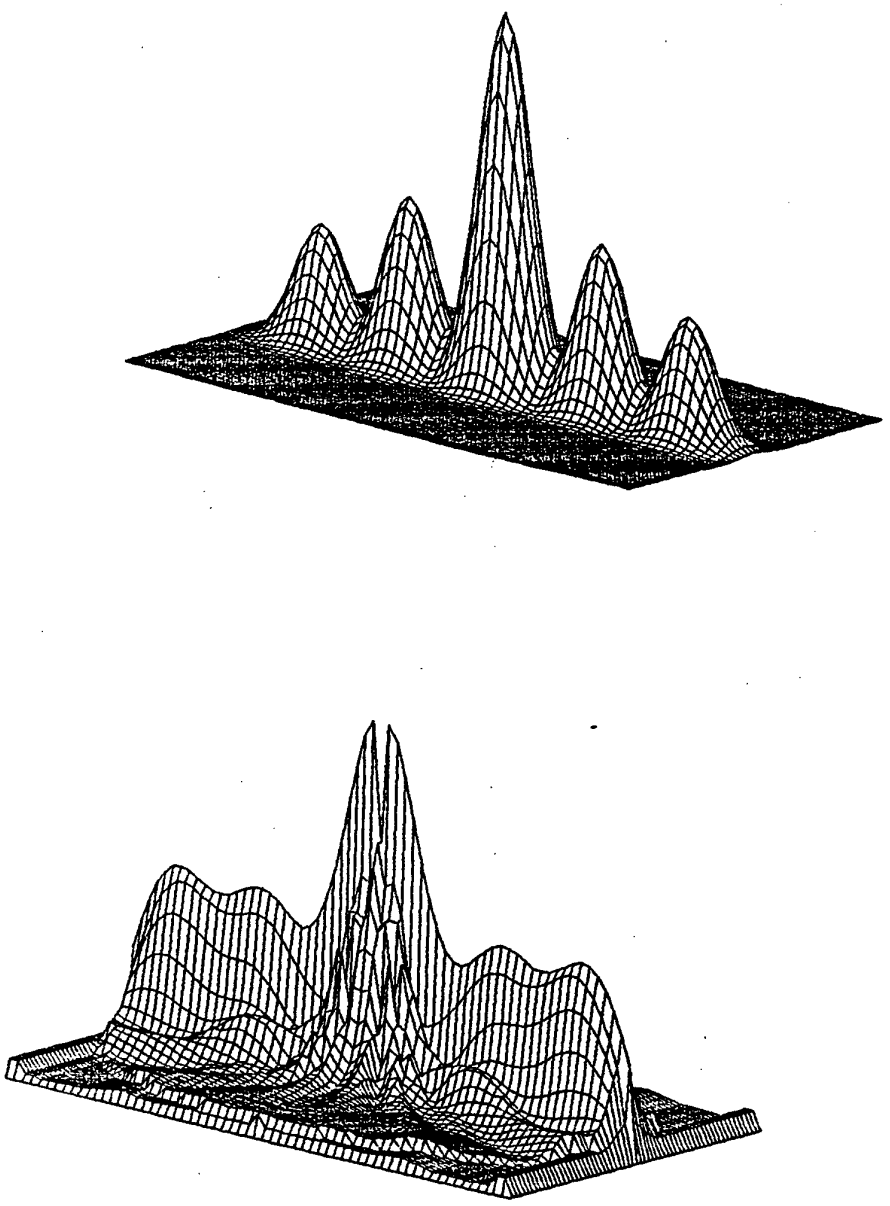

Fig 28

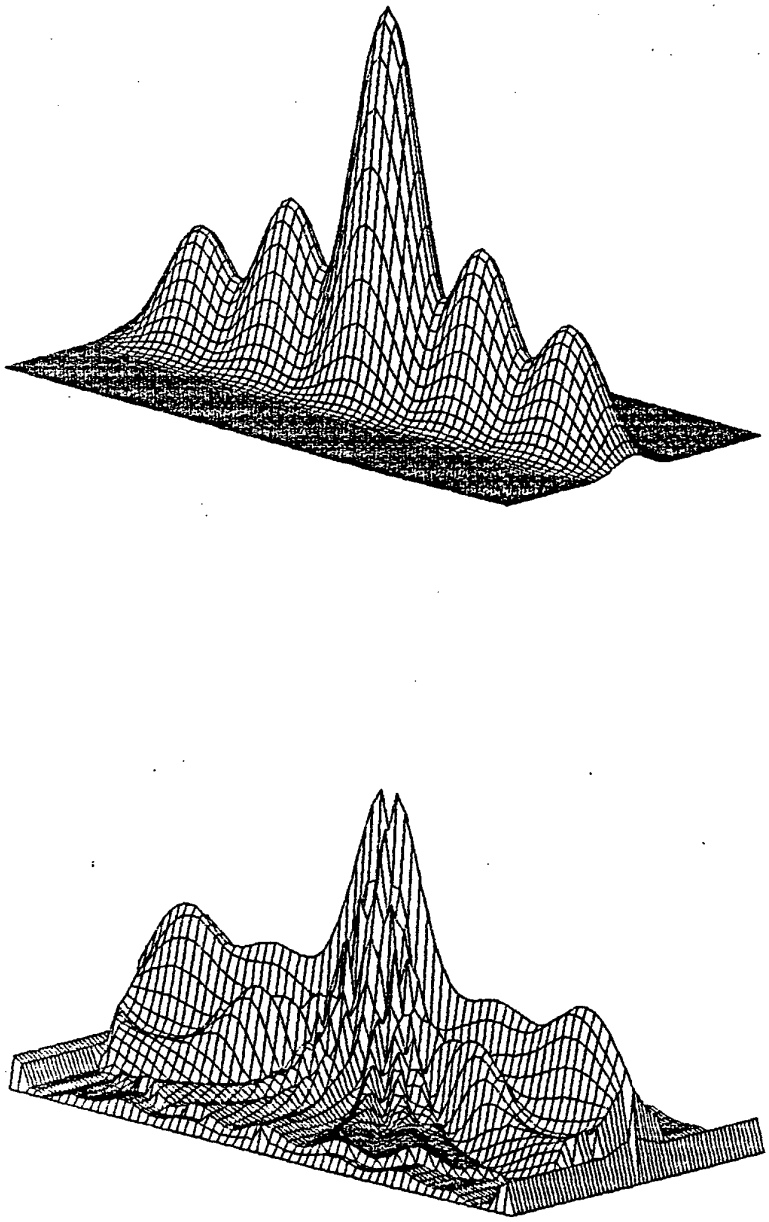

Fig. 29

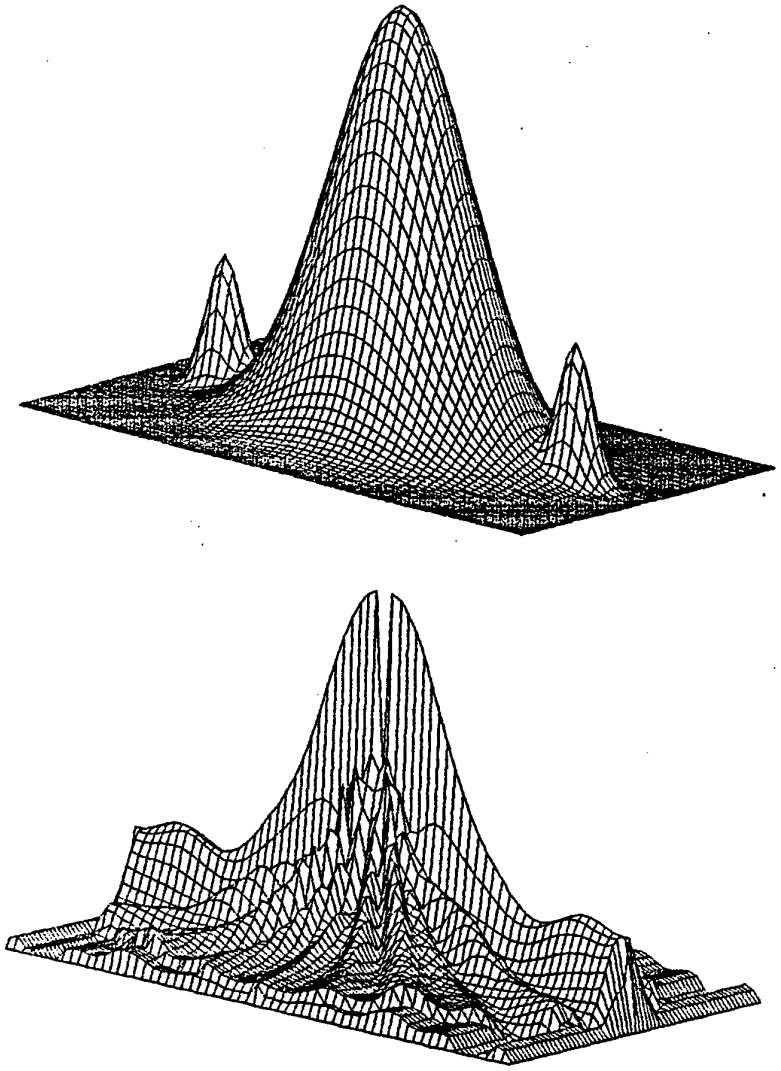

Fig. 30

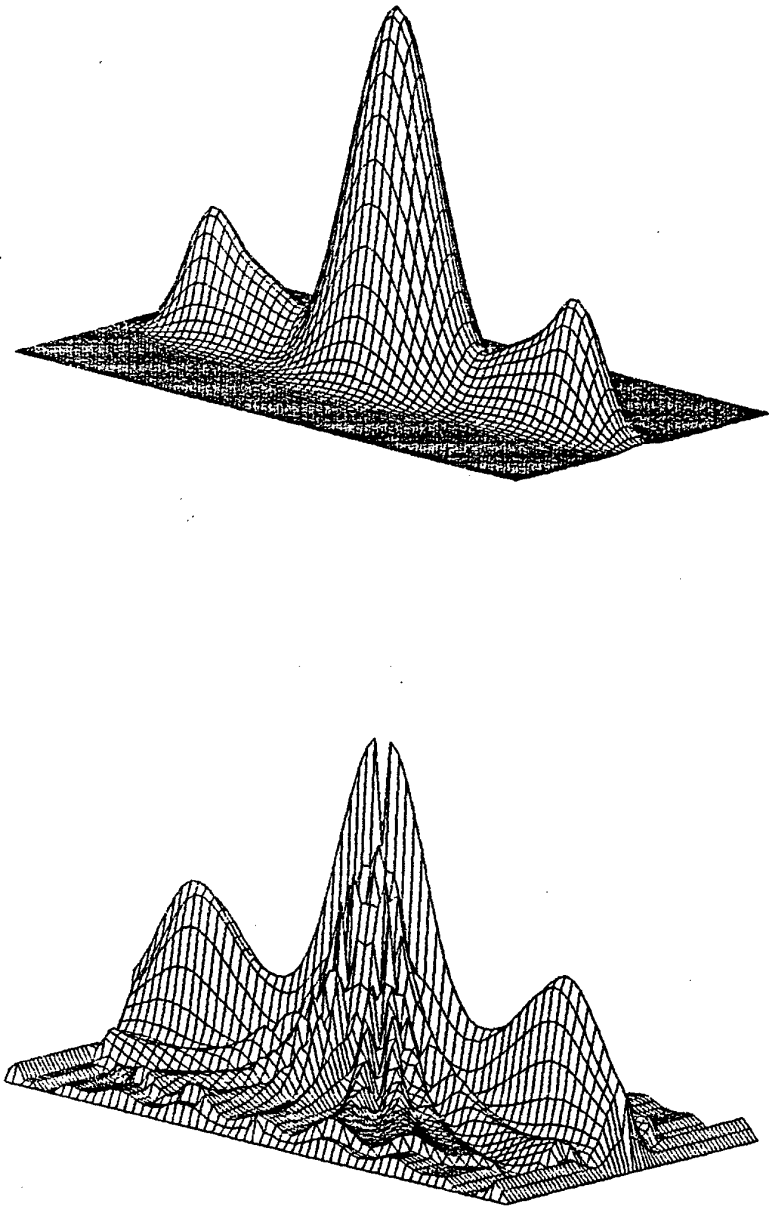

Fig. 31

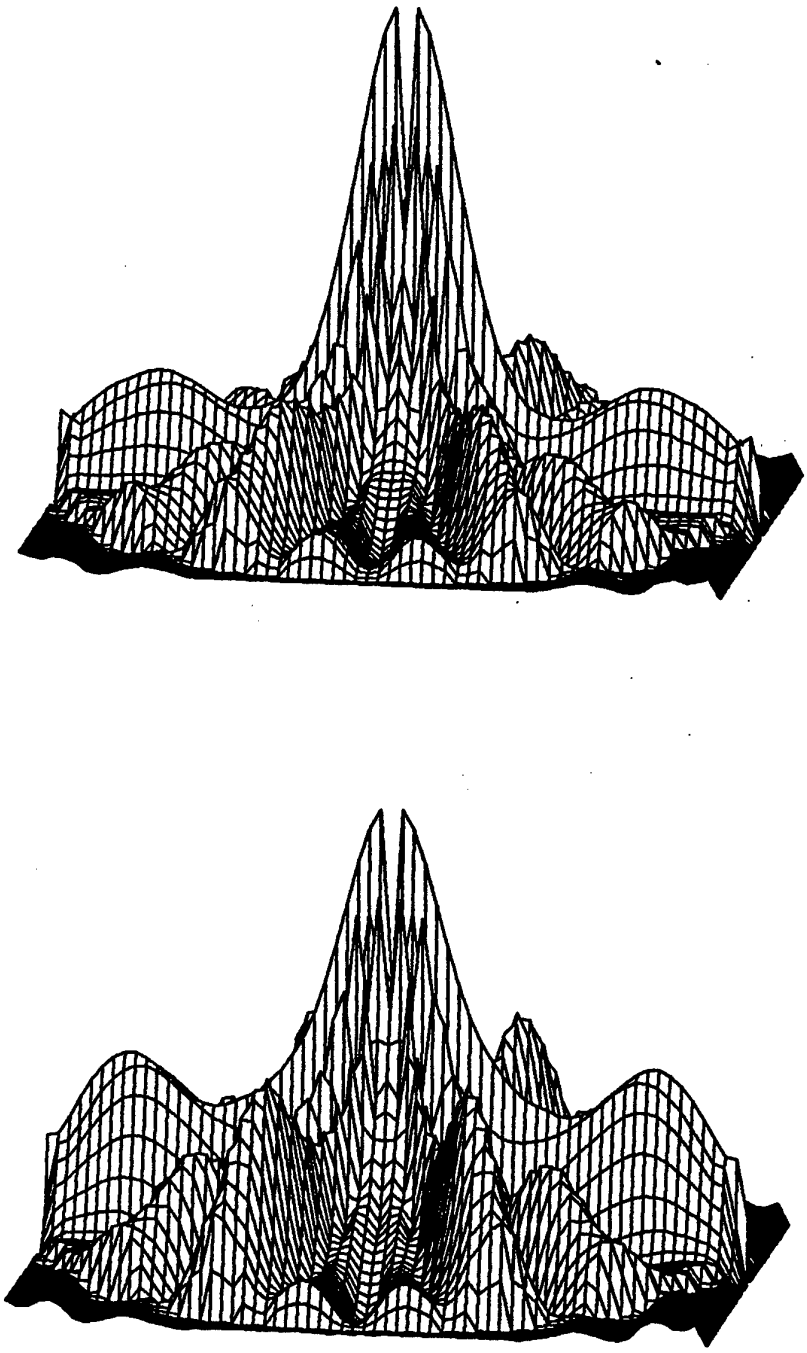

Fig. 32

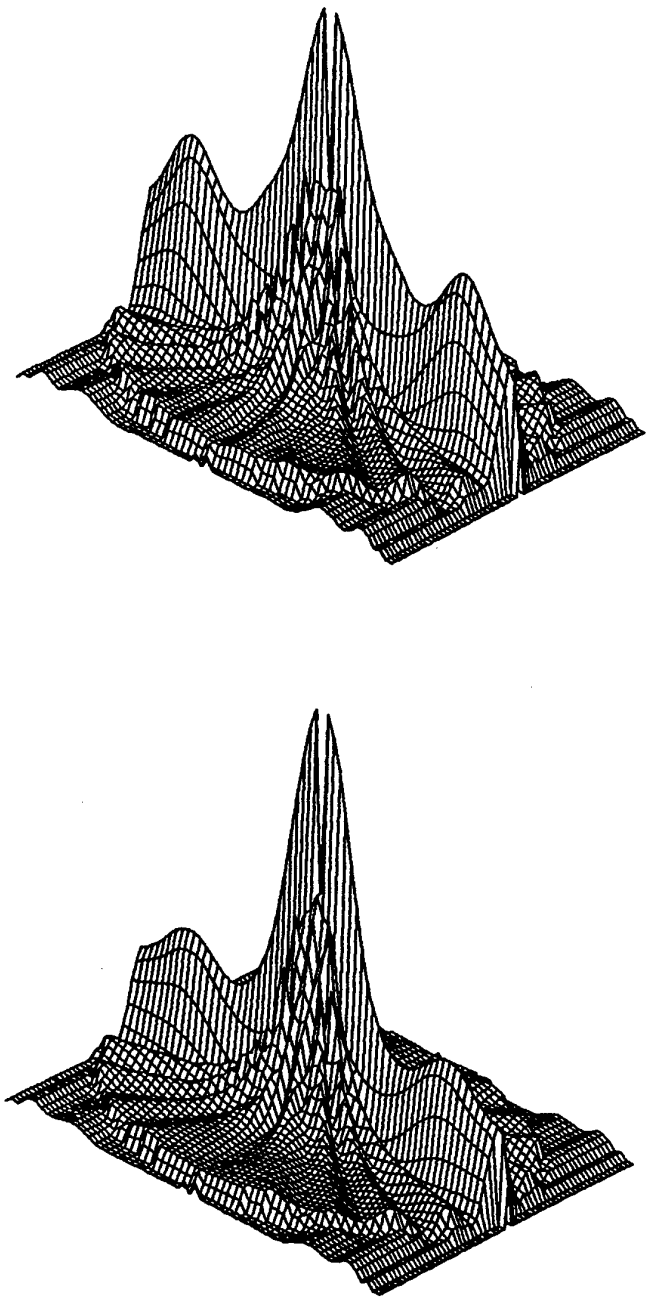

Fig. 33

Development of Algorithms and Programs for the Diffraction and Statistical Radiotomography of the Ionosphere.

Final (12-month) report (EOARD Contract SPC 93-4063)

CONTENT

Principal investigator

Professor V.Kunitsyn

1. Introduction

The aim of this work was to develop efficient algorithms and programs for the solutions of the ionospheric diffraction and statistical radiotomography (RT) problems. The diffraction and statistical RT problems are related with reconstruction of the scattering ionospheric irregularities structure. The use of tomographic methods is perhaps an unavoidable stage in evolution of nearly all diagnostic systems. At a sufficiently high level of development of remote sensing technology and data processing resources, it become possible to reconstruct the spatial structure of a medium on the basis of tomography. Tomographic approaches have already transformed sensing methods in many fields and provided fundamentally new results. The major achievements of tomography in medicine and molecular biology are widely known. Tomographic methods have made it possible to detect previously unknown phenomena in geophysics (seismotomography of the Earth and acoustic tomography of the ocean). At the present stage, radio sounding technology makes it possible to use satellite resources to perform ionospheric sounding in a wide range of different positions of the transmitting and receiving systems and to use tomographic methods. In connection with this, work on RT of the ionosphere has began actively in recent years.

The purpose of this paper is to describe shortly the RT methods [1-8] and program developed for reconstruction ionospheric irregularities structures together with some results of computer simulation. We are dealing with reconstruction of the irregularities of the electron density and of the effective collision frequency by scattered radio waves field. Mathematicians used very often designations the inverse problem (IP) or the

inverse scattering problem (ISP) for such problems of structure reconstruction owing to the scattered field. Here we used the terms IP or ISP and diffraction tomography as synonims. The ionosphere has a rather complex structure; local irregulariries of various scales, including turbulent regions, are present in addition to a quasi-stratified background with large scales. Therefore, problems of satellite RT of the ionosphere should be divided into statistical RT and deterministic RT problems. The latter, in turn, are divided into problems of diffraction RT and ray RT of large structures, where diffraction effects are not significant.

There is no special reason to provide a strict classification of any field of science developing, but certain delimitations and explanations of the terminology must be provided so that we will not later be reproached for "inventing" new terms unnecessarily. In the cases where any projections or "cross sections" of an inhomogeneous object (or a certain transformation of the object, such as Fourier transform) are known from remote sensing data and the problem is to reconstruct the structure of the object, the problem should be considered as a tomographic problem. At present, the mathematical foundation for tomography is related to integral geometry, where it is necessary to reconstruct an object using data on it in the form of integrals with respect to small-dimension manifolds. Therefore, the term tomography is understood not in narrow initial sense, as layer-by-layer study of the structure of the inhomogeneous objects, but ruther in the wider sense, as recording of projections or cross-sections of an object and subsequent reconstruction of the structure of the object from them. The projections of an object are various integrals with respect to small-dimension manifolds. The range of

problems of radio remote sensing of the ionosphere using satellites examined in this paper includes reconstruction of the structure of ionospheric irregularities from files of various tomographic-type data (projections, cross sections), which provides the basis for using the term RT of the ionosphere.

Problems of satellite RT should be divided into deterministic and statistical problems. In the case of a deterministic RT problem, it is necessary to reconstruct the structure of certain large irregularities or a group of irregularities. If a large number of irregularities occupies a certain region in space, it is unadvised to reconstruct the structure of all realizations (generations) of irregularities every moment of time. Here, it makes sense to pose the problem of reconstruction of the characteristics of full ensemble of irregularities, the structure of the statistical characteristics of the irregularities such as the correlation function of the electron density, etc.

We will single out a number of fundamental features of problems of RT of the ionosphere or the IP of reconstruction of the structure of the inhomogeneous ionosphere. The dimensions of the transmitting and receiving systems feasible in practice are much less than the distances from them to the irregularities to be reconstructed, which are hundreds of kilometers, i.e., the aperture angles are small. Since it is extremely difficult and expensive to create transmitting and receiving systems with a large number of receivers, the necessity for aperture synthesis in one coordinate becomes clear. Synthesis apertures can be realized, for example, using a moving transmitter on a satellite. We will emphase that satellite radio sounding makes it possible in practice to obtain files of various tomographic data and to actually realize RT of the inhomogeneous ionosphere. In view of

the small aperture angles, it is advisable to pose the problem of reconstruction of the structure of irregularities with dimensions singficantly exceeding the wavelength. Therefore, the IP of reconstruction of the structure of scatterers which are large in compasion with the wavelength will be examined here, but the dimensions of the irregularities may be both greater than or less than Fresnel zone, and diffraction effects must be considered in a number of cases.

2. Physical and mathematical formulation of the radio tomographic sounding problem.

Radio wave propagation in near-earth space and scattering in plasma irregularities in the ionosphere are discribed by a system of Maxwell equations with the corresponding material equations [9]. In the general case, the dielectric permittivity of the plasma is a tensor value due to spatial dispersion, even in the absence of a magnetic field. However, the spatial dispersion can be disregarded for ionospheric irregularities of both natural and artificial origin, since the thermal velocities of the electrons in the plasma are significantly less then than the speed of light, i.e., the approximation of a "cold" plasma is valid. Likewise, the velocities of diffusion, mixing and other transport processes, as well as the velocity of the transmitting and receiving systems, does not exceed 10 km/s ($v/c < 3 \cdot 10^{-4}$), therefore , the quasistationary approximation is valid; within the framework of it, the "slow" time dependence of the characteristics of the medium and fields can be considered as a dependence on the parameter.

In place of the equations for the field $\vec{\mathcal{E}}(\vec{r},t)$ of a radio wave, it is convenient to use equations for the complex amplitudes $\vec{E}$ of the corresponding monochromatic components, i.e., it is advisable to introduce

$$\vec{\mathcal{E}}(\vec{r},t) = \vec{E}(\vec{r},t)e^{-i\omega t} + \vec{E}^*(\vec{r},t)e^{i\omega t}.$$

For brevity, the complex amplitudes $\vec{E}(\vec{r},t)$ with a "slow" time will be called the field hereafter. Subject to the observations made above, within the framework of the quasistationary approximation and a "cold" plasma, from the Maxwell equations we have the equation for the field

$$\Delta\vec{E} + \frac{\omega^2}{c^2}\hat{\varepsilon}\vec{E} - \text{grad div}\,\vec{E} = 0, \qquad (1)$$

where $\hat{\varepsilon}$ is the complex dielectric permittivity tensor, $f = \omega/2\pi$ is the frequency. Analysis of radio wave propagation in an inhomogeneous magnetoactive plasma with a tensor dependence of $\hat{\varepsilon}$ is a difficult problem. There are no algorithms for calculating the parameters of radio signals and the characteristics of the scattered fields in the general case of an arbitrary dependense of $\hat{\varepsilon}(\vec{r})$ on the coordinates. Therefore, the statement of the ISP of reconstruction of the structure of the tensor characterizing an ionospheric irregularity using data on the measured field is unrealistic at present, and hardly advisable in general. The non-diagonal elements of the tensor can be disregarded at high frequencies, since they do not exceed the square of the ratio of the plasma frequency f_N to the sounding frequency, i.e., $\sim (f_N/f)^2(f_H/f)$ (f_H is the gyrofrequency) [9]. For example, the typical maximum concentration in the ionosphere is $N_0 \sim 10^6$ cm^{-3}. For it and where $f > 50$ Mhz, $(f_N/f)^2(f_H/f) \leqslant 0{,}001$. Likewise, the

last, "depolarization" term of equation (1), the order of which is determined by the ratio of the emission wavelength to the characteristic scale of variation of the concentration, can also be disregarded at high frequencies.

Thus, in the case of high sounding frequencies vector equation (1) decomposes into three scalar equations, and it is sufficient to examine the equation for one field component

$$\Delta E + k^2\hat{\varepsilon}(\vec{r},k)\, E = 0, \qquad (2)$$

where $\varepsilon(\vec{r},\omega) = 1 - \dfrac{4\pi r_e N(\vec{r})}{k^2(1 + i\nu(\vec{r})/\omega)}$, $k = 2\pi f/c = \omega/c$ is the wave number, r_e is the classical electron radius, $\nu(\vec{r})$ is effective collision frequency, $N(\vec{r})$ is the electron concentration; "ion" contribution to the dielectric permittivity can be disregarded [3]. The relation for ε has the same form in both the International System of Units (SI) and CGS system; only the expression for r_e changes.

Then, it will be convinient to introduce the complex function $q(\vec{r},\omega) = k^2(1-\varepsilon) = 4\pi r_e N(\vec{r})/(1 + i\nu(\vec{r})/\omega)$ and divide it into two parts: $q \to q_0(z,\omega) + q(\vec{r},\omega)$, one of which corresponds to the regular stratified ionosphere with the dependencies $N_0(z)$ and $\nu_0(z)$, and the other of which is related to the three-dimension (3D) irregularities on the background of the stratified medium $N(\vec{r})$ and $\nu(\vec{r})$. The specific and concrete form of relations for $\nu_0(z)$ and $\nu(\vec{r})$ depends on the specifics of the problem [1]. By reconstructing the structure of the complex function $q(\vec{r},\omega)$, it is also possible to reconstruct the structure of these 3D disturbances with known information on the regular large scale ionosphere. Therefore we will deal with the two problems: first, the problem of reconstruction of the regular large scale

ionosphere $q_0(z,\omega)$ - ray RT problem; second, the problem of reconstruction the 2D or 3D irregularities structure - diffractional and (or) statistical RT problem. The introduction of q is also justified by the fact that the quantity $q \sim (1 - \varepsilon)$ applies to the generalized susceptibilities [10] characterizing the response of the medium to the field. Furthermore, the scalar Helmholtz eguation assumes the form of stationary Schrodinger equation, where q is the complex potential:

$$\Delta E + k^2 E - q_0(z,\omega)E - q(\vec{r},\omega)E = \delta(\vec{r} - \vec{r}_0) \qquad (3)$$

The delta function in the right side of (3) corresponds to the point sounding source in the majority of satellite radio sounding experiments, since the wave can be assumed to be spherical within the major lobe of the directional pattern of an arbitrary source. The dimensional constant A_0 in front of the δ-function in equation (3) is omitted so that it need not be rewritten in all subsequent formulas. The constant is expressed by means of the total power of a point source [1]. Here, A_0 corresponds to the amplitude value of the field of a point source, i.e.,

$$E_0(\vec{r}) = - A_0 \exp(ikr)/(4\pi r).$$

Hereafter, we can always return to the dimensional field $E \to A_0 E$ when necessary.

The ISP for equation (3) can be formulated in the following manner: it is necessary to reconstruct the structure of the irregularities from measurements of the field in a certain limited region of a fixed surface in a limited range of frequencies and positions of the sounding source. Knowledge of the complex function $q(\vec{r},\omega)$ makes it possible to reconstruct the structure of both $N(\vec{r})$ and $\nu(\vec{r})$. Here $q(\vec{r},\omega)$ is a finite function, since the

irregularities of $N(\vec{r})$ are confined in space. The regular stratified ionosphere is assumed to be known here, i.e., the IP of reconstruction of the regular ionosphere is solved by other, sufficiently well-developed methods, or its influence can be disregarded, for example, as in the UHF/VHF waveband.

The sheme of the experiments on diffraction and statistical RT is presented in Fig.1. The satellite, with a transmitter on board moves at altitude $z = z_0$; the receiving system is located in the plane $z = z_R$ (on the ground). The receiving system can be a transverse array of receivers for diffraction RT or statistical RT (or a collection of transverse arrays). Receivers of array arranged along (the y-axis) a line transverse to the satellite path (the x-axis), arrays being separated by distances of hundreds of kilometers. The scatterer (a group of irregularities) is located near the altitude $z = z_s$.

3. The solution of the diffraction radiotomography problem (inverse scattering problem).

Rigorous results of solution of IP (3) for the complex potential do not exist. We will emphasize that in the case of propagation of waves of various nature in the actual physical media the complex nature of the potential q has a fundamental character and the corresponding dispersion relations relating the real and imaginary parts of the potential can be derived [10]. The fundamental results on solution of the 3D inverse problem for the Schrodinger equation with the real potential $q(\vec{r})$ not depend on the frequency (where $q_0(\vec{r},\omega) = 0$) obtained in [11,12] should be noted here. As to the complex nature of the potentials, there no rigorous results for the 1D IP, i.e the extension of the familiar Gelfand-Levitan-Marchenko algorithm to this case is unknown, even more so for a arbitrary dependence of the potential from the energy (frequency ω) [13].

Approximate approaches to solution of the 3D ISP are therefore of undoubted interest. The approximate approach to solution of inverse RT problem is justified by the properties of the regular ionosphere, the typical scales of essential disturbances of which significantly exceed the radio sounding wavelength. Therefore, the geometrical optics approximation is applicable to description of wave propagation on the background of the regular ionosphere. The scattering in weak irregularities is described within the framework of such familiar approximations as the Born approximation and Rytov approximation (BA and RA). More specialized methods have been used to calculate the scattering in strong-scattering irregularities.

There are many papers connected with the approximate

approaches to ISP [14-18]. The scattering by weak irregularities was described within the BA and RA. The iterative methods were used for strong-scattering irregularities. But there are some specific features of the ionosphere problems, namely: the size of irregularities is very big (it can exceed the probing wavelength in 10^3- 10^4 times), the ionosphere irregularities can be either weak-scattering or strong-scattering. It is very difficult to use iterative methods for big size strong-scattering irregularities directly. However it is sufficient to use the small-angle approximation according to the big size of irregularities or their detailes. In what follows we consider the methods of ISP solutions only, based on the asymptotic approximation for the forward small-angle scattering. It should be noted it is particularly interesting for tomographic methods to consider such cases of small-angle scattering, when a wavelength of sounding radiation is much less compared with the scales of object specific detailes. This is necessary condition to reconstruct the complicated internal structure of the object.

In the beginning it is useful to consider the ISP in the high-frequency limit i.e. the source field freguency is essentially higher than the critical frequency of the regular ionosphere. In this case the refraction index is close to unity, and the influence of the regular ionosphere may be neglected. Then, instead of (1), the following equation should be used:

$$\Delta E + k^2 E - q(\vec{r},\omega)E = \delta(\vec{r}-\vec{r}_0) \qquad (4)$$

This differential equation is equivalent to the Lippmann-Schwinger integral equation

$$E(\vec{r}) = E_0(\vec{r}) + \int G(\vec{r}-\vec{r}')\, E(\vec{r}')\, q(\vec{r}',\omega)\, d^3r' \qquad (5)$$

where $G(r)=-(4\pi r)^{-1}\exp(ikr)$ is the Green's function for a vacuum and $E_0(\vec{r})=G(\vec{r}-\vec{r}_0)$ is the source field.

It is necessary to bear in mind that the potential q depends on N and ν as follows (the usual condition for ionospheric radioprobing $\nu \ll \omega$ is taken into account) [1]

$$q = 4\pi r_e N(\vec{r})/(1 + i\nu(\vec{r})/\omega) \simeq 4\pi r_e N(\vec{r})(1 - i\nu(\vec{r})/\omega) \qquad (6)$$

For the case of small-angle scattering the transmitter, a scattering object and the receiver are situated along a straight line approximately. Assuming that the direction of this straight line is closed to the direction of z-axis one can obtain an approximate equation, describing the forward small-angle scattering, instead of (5) [1,7]

$$U(\vec{r}) = 1 + \int F(\vec{r},\vec{r}')\, U(\vec{r}')\, q(\vec{r}',\omega)\, d^3r' \equiv 1 + \hat{F}Uq \qquad (7)$$

Here $U=E/E_0$ is the normalized field. Under the derivation (7) the Fresnel's approximation was used for the Green function G either as for the sounding wave field. After some transformations we come from (5) to the formula (7), where the kernel F of the equation (7) contains coordinates of the transmitter z_0, the finite scatterer z_s and the receiver z_R

$$F(\vec{r},\vec{r}') = -\frac{1}{4\pi\zeta}\exp\left(i\frac{k}{2\zeta}(\vec{\rho}' - \vec{s})^2\right), \qquad (8)$$

$$\vec{s} = \vec{\rho}_R(z_0 - z_s)/(z_0 - z_R) + \vec{\rho}_0(z_s - z_R)/(z_0 - z_R),$$

$$\zeta = (z_0 - z_s)(z_s - z_R)/(z_0 - z_R).$$

In general case the formulae for s and ζ have to include the integration variable z' instead of z_s. But if the object scale is less than longitudinal Fresnel resolution the varriable z' can be

changed on the constant z_s.

There is another form of the equation (7), using the complex phase $\Phi = \ln E$, $\Phi - \Phi_0 = \ln U$

$$\Phi - \Phi_0 = \ln (1 + \hat{F}q \exp(\Phi - \Phi_0)) \qquad (9)$$

which includes the RA (the first iteration of the non-linear equation (9))

$$\Phi - \Phi_0 = \ln (1 + \hat{F}q) \simeq \hat{F}q \quad \text{or} \quad U = \exp(\hat{F}q) \qquad (10)$$

Taking into account (7,10) and making use of the Fresnel's transformation we have the algorithm for reconstruction of 2D cross-section of potential q [1,2]

$$q_z(\vec{\rho}, \omega) \equiv \int q(\vec{r},\omega)\, dz = (k/2\pi\zeta)^2 \int V(\vec{s}) \exp(-ik(\vec{s}-\vec{\rho})^2/2\zeta) d^2s. \qquad (11)$$

The integral projection $q_z(\vec{\rho})$ can be obtained after transformation of field data. For case of the BA we have $V=-4\pi\zeta(E-E_0)/E_0$ and for the case of the RA $V = -4\pi\zeta(\Phi-\Phi_0)$ [1,2]. Changing the direction of the sounding wave incident ("turning" the z-axis) one can obtain a set of 2D-projections, which makes it possible the tomography reconstruction of the 3D structure.

Determination of the linear potentials $q_z(\vec{\rho},\omega)$ (11) from complex potential $q(\vec{r},\omega)$ in the case of forward scattering reduces the ISP to a problem of tomographic reconstruction - the problem of reconstruction an object from projections. The intensive development in the past decade of tomographic methods for studying the structure of objects is to a significant extent the result of advances in x-ray tomography. The reconstruction algorithms used in practical x-ray tomography are based on a linear approximation of the ray trajectories. In mathematical respects, such problems

reduce to reconstruction of the attenuation function or refractive index from group of linear integrals and to reconstruction of an object from its small-dimensional projections. In addition to x-rays, practically all known types of emissions and waves are now used for tomographic purposes. The linear approximation frequently does not provide good results in tomographic investigations using optical and ultrasonic waves, microwaves and other waves. Therefore, methods for reconstruction with consideration of reflection and diffraction effects have been developed intensively in recent years, and a special term - diffraction tomography - has appeared [8-12,4].

The solutions of the IP of reconstruction of the structure of a scatterer with diffraction considered in the case of "forward" scattering obtained above can also be applied to the field of diffraction tomography. ISP reduces to the tomographic problem of reconstructing a 3D object from 2D projections $q_z(\vec{\rho},\omega)$ (11). By rotating the object or rotating the transmitting and receiving system in relation to the object (axis z), it is possible to obtain a series of linear integrals of $q_z(\vec{\rho},\omega)$, which can be used for tomographic reconstruction of the refractive index. However, the problem of reconstructing the 2D structure from a set of 1D "cross sections", i.e., functions measured by one receiver as the transmitter on a satellite moves, is also a tomographic problem. Furthermore, the physical meaning of the quantities measured by one receiver is of integrals over the cross section of the spectrum of the irregularity. A set of such integrals makes it possible to reconstruct the 2D cross section of spectrum, which is equivalent to reconstruction of 2D integrated projection of $q_z(\vec{\rho},\omega)$. The set of 2D projections makes it possible to perform tomographic reconstruction of the 3D structure.

The influence of diffraction reduces to the fact that the linear integral (11) is dependent not only on the field "on the ray", bur also on the field in vicinity of the intersection point of the ray and recording plane ($z = z_R$). If the emission frequency is high, then at the limit $\omega \to \infty$ the integral (11) should only be dependent on the field on the ray (the eikonal approximation with a stright line trajectory).

Let a plane sounding wave ($\vec{\rho}_0=0$, $z_0 \to \infty$) strike the object. Then, by calculating the integral (11) at the of high k ($kr_m^2/2\zeta \gg 1$) by the saddlepoint method (assuming that $V(\vec{s},\omega) = -4\pi\zeta\Phi_1$ in accordance with smooth perturbation method approximation), we obtain

$$q_z(\vec{\rho},k) \equiv \int q(\vec{r},k)dz \simeq (k/2\pi\zeta)^2\, V(\vec{\rho}_R)(2\zeta/k)(-i\pi) = 2ik\Phi_1(\vec{\rho}_R). \tag{12}$$

To demonstrate, the advance of the complex phase Φ at the object in the geometrical optics approximation with a linear ray is equal to the integral of complex refractive index $n(\vec{r},\omega) = v\sqrt{1-q/k^2}$

$$\Phi = \Phi_0 + \Phi + \ldots = ik \int n(\vec{r},\omega)\, dz =$$

$$= ik \int v\sqrt{1-q/k^2}\, dz \simeq ik \int (1-q/2k^2)\, dz$$

From this, for the first approximation of the complex phase of the field we have $\Phi_1 \simeq -iq_z/2k$, which agrees with (12), i.e., at the high-frequency limit linear integrals of type (11) are only dependent on the field on the ray. This means that the approximation used here also contains the geometrical optics approximation with linear trajections at the high-frequency limit. The result of the limitation on $\vec{s}$ of the region where the field is recorded is that the function $q_z(\vec{\rho},\omega)$ reconstructed from limited

data on $\Phi_1(\vec{s})$ will be smoothed. The null space of the equation is determined by the parameters of the recording system and defines the Rayleigh resolution limit [1]; then $q_z(\vec{\rho},\omega)$ is an integral over a ray of finite "thickness".

To reconstruct the 2D structure of ionospheric irregularities according to the transformation (11) we need the information about the approximate coordinate of the scatterer z_s. Let us discuss briefly a method for determination of a distance to the scatterer, which is essential for irregularities reconstruction by integral transformations. If only an approximate value of the distance is known then there appear errors in $\vec{s}$ and ζ, and hence, the reconstructed function is destorted. Let us consider an example where a source is placed on board of a satellite and the corresponding distortions arising in this case. The distance between the satellite and the receivers $(z_0 - z_R)$ is known quite precisely, but in determination the distances "source - scatterer" $(z_0 - z_s)$ and "scatterer - receivers" $(z_s - z_R)$ a systematic error Δ is present: $z_s' = z_s - \Delta$. It may be shown that reconstruction errors are small for such values of Δ, which correspond to the longitudinal resolution of the measuring system. This conclusion is also confirmed by numerical simulations [1].

It easy to show that when the error Δ is less than the longitudinal resolution, $\Delta \ll \lambda\, 2\zeta^2/(\max\, s)^2$, the reconstructed function is

$$\tilde{q}_z(\vec{\rho}) \simeq q_z(x/u_x,\ y/u_y)\ \exp\left(i\frac{k}{2\zeta u_x u_y}\ (y^2 - x^2)\right), \qquad (13)$$

where $u_x = 1 - \Delta/(z_s - z_R)$, $u_y = 1 + \Delta/(z_0 - z_s)$. This equation makes it possible to determine the distance to the scatterer by performing reconstruction with different values of Δ. At the true location of the scatterer (Δ=0) the "phase front" curvature of the

function $\tilde{q}_z$ under reconstruction changes to the opposite with respect to each coordinate. These problems are considered in detail in [1] and partly in [6]. There one can find the generalization of the method for the ionosphere with the stratified background; the method for determination of inhomogeneities parameters ("mass", space coordinates, size and other moments of potential q) by means of a small number of receivers and solutions of IP due to data of back- scattering.

It is possible to consider the more general case, namely, the strong scattering case. For this case in accordance with (7,10) we reconstruct the projection Q_z of the product of the potential and the normalized field Q=qU, namely,

$$\int qU\, dz = Q_z(\vec{\rho}) \qquad (14)$$

It should be stressed that in general the normalized field U[q] depends on the potential and on the direction of the sounding wave incident. So it is impossible to solve the problem of the product qU reconstruction by means of the direct transformation of a set of projections (14). It is possible to suggest iteration procedures of the ISP solution to the equation (14) directly. But, if the scale of ionospheric inhomogeneities more than sounding wavelength in 10^3- 10^4 times, it is even complicated to solve the direct scattering problem. So for such cases it is necessary to use asymptotic methods. The special asymptotic methods of the solution of the ISP for the case of strong and large scatterers were developed in [1,18]. For example the following asymptotic representation of normalized field was obtained

$$U(\vec{\rho},z) = \exp\Big[-\frac{i}{2k}\int_{-\infty}^{z} q(\vec{\rho}+z')dz + \frac{1}{4k^2}\int_{-\infty}^{z}(z-z')\frac{\partial^2 q(\vec{\rho}+z)}{\partial\vec{\rho}^2}dz' + O(k^{-3})\Big] \qquad (15)$$

This formula is correct for infinitly smooth potential. The corresponding additional terms in the sum (15) will appear in the presence of derivatives discontinuities. The formula (15) permits us to construct the simple iteration procedure of the ISP solution, when it is not necessary to solve numerically neither the direct scattering problem, or the ISP. The given first guess of the potential q_1 (a priori information or transformation under the condition of weak-scattering) defines the approximation of the normalized field functional $U[q_1]$ according to (15). Using this approach it is possible to solve the usual tomographic problem of the reconstruction $q(\vec{r})$ (14) with known "weight" U due to $Q_z(\vec{\rho})$ under the different directions of the sounding wave incident. Later on the iteration procedure with the potential approximations obtained is repeated.

The formula representation (15) permits us to formulate the conditions of applicatability of the weak-scattering approximations. According to this condition the first term ($\sim k^{-1}$) and all successive terms of the expansion (15) have to be small. The restriction on the first term gives us the well-known condition of the BA applicatability.

$$qr_m/2k \ll 1 \qquad (16)$$

Here q is the typical (mean) value of the potential, r_m is the maximum size of the inhomogeneity. In the case when the wavelength of the sounding radiation λ=2m and the value of disturbances of the ionosphere electron density $N \sim 10^{11}$el/m^3 the condition (16) leads to the inequality $r_m \ll$ 2 km. The disturbances of the electron density, scattering radiowaves, have to be measured relative to the background of the regular stratified ionosphere. So, if the background value $N \approx 10^{11}$el/m^3 and the disturbances are

sufficiently strong (10%), the BA is valid up to the sizes of dozens km. But for the case of the main ionosphere maximum ($N \sim 10^{12}$ m^{-3}) the scale restriction is significant and it is necessary to take into consideration the first term of (15). The second term of (15) for simple scatterers without internal structure is less ($kr_m \gg 1$) than the first one. In the case when there are some internal details inside the scatterer with the scale $a \gg \lambda$ and the typical value of the potential q', the second term can be more than the first. Hence the other necessary condition of the BA is the condition that the second term with the transverce derivative is small

$$q' r_m / (4k^2 a) \ll 1. \qquad (17)$$

In many practical cases it is sufficient to take into account the first term of (15) only, but the scatterer is not the Born's scatterer according to (16) and the inequality (17) is valid. Such conditions allows us to get the simple analytic formula [1,14], which connects the function Q_z reconstructed due to the experimental data and the projection of the scattering potential q_z (15).

$$Q_z(\vec{\rho}) = 2ik\,[\exp(-iq_z(\vec{\rho})/2k) - 1] \qquad (18)$$

This formula is the basis of the tomography reconstruction for the most of ionospheric applications. Really, the inhomogeneities with the scale about ten or more kilometers, the deviations of which are about 10% with respect to the background, are the strong inhomogeneities (the left hand side of (16) is more or approximately equal to 6, when $\lambda = 2$ m), but the inequality (17) is valid for the internal details with the scale more than hundreds of meters and with the electron density disturbances about 100% compared with the background.

The uniqueness of solutions of the similar ISP was considered many times earlier [1-3]. Some exact results are known. For the problems in question the uniqueness of the transformation q_z (11) and the following reconstruction (14,18) of projections can be easily proved for the finite volume.

The results described above allow us to get 2D projections of localised ionospheric inhomogeneities with the help of the moving satellite transmitter and the transverse arrow of Earth receivers. If there are some arrows of receivers separated by distances about hundreds kilometers along the line of the satellite flight, it is possible to obtain some 2D projections. Having a set of 2D projections one can reconstruct the 3D structure also. Such experiment (with some arrows of receivers) is rather complicated and it was not realized yet. Nowadays experiments connected with the reconstruction of the 2D localized inhomogeneities were carried out [1,5]. This is the tomography problem also because it is possible to reconstruct the 2D inhomogeneity projection or the 2D cross-section of its spectrum after the corresponding transformations by means of a set of 1D field records in each receiver.

We will consider the examples of numerical calculations by means of eleborated programs.

Using the first numerical example, we will illustrate the necessity for considering diffraction effects in RT reconstruction of objects with dimensions r_m comparable to the dimensions of the Fresnel zone $\sqrt{\lambda\zeta}$. As was demonstrated above (12), diffraction effects are insignificant where $kr_m^2/2\zeta \gg 1$ and can significantly distort the results where $kr_m^2/2\zeta \leqslant 1$. Fig. 2a shows $q_z(\vec{\rho})$, consisting of two irregularities - two Gaussians ($\sim \exp(-\rho^2/r_i^2)$

with parameters ($r_1/\sqrt{\lambda\zeta}$ = 5, $r_2/\sqrt{\lambda\zeta}$ = 1/3, for the λ=2m, ζ=200km, $2r_1$ = 6.3km, $2r_2$ = 420m). If we reconstruct the complex phase after the emission passes through one large irregularity, then according to (12) Im Φ_1 is proportional with a high accuracy to the function $q_z(\rho)$ from a large irregularity. However, the imaginary part of the complex phase Φ_1 (Fig. 2b) from a pair of irregularities bears little resemblance to Fig. 2a due to diffraction effects in small irregularity. Fig. 3 shows the similar picture for the two irregularities with parameters ($r_1/\sqrt{\lambda\zeta}$ = 5, $r_2/\sqrt{\lambda\zeta}$ = 1/8). The pair of irregularities is reconstructed very accurately in the case where the Fresnel inversion (11) is used.

For reconstruction of the structure of ionospheric irregularities the questions about sampling data and reconstruction procedure are significant. The sounding radio signals are always recorded by point receivers. The signal from each receiver recording the emission of the moving transmitter on the satellite is also sampled by an electronic circuit with a fixed interrogation frequency. Moreover, the integral transformations as a result of which the structure of the scattering irregularities is reconstructed can be realized numerically on a computer only after the appropriate digitization. Therefore, both the form of the data recorded and the nature of the numerical processing and the reconstruction of the objects lead to the necessity for performing purely discrete operations. However, in theoretical examination of the solution of the inverse scattering problem the immediate switch to discrete formulas is hardly advisable in the majority of cases. Usually, the discrete analogues to the reconstruction formulas are significantly more

cumbersome, and besides the discrete form hinders analysis of the results obtained. On the other hand, the switch from continual relations to their discrete analogues does not cause difficultes in the majority of cases and is performed in a unique manner. So, continual formulas can be considered a compact notation of their discrete analogues for further practical reconstruction.

Let us consider the switch to discrete analysis of the reconstruction procedure and the questions associated with this switch using the transformations (8), (11). It should be noted that, the methods for digital processing of signals and fields have been developed rather well and covered in the literature [19,20].

First, we switch in (8, (11) to the dimensionless variables $\vec{P} = \vec{\rho}/\sqrt{v\,\lambda\zeta}$; $\vec{S} = \vec{s}/\sqrt{v\,\lambda\zeta}$, normalized to the radius of the Fresnal zone. Intriducing the quantities

$$F_q(\vec{P}) \equiv \frac{q_z(\vec{\rho})\lambda}{4\pi} e^{i\pi P^2} \quad \text{и} \quad F_v(\vec{S}) \equiv \frac{V(\vec{s})}{4\pi\zeta} e^{-i\pi S^2} \tag{19}$$

from (11) we obtain the pair of integral Fourier transforms for them [1]

$$\begin{aligned} F_q(\vec{P}) &= \int F_v(\vec{S})\, e^{-2i\pi\vec{S}\vec{P}}\, d^2S \\ F_v(\vec{S}) &= \int F_q(\vec{P})\, e^{+2i\pi\vec{S}\vec{P}}\, d^2P \end{aligned} \tag{20}$$

By virtue of the definition $F_q(\vec{P})$ is a finite function due to the finiteness of $q_z(\rho)$. Let the dimensions of the object not exceed the limits of the segment $[-P_{Ox}, P_{Ox}]$ in axis x and $[-P_{Oy}, P_{Oy}]$ in axis y, i.e., the carrier of the function $F_q(\vec{P})$ is contained in a fixed rectangle. Then, $F_v(\vec{S})$ will be an infinite

and analytical function with a finite spectrum $F_q(\vec{P})$. According to the Kotel'nikov theorem $F_v(\vec{S})$ can be represented in the form of an infinite series in terms of sample functions with the sampling intervals $\Delta S_x = P_{Ox}/2$, $\Delta S_y = P_{Oy}/2$:

$$F_v(S_x,S_y) = \sum_{m_x m_y} F_v\left(\frac{m_x}{2P_{Ox}}, \frac{m_y}{2P_{Oy}}\right) \operatorname{sinc}(2\pi P_{Ox}S_x - \pi m_x) \operatorname{sinc}(2\pi P_{Oy}S_y - \pi m_y)$$

Substituting this representation in (20) and integrating with respect to S_x, S_y, we obtain the relation

$$F_q(\vec{P}) = \sum_{m_x\, m_y} F_v\left(\frac{m_x}{2P_{Ox}}, \frac{m_y}{2P_{Oy}}\right) e^{-2i\pi[P_x\Delta S_x m_x + P_y\Delta S_y m_y]} (2P_{Ox}\, 2P_{Oy})^{-1}. \qquad (21)$$

Using the concept of signals which are really indistinguishable at the level ε [21], it is advisable to introduce a finite function which is really indistinguishable at a fixed level from $F_v(\vec{S})$. Let the carrier of this function be contained in the rectangle $[-S_{Ox},S_{Ox}]$ x $[-S_{Oy},S_{Oy}]$. Then, according to the Landau-Pollack theorem [21,22] the approximate dimension of the set of all functions $F_v(\vec{S})$ finite at a fixed level with a carrier in the rectangle $[-S_{Ox},S_{Ox}]$ x $[-S_{Oy},S_{Oy}]$ and with a finite spectrum supp $F_q(\vec{P}) \in [-P_{Ox}, P_{Ox}] \times [-P_{Oy}, P_{Oy}]$ is close to $N_xN_y = (2S_{Ox}\times 2P_{Ox})$ x $(2S_{Oy}\times 2P_{Oy})$. In other words, due to the finite accuracy in measurement of the signals it can assumed that both the signal and its spectrum are finite. The limitation on the carrier of the spectrum leads to a finite sampling frequency and

$$F_q(\vec{P}),\ \Delta P_x = 1/2S_{Ox},\ \Delta P_y = 1/2S_{Oy},$$

here, the number of sampling intervals on the Cartesian axes is equal to $N_x = = 2S_{Ox}/\Delta S_x = 2P_{Ox}/\Delta P_x$, $N_y = 2S_{Oy}/\Delta S_y = 2P_{Oy}/\Delta P_y$. From this, assuming $P_x = n_x\Delta P_x$, $P_y = n_y\Delta P_y$, it is simple to switch

from (19), (20) to a pair of discrete transformations for $\tilde{F}_v = F_v/(\Delta P_x \Delta P_y)$ и $\tilde{F}_q = F_q$

$$\tilde{F}_q(n_x,n_y) = \frac{1}{N_x N_y} \sum_{m_x=-N_x/2}^{N_x/2-1} \sum_{m_y=-N_y/2}^{N_y/2-1} \tilde{F}_v(m_x,m_y)\, e^{-2i\pi\left(\frac{m_x n_x}{N_x} + \frac{m_y n_y}{N_y}\right)}, \tag{22}$$

$$\tilde{F}_v(m_x,m_y) = \sum_{n_x=-N_x/2}^{N_x/2-1} \sum_{n_y=-N_y/2}^{N_y/2-1} \tilde{F}_q(n_x,n_y)\, e^{-2i\pi\left(\frac{m_x n_x}{N_x} + \frac{m_y n_y}{N_y}\right)}.$$

Later on, the fast Fourier transformation algorithms are used in the numerical modeling and the numbering of the sums over m_x, n_x is shifted from 0 to $N_x - 1$, and likewise for m_y, n_y.

The dimensions of the reception region S_{Ox}, S_{Oy} and, consequently, the sampling intervals ΔP_x, ΔP_y also determine the resolutions. To demonstrate, the minimum resolvable interval δ_x in x is equal to $\delta_x = \sqrt{\lambda\zeta}$, $\Delta P_x = \sqrt{\lambda\zeta}/2S_{Ox} = = \lambda\zeta/2S_m$. A limitation of the reception region always limits the resolution or the sampling interval and the function with a finite spectrum. Therefore, generally speaking, with a limited reception region it is possible to switch immediately from (21) to the finite, discrete Fourier transform (22).

The switch from other continual reconstruction formulas containing the Fourier and Fresnel transforms to their discrete forms is also made according to this scheme.

The practical realization of reconstruction of the structure is governed to a great extent by the resistance of the reconstruction procedure to the various types of noises and distortions which unavoidably appear in measurements and processing of experimental data. Let us illustrate the influence

of noises and distortions on reconstruction of the structure on the examples of numerical simulation. Briefly discribe a modeling scheme using the example of two-dimensional Fresnel reconstruction.

The modeling scheme

$$q_z(\vec{\rho}) \Rightarrow F_q(\vec{P}) \Rightarrow F_v(\vec{S}) \Rightarrow V(\vec{S}) \Rightarrow \underset{\uparrow}{\ldots\ldots} \Rightarrow \tilde{q}_z(\vec{\rho})$$

noises, distortions

The function $q_z(\vec{\rho})$ characterizing the two-dimensional structure of the electron concentration irregularities and the effective collision frequency is defined. Then, the quantity $F_q(\vec{P})$ is calculated using formula (19). After performing the discrete Fourier transform (22) corresponding to (20), $F_v(\vec{S})$ is obtained and, thus, the field $V(\vec{S})$ in a discrete grid. This stage of modeling is related to the direct scattering problem, where it is assumed that the scattering is calculated well within the framework of the corresponding approximations. Further, the noise can be added to the data on the field obtained, after which the inverse discrete Fourier transform (22) corresponding (20) is performed, and the result of reconstruction $\tilde{q}_z(\vec{\rho})$ is obtained as a result. The influence of distortions is modeled in asimilar manner: in the inverse transformation stage, the parameters of the transformation are changed or "distorted".

The results of numerical modeling of the influence of noises have demonstrated the stability of the reconstruction procedure. Fig.4 shows two actual irregularities of $q_z(\vec{\rho})$ - two Gaussians with various dimensions on a 64x64 grid. The total size of the image frame in units of the scale of the Fresnel zone $\sqrt{\lambda\zeta}$ is

equal 5x5. After calculating the complex phase of the field scattered by these irregularities, the data on V were disturbed by noise. Then, reconstruction was performed; the quality of it was sufficient even with comparatively large errors in the measured field [23]. For example, Fig.5 shows the result of reconstruction of these irregularities according to data on Φ_1 with additive complex Gaussian noise having a variance of 0.05 of maximum amplitude of the change in the real and imaginary parts of complex phase of the field. Fig.6. illustrates reconstruction with double the noise (a variance level of 0.1). Another numerical example: actual irregularities - "cylinder" and "parabola" are represented in Fig.7. The result of reconstruction of this model structure with additive noise (a variance level of 0.05) is shown in Fig.8. Fig.9 illustrates the reconstruction with double noise (0.1). If we perform preliminary processing of the data, then even higher noise levels will not noticeably influence the results of reconstructions.

Numerical estimation of the level of influence of the noises is of interest for practical applications. It is advisable to characterize the level of influence of the noises in the metric C and L^2. In a discrete reconstruction procedure, it is better to use their discrete, normalized analogues, i.e. we will estimate the difference between the function $\tilde{f}$ reconstructed from noisy data and real function f by the numbers

$$\rho_C(f,\tilde{f}) = \frac{\max\limits_i |f_i - \tilde{f}_i|}{\max\limits_i |f_i|}; \quad \rho_{L^2}(f,\tilde{f}) = \left[\frac{\sum\limits_i (f_i - \tilde{f}_i)^2}{\sum\limits_i f_i^2} \right]^{1/2}, \quad (23)$$

where summation and selection of maximum are performed for all increments of recorded function.

The dependence of the normalized disturbance of the reconstructed two-dimensional structures (i.e., the difference between the true real $q_z(\vec{\rho})$ and reconstructed $\tilde{q}_z$ in the metrics ρ_c and ρ_{L^2}) on the amplitude Δ of normalized (to the maximum amplitude of the change in the field) complex Gaussian noise is shown in Tabl.1 for the irregularities in Fig.7. It is clear that the normalized deviations of the reconstructed two-dimensional structures are comparable to the noise level. The absolute disturbances of the real part, although the true function is real.

Distortions of irregularities reconstructed by radio tomographic methods appear due to imprecise determination of the distance to the irregularities and, as a result, incorrect knowledge of the given parameters of the integral transformations. The influence of distortions was modeled by the scheme described above. The model in Fig.10 (two irregularities: "cos" and "cos^2" ellipse) is the object of reconstruction. The imprecisely determined coordinate of the scatterer $z_s' = z_s - \Delta$ with an error Δ was substituted in the parameters of the Fresnel transformation. Numerical values $z_0 - z_s = 700$ km, $z_s - z_R = 300$ km, $\lambda = 2$ m typical for satellite sounding were used in the calculations. The dimension of the Fresnel zone here $\sqrt{\lambda\zeta} \approx 0{,}65$ km, the frame dimension was 6,4x6,4 km and the transverse resolution δ was of the order of a hundred meters. Fig.11-15 provide reconstructed two-dimensional structures with various values of the error in determination of the coordinates Δ measured in kilometers; Δ is successively equal to -10, +20, -20, +30, +40 km. It is clear that an error of 10 km has little influence on the reconstruction. Errors Δ of the order of 20 km distort the object, but the characteristic details of the object are reconstructed fairly.

Only errors exceeding 30-40 km noticeably distort the reconstructed irregularity and may lead to incorrect conclusions on the structure of the object. The values of the errors in reconstruction in normalized metrics are shown in Tabl.2. The modeling was performed for two Gaussians. The analogy dependence of error reconstruction on the Δ is shown in the graphs in [1]. The reconstruction errors have a clearly pronounced minimum and are minor ($\leqslant 0{,}1 \div 0{,}2$) within $\pm$ (5 - 10)km. We will note that dimension of this minimum agrees in order of magnitude with the longitudinal resolution δ_z of the system; here, the transverse resolution $\delta \sim \lambda/\theta \sim 100$ m, the aperture angle $\theta \sim 0{,}02$ и $\delta_z \sim \lambda/\theta^2 \sim 5$ km. Therefore, determination of the distance to scatterer with accuracy of the order of the longitudinal resolution of the recording system is sufficient for high-quality reconstruction. The method for determining the distance according to the change in the curvature of the "phase" of the reconstructed function makes it possible to achieve this accuracy in insignificant noises [1].

On reconstruction of q_z using the formula (18) the main obstacle is that Qq_z is a periodical function of q_z, therefore, a real part of q_z is not unambigiously defined by Q_z, which we get from experimental data. Since that, making use the formula (18) one cannot immediately reconstruct scatterers that exceed $4\pi k$. It should be noted here that it's much more than BA-based reconstruction procedures are applicable to. Namely, we have found using numerical simulations that BA holds for scatterers satisfying the inequality

$$q_z/2k < 0.1.$$

In principle, one can reconstruct more intensive scatterers, assuming that Q_z is zero if q_z crosses πk level, or if any additional information about the scaterer structure is available.

We have derived an algorithmic procedure for finite scatterers, which allows one to reconstruct scatterers exceeding $4\pi k$. We have seen that the main obstacle which restricts this procedure capabilities is the finite number of receivers which register the scattered field. From the formal mathematical point of view, that simply means we get only finite number of Fourier expansion terms , i.e. we deal with the truncated Fourier series of Q_z.

Thus to obtain q_z we have to derive it from a truncated Fourier expansion of Q_z, which in turn is a nonlinear transcendent function of q_z. This makes us use the numerical simulations to investigate the domain of applicability of this procedure, because immediate analysis of that algorithm is extremely difficult.

We have performed such an investigation of this procedure applying it to various scatterers. The examples of such numerical simulations of reconstruction of 1D projections of 2D scatterers are presented on Fig.16-18. The scatterer - receiver distance was assumed to be 300 km, the sounding wavelength was 2m. Thick curves correspond to initial projections q_z which had to be reconstructed, thin curves are the reconstructed images of q_z using the procedure described above. Just for checking, the Q_z patterns are also shown (small amplitude fast oscillating curves of normal thickness). On the Figure 16, the scatterer is not too strong, so two curves simply coincide (the projection is exactly reconstructed). On the Fig.17-18, where stronger patterns are given, one can see the discrepancy between exact image and

reconstruction. One can see very easy that mistakes in the procedure work arise mostly on those fragments of scatterers where the transverse derivative $|dq_z/dx| = |dQ_z/dx|$ is big enough, so the oscillations of Q_z become so fast that Q_z is no longer approximated by the truncated Fourier expansion well enough. They may cause the loss of zeros of Q_z, which correspond to increments or decrements of $4\pi k$. The numerical simulations using wide variety of scatterers have confirmed this conclusion. Moreover, they have shown that only the transverse derivative absolute value $|dq_z/dx|$ is critical for the correct reconstruction. Of course, it causes the limitation on the maximal intensity of the scatterer, since for continuous function $q_z(x)$ $|q_z| < a\,|dq_z/dx|$. For this reason, the problem to calculate this boundary value for $|dq_z/dx|$ had also been posed. The value which we get estimating the supremum of the truncated Fourier expansion derivative (it is bounded as a derivative of polynom) is much more than actual value. Fig.19 shows the normalized derivative value times $2\pi N$ plotted versus N, where N is the number of terms retained in the Fourier series. We assumed that well-approximating reconstruction it that one which has the maximal normalized discrepancy between exact and reconstructed images less than 0.1.

The description of Fortran Programs

System Requirements

- Computer:	IBM AT or compatible (with coprocessor)
- Operating System:	MS-DOS or PC-DOS version 3.0 and later
- Memory:	at least Extended memory 4 Mbytes (depends on geometry and type of approximation reconstructed function)
- Hard Disk Space:	4 Mbytes
- Software:	compiler 1.4e and linker 2.2d NDP-FORTRAN-386(c) MicroWay or later

1. Program <DT_DIR.for>

This program solves direct problem, namely, determines complex field $V(\vec{S})$ by means of Fast Fourier Transformation (FFT) based on the model structure of irregularities.

Input parameters and files:

(the determination of the irregularities parameters)
file <mod_par.tsk> contains the following parameters:

```
<< line 1 in file
      'wave length (km):'                    0.002    (DLV in program)
   line 2
   'distance to satellite (km):'             1000.    (ZZO in program)
   line 3
   'distance to irregularities (km):'        300.>>   (Z in program)
```

These parameters you can change in the file.

NY - number of receivers
MNY - the degree of 2 for NY (namely, 2^MNY=NY)
NX - number of discrete intervals on the axis X
MNX - the degree of 2 for NX (namely, 2^MNX=NX)
RMN - the radius of the Fresnel zone.
PX,PY - the limits of segments [-PX/2, PX/2] in axis X and [-PY/2, PY/2] in axis Y; object (model structure not exceed these limits; variable $\vec{P}$)
SX,SY - the limits of rectangle [-SX/2, SX/2]x[-SY/2,SY/2] (variable $\vec{S}$)

YR - the size of the receiving system (km)
XO2 - the size of aperture "synthesized" by satellte (km)
DXX, DYY - the size of frame (km*km)
NMOD - number of model structure (1-10):
1 - the gaussians
2 - "homogeneous" ellipse
3 - "parabolic" ellipse
4 - " 2 + 3 "
5 - " 2 " with absorption 10%
6 - " 3 " with absorption 20%
7 - "cos" ellipse
8 - "cos^2" ellipse
9 - " 7 + 8 "
10 - arbitrary

Nmod is introduced from the screen
Const5=0.1 (namely,10%) - constant for NMOD=5
Const6=0.2 (20%) - constant for NMOD=6

Z1,Z2,Z3,UG ——————————————
A1,B1,A2,B2,XO,YO,Y1,A3,FPC,FPS | parameters for
AELP,BELP |
APAR,BPAR | models
AELP1,BELP1,APAR1,BPAR1 ——————

RN - complex field
Subroutine <SMAXMI> calculates min and max of array
Subroutine <FFT> calculates 1-D Fast Fourier Transformation

Output files:
<MODEL.GRD> - contains the model structure of irregularities and the number of the model (NMOD) and constans VMD and ZRD (for determination of reconstruction's errors)
<V_real.grd> - the array of real parts of the field RN
<V_imag.grd> - the array of imaginary parts of the field RN
Execution
f77 dt_dir.for
RUN
dt_dir.exp

2. Program <DT_INV.for>

This program solves inverse scattering problem for weak-scattering irregularities in the case when noise is present in the measurements of the field and calculates the errors of the reconstruction in metric C and L2 in dependence on level of noise.

Input parameters and files:

Parameters < NX, MNX, NY, MNY, PX, PY, SX, SY >are similar to same parameters of program <DT_DIR.FOR>.

FILES (from program <DT_DIR.for>):

<MODEL.GRD> - input file of model structure.

<V_real.grd> - the array of real parts of the field RN.

<V_imag.grd> - the array of imaginary parts of the field RN.

Parameter <Error> - the level of noise (0 < error < 1)

Error is introduced from the screen.

Const5, Const6 - are similar to same parameters of program <DT_DIR.for>

Subroutine <SMAXMI> calculates min and max of array

Subroutine <FFT> calculates 1-D Fast Fourier Transformation

Function <RAN> - determinates random values in [0,1].

K33 - the constant for function <RAN>

Output files:

REC_er.GRD - the reconstruction

er_r!er.dat - contains the errors of reconstruction in metric C and L2

Same errors are shown on the screen.

Execution

f77 dt_inv.for

RUN

dt_inv.exp

3. Program <DT_ERR.for>

This program solves inverse scattering problem for weak-scattering irregularities in the case when distortions are present in the measurements of the field and calculates the errors of the reconstruction in metric C and L2 in dependence on distortions.

Input parameters and files:

Parameters < NX, MNX, NY, MNY, PX, PY, SX, SY > are similar to same parameters of program <DT_DIR.FOR>.

FILES (from program <DT_DIR.for>):

<MODEL.GRD> - input file of model structure.

<V_real.grd> - the array of real parts of the field RN.

<V_imag.grd> - the array of imaginary parts of the field RN.

<mod_par.tsk> is similar the same file in program <DT_DIR.for>.

Parameter <DEL> - the error of irregularities coordinate in km

DEL is introduced from the screen.

Subroutine <FFT> calculates 1-D Fast Fourier Transformation

Output files:

REC_cr.GRD - the reconstruction

er_r!cr.dat - contains the errors of reconstruction in metric C and L2

Same errors are shown on the screen.

Execution

f77 dt__err.for

RUN

dt_err.exp

4. The solution of the statistical radiotomography problem (statistical inverse scattering problem)

Rather frequently, the ionosphere contains entire regions filled with large numbers of irregularities of various dimensions. Such a state is typical for the equatorial and polar regions, especially at night. In this case it is advisable not to reconstruct individual realization of such disturbed ionosphere, but rather to pose the problem of reconstruction of the statistical characteristics of the turbulent random ionosphere such as correlation function or spectrum of fluctuations. So, such reconstruction of random ionosphere statistical properties by the measured field statistics it is reasonable to name the statistical ISP or the statistical RT problem [24,25].

We consider the reconstruction of ionosphere electron density fluctuations spectrum by means of satellite radioprobing data. Integral equations, which relate the measured field to the medium structure are probably the most convenient and adequate mathematical technique for the tomography. In this paper we shall show how to derive such equations. For simplicity it is reasonable to use two frames of reference. The first "global" frame of reference $\vec{r}=(x,y,z)=(\vec{\rho},z)$, its origin is related to the receiving system as in the previous section (Fig.1). The origin of the second frame of reference $\vec{\mathcal{R}}=(\mathcal{X},\mathcal{Y},\mathcal{Z})=(\vec{\mathcal{P}},\mathcal{Z})$ is reasonable to locate at one of the transmitter positions and the $\mathcal{Z}$ axis to direct to the center of the receiving system. As the transmitter moves it is convenient to use several such "local" frames with different orientations. Such frames are introduced to make derivations shorter, because the probing wave scattering in each local frame may be treated as "almost forward" small-angle scattering. The

lower boundary of the layer of irregularities is z_d, the upper - z_u in the global frame $\vec{r}$. After performing the Fresnel expansions of exponents in the (5) for small-angle scattering, we obtain the integral equation for U (7). This equation is written in the local reference frame, $\vec{S}(Z-Z_0) = (Z'-Z_0)\vec{R} + (Z-Z')\vec{R}$; $D(Z-Z_0) = (Z'-Z_0)(Z-Z')$. For making formulas shorter we assume, that the transmitter is located exactly at the local frame origin, i.e. $\vec{R}_0 = (\vec{P}_0,Z_0)=(0,0,0)$.

To reduce calculations and to use known results we transform (7) to the parabolic equation in new variables $\xi = 1/Z$, $\vec{\sigma} = \vec{P}/Z$, $\xi'= 1/Z'$. Then $(\vec{S}-\vec{P}')^2/D = (\vec{\sigma}-\xi'\vec{P}')^2/(\xi'-\xi)$ and U satisfies the differential equation

$$(-2ik\frac{\partial}{\partial\xi} + \Delta_\sigma - \xi^{-2}q)\ U(\xi,\vec{\sigma}) = 0 \qquad (24)$$

Equation (24) is derived from (7) by differentiating and making use of the following relation for the fundamental solution of the Schrodinger operator [24]. Having derived the parabolic equation we use the methods developed to obtain equations for the first and the second moments of U [26,27]. Let us assume also that the random field q to be Gaussian and δ-correlated along Z,

$$B(\vec{R}_1,\vec{R}_2)\equiv \langle q(\vec{P}_1,Z_1)\ q(\vec{P}_2,Z_2)\rangle = \delta(Z_2-Z_1)\ A_q(\vec{P}_2-\vec{P}_1) \qquad (25)$$

In the similar way in the variables $(\vec{\sigma},\xi)$ it is possible to derive from (24) equations for the second moments of the normalized field $\gamma(\vec{R}) = E(\vec{R})/\langle E(\vec{R})\rangle$,

$\Gamma_{1,0}(\vec{P},Z) = \langle\gamma(\vec{P}_2,Z)\ \gamma^*(\vec{P}_1,Z)\rangle$ - the first coherence function,

$\Gamma_{2,0}(\vec{P},Z) = \langle\gamma(\vec{P}_2,Z)\ \gamma(\vec{P}_1,Z)\rangle$ - the second coherence function of

the second order. As the calculations are described in the papers mentioned above, we present only the final result in the variables $\vec{\mathcal{P}}_+ = (\vec{\mathcal{P}}_1+\vec{\mathcal{P}}_2)/2$, $\vec{\mathcal{P}} = \vec{\mathcal{P}}_2-\vec{\mathcal{P}}_1$ and for statistically homogeneous layer, when the dependence on $\vec{\mathcal{P}}_+$ is absent.

$$[ik(\frac{\partial}{\partial \mathcal{Z}} + \frac{\vec{\mathcal{P}}}{\mathcal{Z}}\frac{\partial}{\partial \vec{\mathcal{P}}}) + \Delta_\perp + \frac{i}{4k} A_q(\vec{\mathcal{P}})]\, \Gamma_{2,0} = 0, \quad \Gamma_{2,0}(\vec{\mathcal{P}},\mathcal{Z}_u) = 1 \tag{26}$$

The integral equation, corresponding to (21), has the form

$$\Gamma_{2,0}(\vec{\mathcal{P}},\mathcal{Z}) = 1 + \frac{i}{16\pi k}\int d^3\mathcal{R}'\, \frac{A_q(\vec{\mathcal{P}}')}{\mathcal{D}}\, \Gamma_{2,0}(\vec{\mathcal{P}}',\mathcal{Z}')\, \exp(\frac{ik}{4\mathcal{D}}(\vec{\mathcal{S}}-\vec{\mathcal{P}}')^2) \tag{27}$$

The following formula for $\Gamma_{1,1}$ is well known [26,27].

$$\Gamma_{1,1}(\vec{\mathcal{P}},\mathcal{Z}) = \exp(\frac{1}{4k^2}\int_{\mathcal{Z}_u}^{\mathcal{Z}} A_q(\vec{\rho}-\frac{\mathcal{Z}'}{\mathcal{Z}}\vec{\mathcal{P}})\, d\mathcal{Z}') \tag{28}$$

Eguation (27) follows from (26). The resulting integral equation is valid also at $\vec{\mathcal{P}}_0 \neq 0$, $\mathcal{Z}_0 \neq 0$.

The integral equation (27) is the basis of the statistical RT. According to (20) $A_q(\vec{\mathcal{P}})$ is the correlation function projection, $\int B(\vec{\mathcal{P}},\mathcal{Z})\, d\mathcal{Z} = A_q(\vec{\mathcal{P}})$. Measured wave coherence functions allow us to determine projections of the complex potential q correlation function by the (27,28). To begin with, let's assume, that irregularities occupy a sufficiently extensive layer, oblique to the probing wave propagation direction. To reconstruct projection $A_q(\vec{\mathcal{P}})$ it's necessary to determine the layer coordinate $\mathcal{Z}_s$. It may be done by a single receiver. The special procedure for determination of the scattering layer $\mathcal{Z}$-coordinate by equation (22) was developed [1,24].

In many situations randomly inhomogeneous media represent

statistically quasi-homogeneous fields with slowly varying statistical properties, i.e. such fields, for which the correlation radius of the differential argument is essentially less than the scale of the variance σ. In other words, the correlation function is represented as a product $B(\vec{\mathcal{R}}_1,\vec{\mathcal{R}}_2) = \sigma^2(\vec{\mathcal{R}})\mathcal{K}(\Delta\vec{\mathcal{R}},\vec{\mathcal{R}})$, where $\vec{\mathcal{R}} = (\vec{\mathcal{R}}_1+\vec{\mathcal{R}}_2)/2$, $\Delta\vec{\mathcal{R}} = \vec{\mathcal{R}}_1-\vec{\mathcal{R}}_2$. A randomly inhomogeneous field with the costant correlation coefficient $\mathcal{K}(\Delta\vec{r})$ but with varying fluctuations variance $\sigma^2(\vec{\mathcal{R}})$ may be called an "additive" field, because the electron density changings influence only the fluctuations intensity, but the correlation coefficient dependence on the summarize argument $\vec{\mathcal{R}}$ is absent. Assuming the field q to be δ-correlated, as was done above, it is possible to obtain similar equations by the same technique. The correlation function projection $A_q(\vec{\mathcal{P}})$ in the integrands should be replaced by $\sigma^2(\mathcal{Z})\ K(\vec{\mathcal{P}})$. Here $K(\vec{\mathcal{P}}) = \int \mathcal{K}(\Delta\vec{\mathcal{R}})\ d(\Delta\mathcal{Z}')$ is the correlation function projection. Then formula for $\Gamma_{1,1}$ and the equation for $\Gamma_{2,0}$ have the form

$$\Gamma_{2,0}(\vec{\mathcal{P}},\mathcal{Z}) = 1 + \frac{i}{16\pi k}\int d^3\mathcal{R}'\ \frac{\sigma^2(\mathcal{Z}')K(\vec{\mathcal{P}}')}{\mathcal{D}}\ \Gamma_{2,0}(\vec{\mathcal{R}}')\ \exp\left(i\frac{k}{4\mathcal{D}}(\vec{\mathcal{S}}-\vec{\mathcal{P}}')^2\right) \tag{29}$$

$$\Gamma_{1,1}(\vec{\mathcal{P}},\mathcal{Z}) = \exp\left(\frac{1}{4k^2}\int_{\mathcal{Z}_u}^{\mathcal{Z}} \sigma^2(\mathcal{Z}')\ K\left(\vec{\rho}\ \frac{\mathcal{Z}'}{\mathcal{Z}}\right)\ d\mathcal{Z}'\right) \tag{30}$$

The equations (29,30) contain the unknown function $\sigma^2(\vec{\mathcal{R}})$. So, the problem of the correlation function reconstruction is divided into two ones: the problem of reconstruction of the fluctuations variance $\sigma^2(\vec{\mathcal{R}})$, and the problem of the $\mathcal{K}(\Delta\vec{\mathcal{R}})$ reconstruction given the measured projections $K(\vec{\mathcal{P}})$.

The formula (30) allows us to determine integrals of $\sigma^2(\mathcal{Z})$ along the direction ($\mathcal{Z}$ axis) of the probing wave propagation. If a

set of different integrals is given for a region filled with irregularities we arrive at a tomography problem. Usually in the experiments there exist a natural limit to the number of projections and angular range of probing waves propagation directions. Hence, the problem when data are known in the small angle range should be solved. A similar problem was solved in the ray RT. Information about the fluctuations intensity $\sigma^2(\vec{\mathcal{R}})$ distribution is sufficient to reconstruct a set of correlation function projections given by measured coherence functions. Methods of the statistical RT problem solution are similar to the discussed above, with the substitution of the product $\sigma^2(\vec{\mathcal{R}})K(\vec{\mathcal{P}})$ of the known function $\sigma^2(\vec{\mathcal{R}})$ and the correlation function projection $K(\vec{\mathcal{P}})$ instead of A_q. A set of projections $K(\vec{\mathcal{P}})$ allows us to perform tomography reconstruction of the correlation coefficient $\mathcal{K}(\Delta\vec{\mathcal{R}})$ or its spectrum.

With the help of examples we want to illustrate the results of programs and numerical pattering. Reconstruction of electron concentration fluctuations spectra was made in two steps: pattering of environment fluctuation spectra and recovery of the power angle spectra of the dispersive environment.

I. Pattering of environment fluctuation spectra. In the given program <ST-DIR.FOR> the account of accidental realisations of electron concentration power fluctuation spectra is made. The pattering scheme is given of tabl.3.

1. The sum of three (of five) Gauss lines with defferent width and intensivity was taken as a pattern of spectra with a few maximums. The location of local maximums and their width depend on the dimentions of the area (32*32,64*64,etc.) and were given by the quantity of accounts from the beginning of the area.The intensivity of local maximums was given in the percent relativity

from the intensivity of the center maximum.

2. The computation of correlation function projections of dispersed field Γ_{11} is made in polar coordinates for the given reception angles in condition with equation (28). The projections of environment correlation functions $R(\rho,\phi_n)$ calculated with the help of fast Fourier transformation from the spectra $\Phi(\rho,\phi_n)$ for every given reception angle in area $[0,\pi/2]$.

3. The form of casual realisations of the dispersed field is made in two steps. At first, with the help of linear congruent method [28,29] statisticaly independent one-dimentional realisations of casual numbers with proportional spectra were obtained. Then, with the help of spectra method of reorganization [30] the prosess with given correlation function $\Gamma_{11}(\rho,\phi_n)$ was formed.

4. The selected (casual) correlation functions of the field $\tilde{\Gamma}_{11}(\rho,\phi_n)$ were calculated from alone realisations of the field.

5. The selected projections of correlation functions of the environment $\tilde{R}(\rho,\phi_n)$ were calculated by logariphmation of the function $\tilde{\Gamma}_{11}(\rho,\phi_n)$. The appropriate $\tilde{R}(\rho,\phi_n)$ casual power spectra of environment fluctuations $\tilde{\Phi}(\rho,\phi_n)$ are defined with the help of standard procedure fast Fourier transformation. The given model of environment spectra (in Decart coordinates) is given as the illustration on fig.20,a. Area dimentions are 64*64, width of central and local maximums on the level of 0.5 their intensivity is 1/8 from linear dimentions of the area. The local maximum intensivety is $I_1=0.3I_c$ (I_c means intensivity of central maximum). From the fig 20,b one can see casual spectra of environment fluctuations, formed from one field realisation for every given reception angle. It is easy to see, that for more calculations reconstraction of angle spectra) the same casual function need

smoothing, i.e. period of its oscilations is equal to the account step [29]. On fig.21 statistically middled (by 50(a) ond 100(b) realisations) angle spectra of the intensivity of environment fluctuations , took by the given below scheme, are given.

II. Recovery of the power angle spectra of the dispersive environment.

In program <ST-INV.FOR> the account of reconstructions of environment power angle spectra from the information in finit reception angle area. For solving the problem of recovery the method of function decomposition into Lejandr polynoms is used. The system of linear equations, made by this method, is solving by Gordon method [30]. On the last step of the account the linear interpolation of the function $\Phi(\rho,\phi_n)$ in Decart coordinates is made.

On fig.23 one can see reconstructions of power spectra of plasma fluctuations calculated from one realisation of dispersed field in each direction of the reciption of the signal. The account was made for three-racurs reception system (fig.22,b). It was supposed that angle areas makes $0\text{-}20^0$,$35\text{-}55^0$,$65\text{-}85^0$ from vertical. On fig.23 the model and reconstruction of its casual realisation (the width of central and local maximums is 1/8 and 1/10 from the linear dimentions of area (64*64),intensivity $I_l=0.3I_c$) is shown. On fig.24 the results of the same account for the dimentions of local and central maximums of 1/16 and 1/8 is shown. Analising the results, we can see that the best reconstructions are obtained for the models of sufficiently narrow spectra (fig.25-28). In this case (fig.28) the recovery of realisation of pattern from 5 local maximums (width is 1/20, relativity of intensivity is 1:0.3:0.2) is sufficiently good. On fig.29 the reconstruction of realisation of pattern from 5 local

maximums (width 1/16, relativity of intensivity is 1:0.3:0.2) is given.The results of the accounts also show that weak intensive local maximums (1:0.1) recover sufficiently good (fig. 30). But the essential part is played by the width of the spectra.On fig.31 the reconstruction of model, which appropriate to the experimental observations[24]. It is clear, that recovery of the spectra from one realisation allow to underline the particularities of its structure. Comparison analisys shows that in spectra reconstructions the locations of local maximums coincide with the original but the intensivities are differ. It future thes difference can be overcomed by using of correlative filters.

The quality of reconstruction very much depend on the quantity and width of reception areas. On fig.32,a reconstruction of model from fig.24, made by two-racurs scheme(fig.22), is given. Reception angles area - 0^0-30^0 and 50^0-80^0. The same reconstructions are made for the experimental model (fig.30). It is clear, that 3-racurs sceme is prefered. On fig.33 are given spectra reconstructions for three reception areas: 0^0-10^0, 40^0-50^0, 70^0-80^0, which are in connection with fig.32. It is clear that to give more quality to the reconstruction the width of reception area should have optimum value.

The description of Fortran Programs

System Requirements

- Computer: IBM AT or compatible (with coprocessor)
- Operating System: MS-DOS or PC-DOS version 3.0 and later
- Memory: at least Extended memory 4 Mbytes (depends on size of frame and number of rays)
- Hard Disk Space: 4 Mbytes
- Software: compiler 1.4e and linker 2.2d NDP-FORTRAN-386(c) MicroWay or later

1. Program <ST-DIR.**for**>

This program solves direct problem, namely, determines the model structure and calculates the random realizations of angle power spectrum.

Input parameters and files:

M - size of frame
NM - size of half frame
JMN - number of rays in [0;π/2] range
KR1 - local maximum size
KR - central maximum size
NOO - spectrum coordinate of local maximum
OTT - level of local maximum power
array HH - model of angle power spectrum in polar coordinates
array SPAD - correlation function model of scattering field
Subroutine SMAXMI calculates maximum and minimum of one-dimension function
Subroutine SMAXNI calculates maximum and minimum of two-dimension function
Subroutine SPGEN calculates balance multipliers
Subroutine RANFIL calculates random fields(complex)
Subroutine CORPAT calculates random correlation function
Subroutine FORT1 calculates one-dimension Fast Fourier Transformation
Function RAN1 calculates uniform random number

Output files:
<RANDSP.GRD> - contains random realization of angle
power spectrum,size(JMN:M)

Execution
f77 st-dir.for
RUN
st-dir.exp

3. Program <ST-INV.for>

This program solves inverse problem for statistical RT, namely, calculates reconstructions of power spectrum of electron density in Decart coordinates for varios namber of receivers.

Input parameters and files:
Parameters
M - size of frame
NM - half size of frame
NN - half size of frame +1
ITER - number of iterations
JPI - number of reseivers
JMN - numer of rays in [0,π/2] range
JT1, JT2, JT3, JT4,JT5,JT6 - boundaries of angle ranges of reception in degrees
NU - number of rays in angle ranges of reception
NXX -number of Lejandr cofficient
FILE <RANDSP.GRD> contains realization of angle power spectrum (OUTPUT file of progpam ST-DIR.for)
OUTPUT FILE:
< RECONS.GRD> contains the reconstraction of realizations angle power spectrum in Decart coordinates,size(M:M).

Execution
f77 st-inv.for
RUN
st-inv.exp

References.

1. V.E.Kunitsyn, E.D.Tereshchenko, *Tomography of the Ionosphere*, Moscow, Nauka, 1991 (in Russian).
2. V.E.Kunitsyn, "Inverse Scattering Problem in the Layered Medium", Moscow University Physics Bulletin, Vol.26, No 6, pp.33-40, 1985.
3. V.E.Kunitsyn, "Determination of the structure of ionospheric irregularities", Geomagnetizm and Aeronomy, Vol.26, pp.75-81, 1986.
4. V.E.Kunitsyn, "Diffraction Tomography in the Fresnel Zone", Moscow University Physics Bulletin, Vol.41, No 2, pp.43-48, 1986.
5. V.E.Kunitsyn, N.G.Preobrazhensky, E.D.Tereshchenko, "Reconstruction of ionospheric irregularities structure based on the radioprobing data", Dokl.Akad.Nauk USSR, Vol.306, pp.575-579, 1989.
6. V.E.Kunitsyn, E.D.Tereshchenko, *The reconstruction of the ionosphere irregularities structure*, Preprint Polar Geophys. Inst., № 90-01-69, pp.1-60, 1990.
7. V.E.Kunitsyn, "Diffraction Tomography based on small-angle scattering data", Transactions SPIE, Vol.1843, pp.172-182, 1992.
8. V.E.Kunitsyn, E.D.Tereshchenko, "Radio Tomography of the Ionosphere", Antennas Rropagation Magazine, Vol.34, pp.22-32, 1992.
9. V.L.Ginzburg, *Propagation of electromagnetic waves in plasma*, New York, Gordon and Breach Science Publishers, Inc., 1961.
10. L.D.Landau, E.M.Lifshits, *Statistical physics*, New York, Pergamon Press, 1980.
11. L.D.Faddeev, "Three-dimensional inverse scattering problem", J.Sov.Math., Vol 5, pp. 334-360, 1976.
12. R.G.Newton, "Inverse scattering II. Three dimentions" J.Math. Phys., Vol.21, pp.1698-1715, 1980.
13. K.Chadan, P.C.Sabatier, *Inverse problems in quantum theory*, New York, Springer-Verlag, 1977.
14. A.J.Devaney, "Geophys. diffraction tomography", IEEE Trans. Geosci. and Remote Sencing, Vol.22, pp.3-13, 1984.
15. R.K.Mueller, M.Kaveh, G.Wade, "Reconstructive tomography and applications to ultrasonics", Proc. IEEE, Vol.67, pp.567-587, 1979.
16. D.Lesselier, D.Vuillet-Laurent, F.Jouvie at al., "Iterative solutions of some direct and inverse problems in electromagnetics and acoustics", Electromagnetics, Vol.5, pp.147-189, 1985.

17. K.J.Langeberg, "Applied inverse problems for acoustic, electromagnetic and elastic wave scattering", in P.Sabatier (ed.), Basic methods of tomography and inverse problems, Bristol, Adam Hilger, pp.127-467, 1987.
18. W.Tabbara, B.Duchene, C.Pichot. et al, "Diffraction tomography: contribution to the analysis of some applications in microwaves and ultrasonics", Inverse Problems, Vol.4, pp.305-331,1988.
19. W.K.Pratt, Digital Image Processing, New York, A Wiley Interscience Publ., 1978.
20. D.E.Dadgeon, R.M.Mersereau, Multidimensional Digital Signal Processing, Prentice-Hall, Inc., 1984.
21. D.Slepian, "About bandwidth", Proc.IEEE, Vol.64, No.3, pp.292-300.
22. H.J.Landau, H.O.Pollak, "Prolate spheroidal wave functions, Fourier analysis and uncertainty", Bell Syst.Tech.J., Vol.40, pp. 65-84; Vol.41. pp.1295-1336, 1961.
23. E.S.Andreeva, V.E.Kunitsyn, "The reconstruction of the projections of scattered irregularities by inexact wavefield data", In: Waves propagation and diffraction in inhomogeneous media, Moscow, Moscow Inst. Physics and Technology, pp. 9-14, 1989.
24. V.E.Kunitsyn, E.D.Tereshchenko, "Determination of the turbulent spectrum in the ionosphere by a tomographic method", Journ.Atm.Terr.Phys., Vol.54, pp.1275-1282, 1992.
25. A.V.Galinov, V.E.Kunitsyn, E.D.Tereshchenko, "A tomographic approach to the investigation of a randomly nonuniform ionosphere", Geomagnetism and Aeronomy, Vol.31, No.3, pp.351-356, 1991
26. V.I.Tatarski, *Wave propagation in a turbulent medium*, New York, McGraw-Hill, 1961.
27. A.Ishimaru, *Wave propagation and scattering in random media*, Orlando (Florida), Academic Press; 1978.
28. I.M.Sobol, *Monte-Carlo method*, Moscow, Nauka, 1978 (in Russian).
29. S.Chakrabarti, S.K.Mitra, "Calculations of two dimensional digital filters by spectral convolution", Proc.IEEE, Vol.65, No.6, 1977.
30. R.Gordon, R.Bender, A.Lent, Journ.Theor.Biol., Vol.29, 1970.

σ	ρ_c	ρ_{L^2}
$1*10^{-2}$	0.034	0.033
$2*10^{-2}$	0.066	0.067
$3*10^{-2}$	0.100	0.101
$4*10^{-2}$	0.134	0.135
$5*10^{-2}$	0.165	0.167
$6*10^{-2}$	0.201	0.200
$7*10^{-2}$	0.229	0.232
$8*10^{-2}$	0.267	0.270
$9*10^{-2}$	0.302	0.327
10^{-1}	0.337	0.332

Tabl. 1

Δ (км)	ρ_c	ρ_{L^2}
-10	0.154	0.183
-20	0.345	0.436
-30	0.439	0.675
-40	0.672	0.882
10	0.093	0.101
20	0.241	0.253
30	0.468	0.475
40	0.654	0.717

Tabl. 2

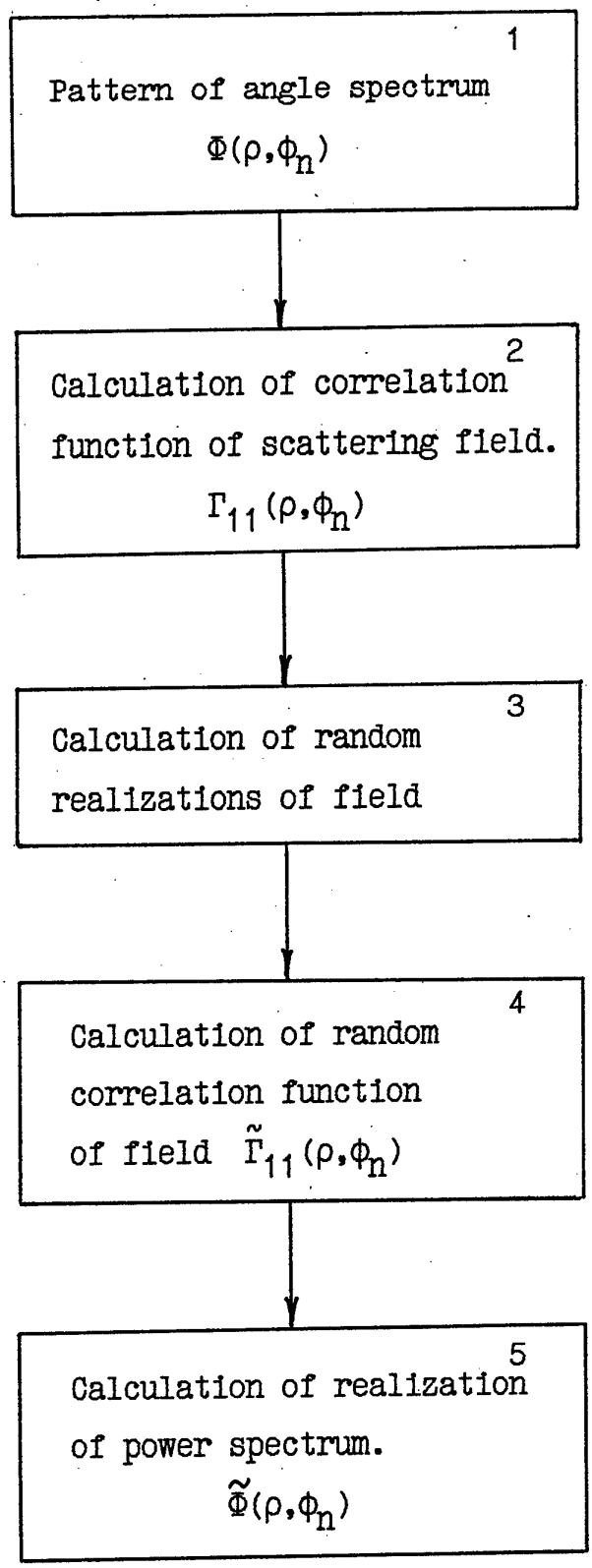
1
Pattern of angle spectrum
$\Phi(\rho,\phi_n)$
2
Calculation of correlation function of scattering field.
$\Gamma_{11}(\rho,\phi_n)$
3
Calculation of random realizations of field
4
Calculation of random correlation function of field $\tilde{\Gamma}_{11}(\rho,\phi_n)$
5
Calculation of realization of power spectrum.
$\tilde{\Phi}(\rho,\phi_n)$

Tabl. 3

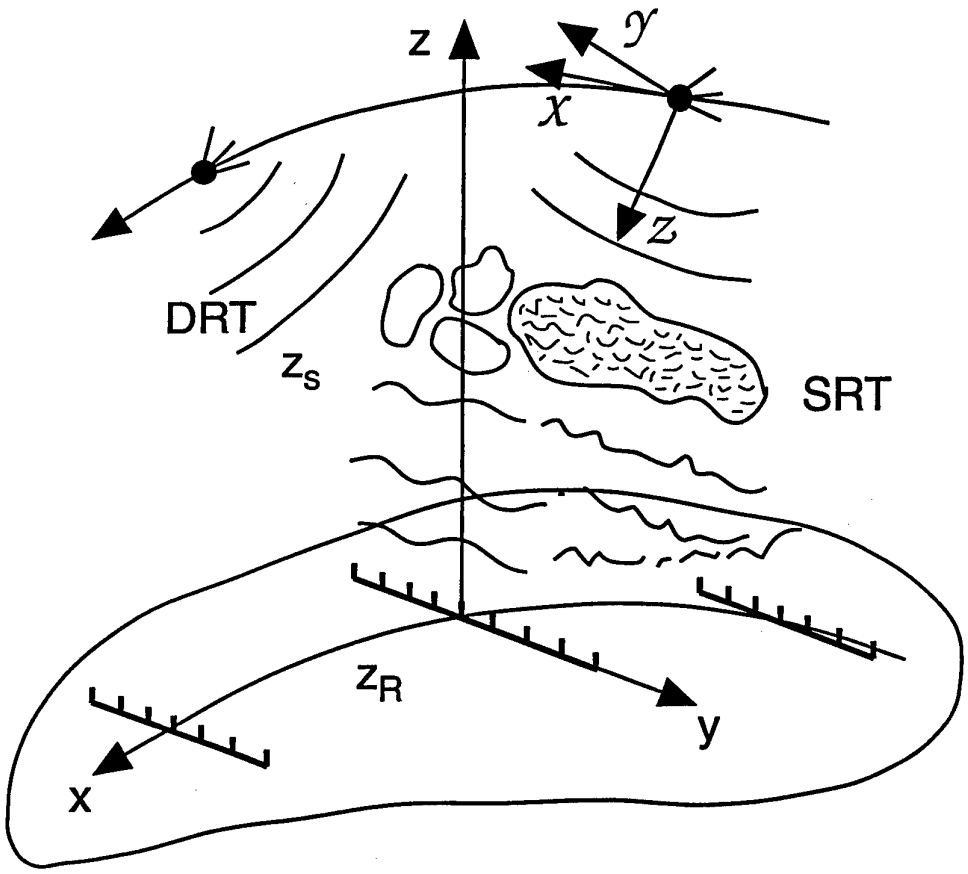

Figure 1.

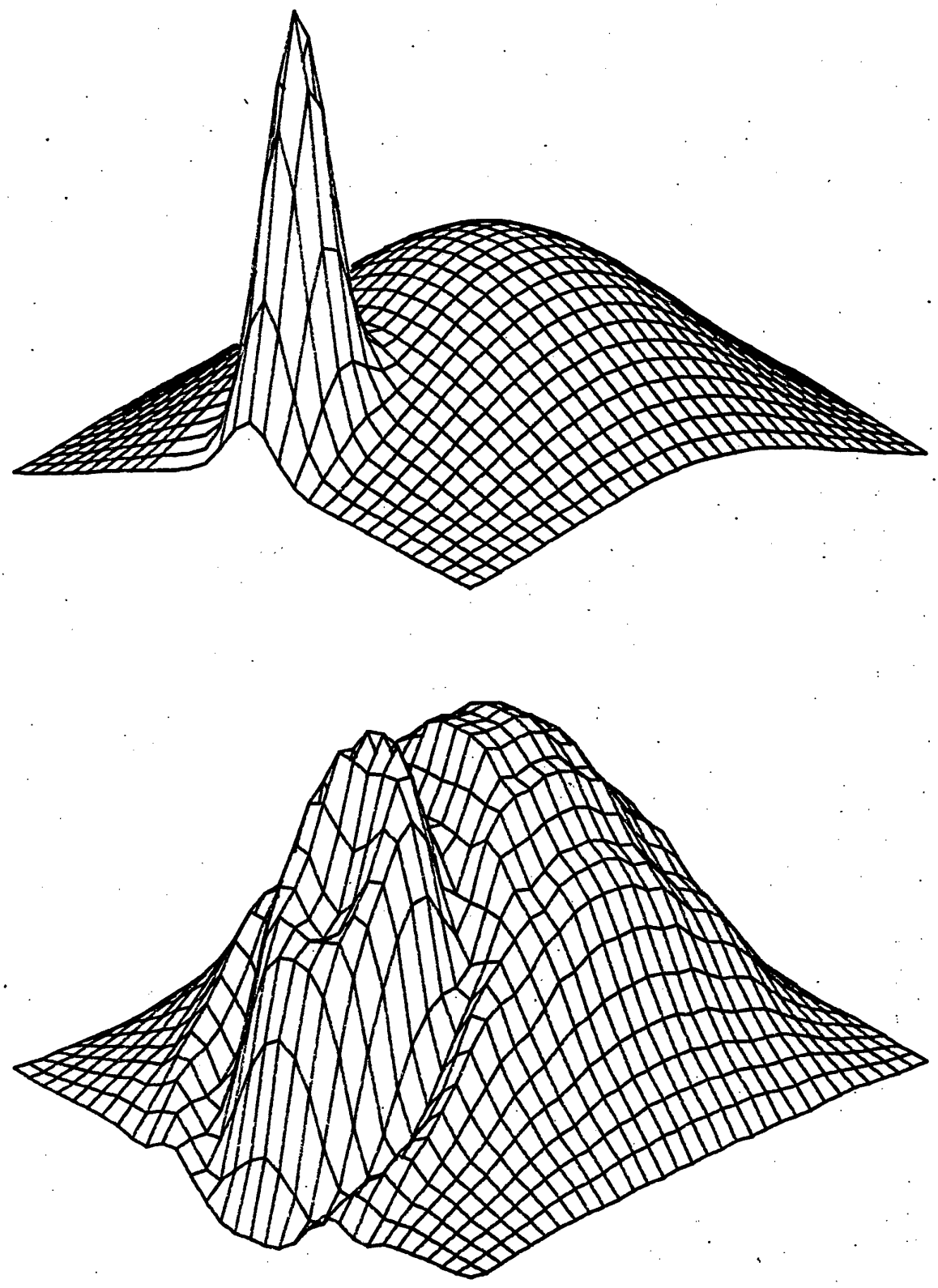

Fig. 2

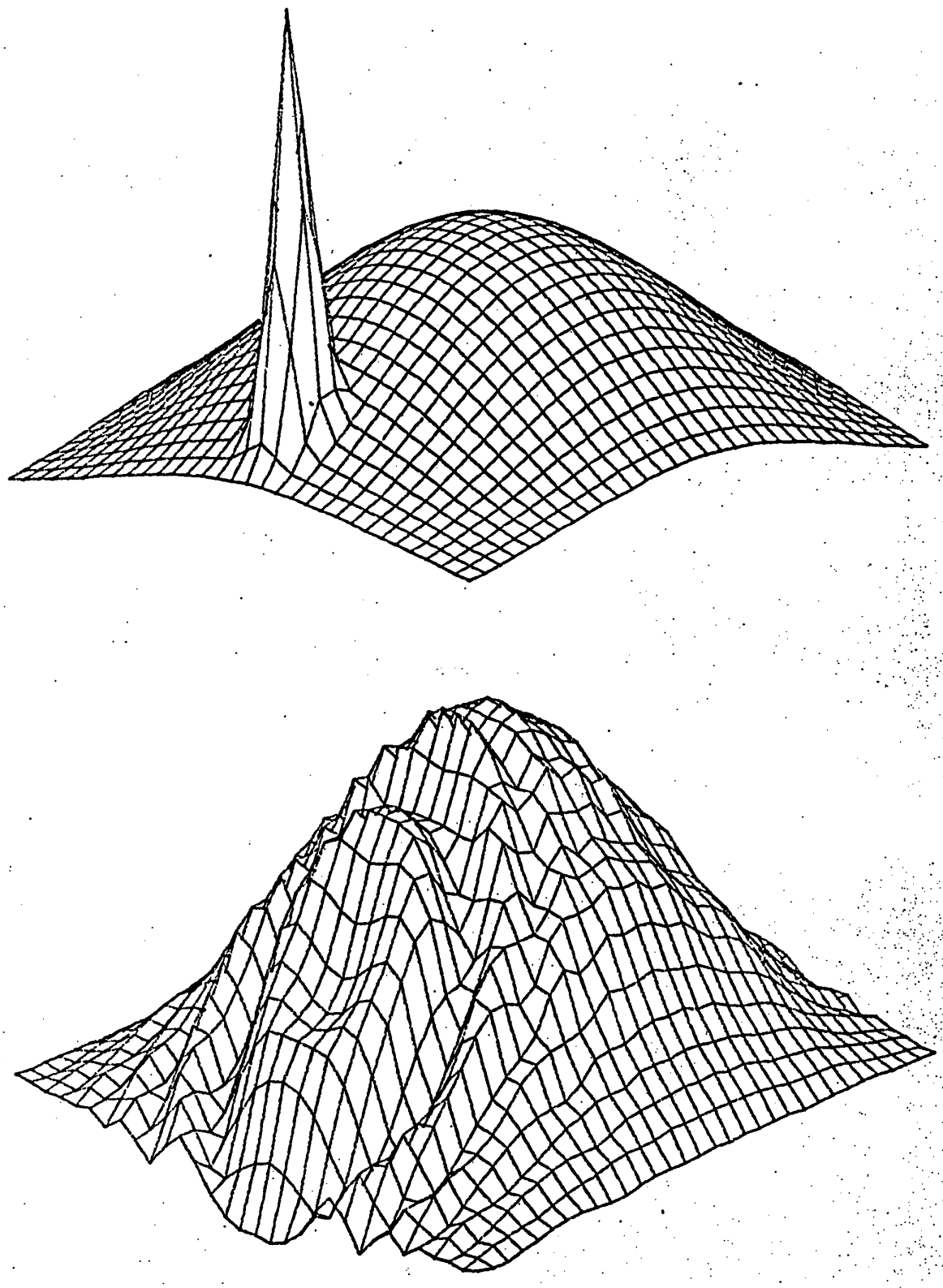

Fig.3

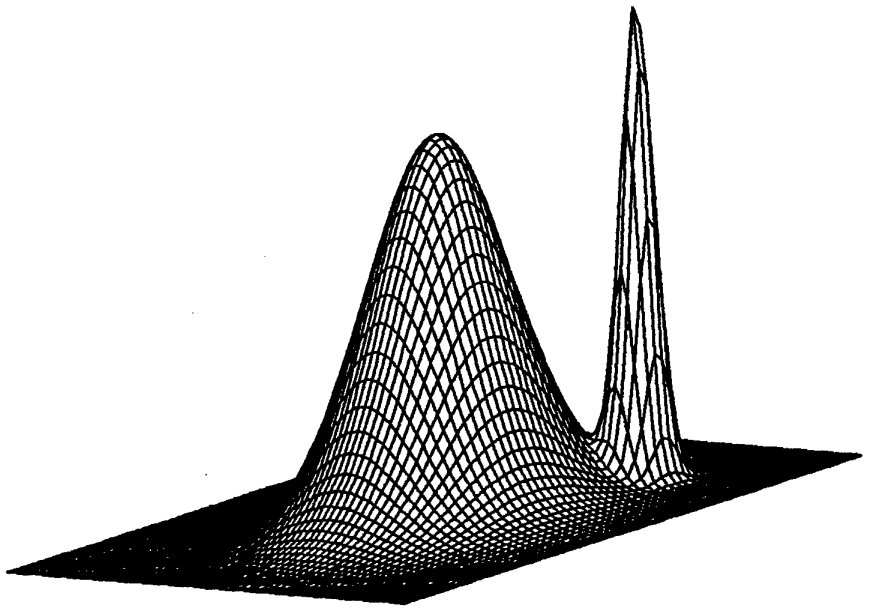

Fig 4.

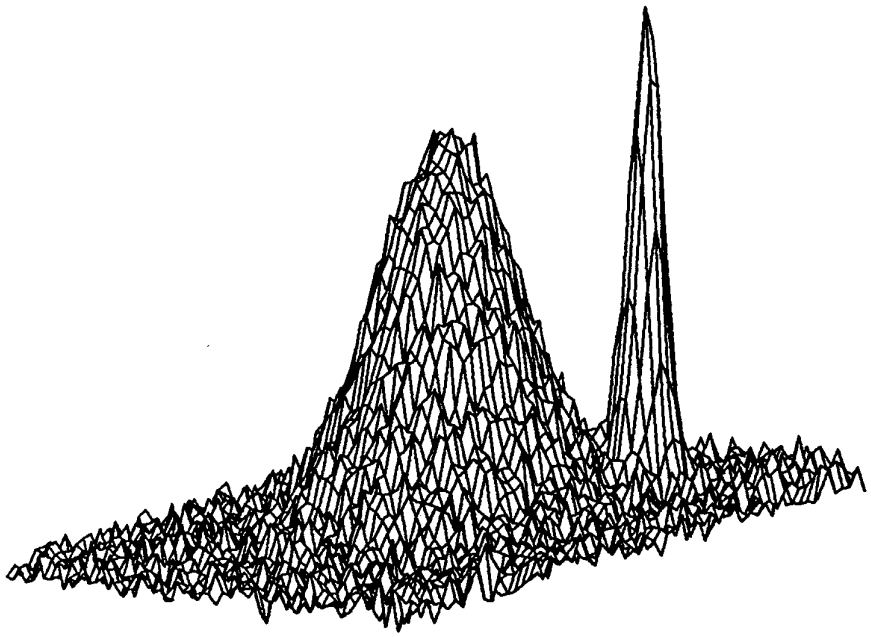

Fig.5

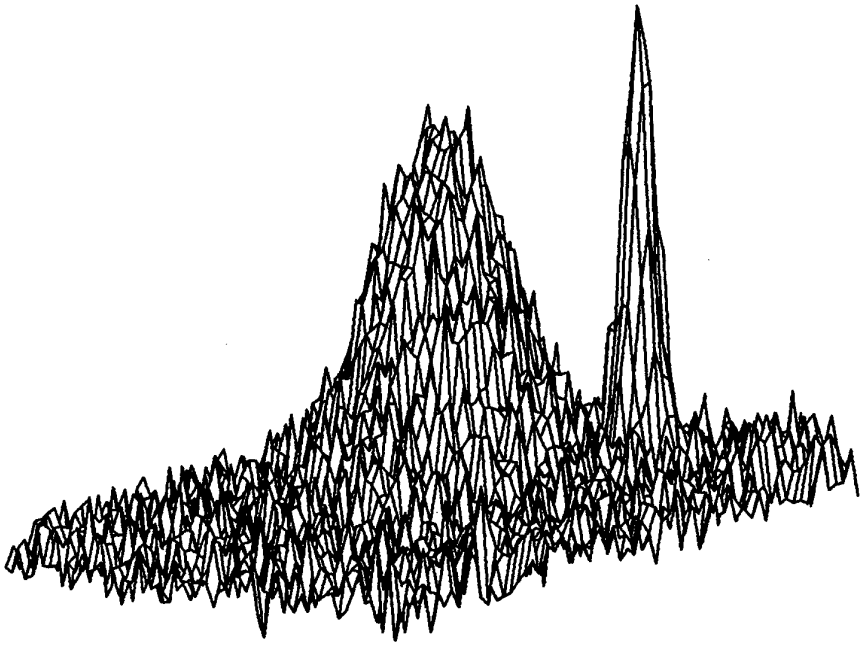

Fig 6.

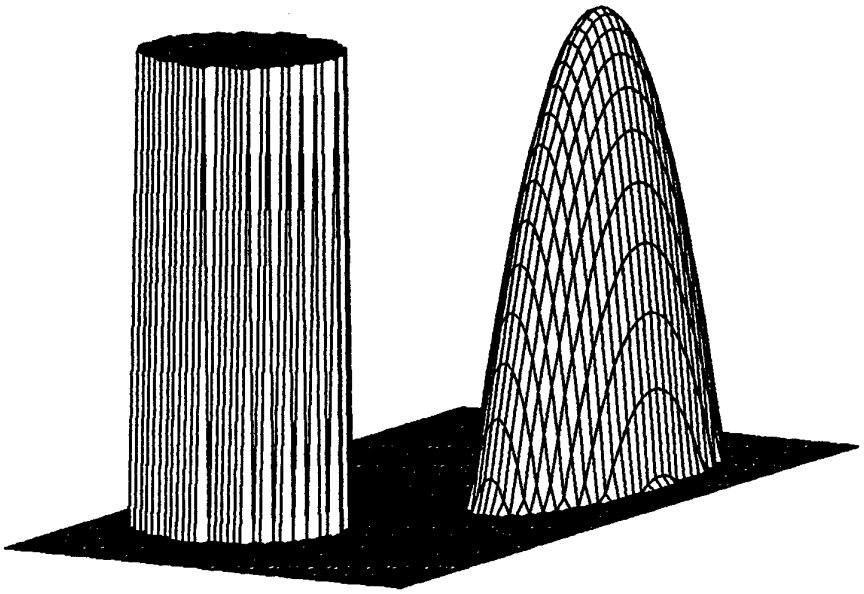

Fig. 7

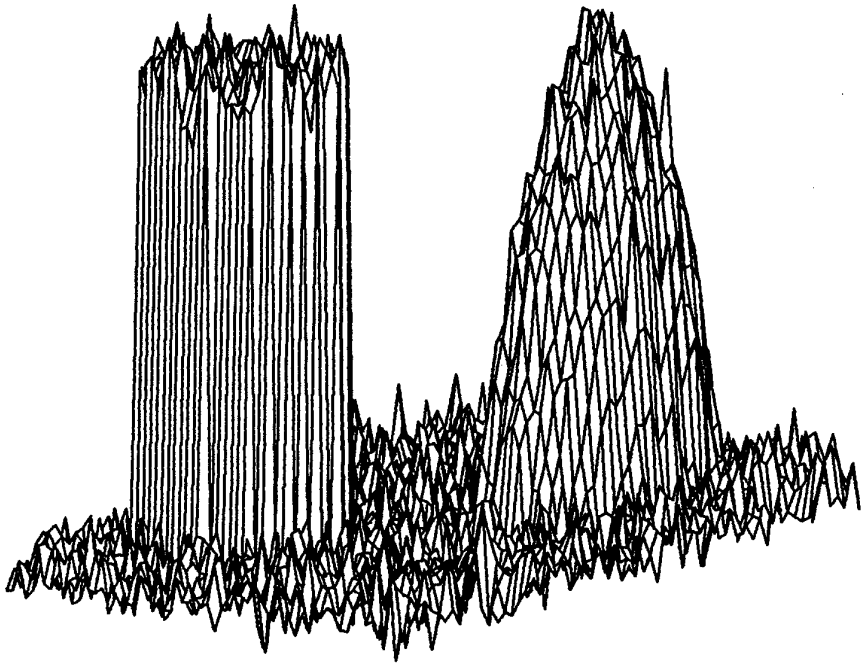

Fig. 8

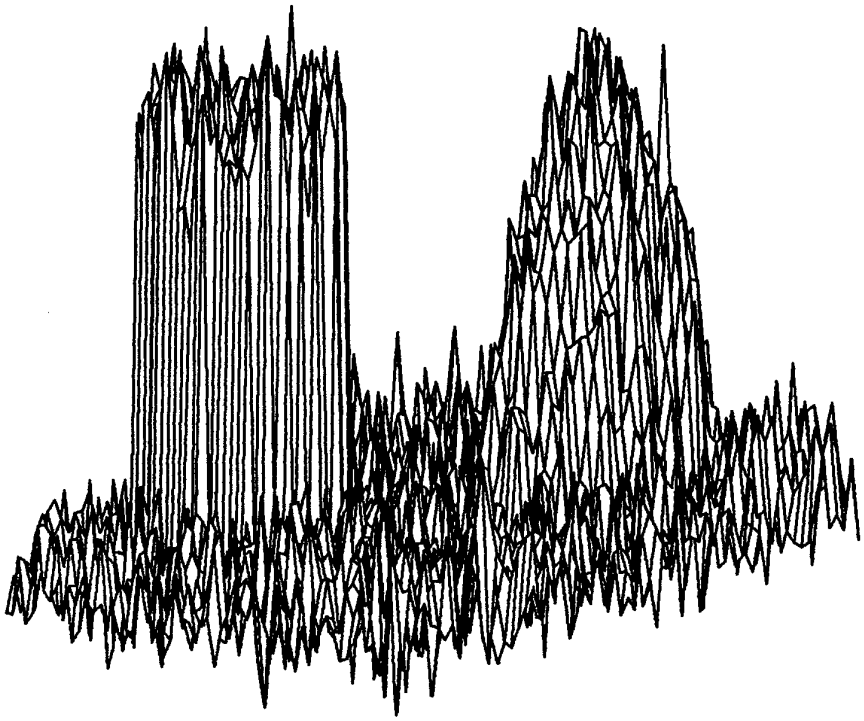

Fig. 9

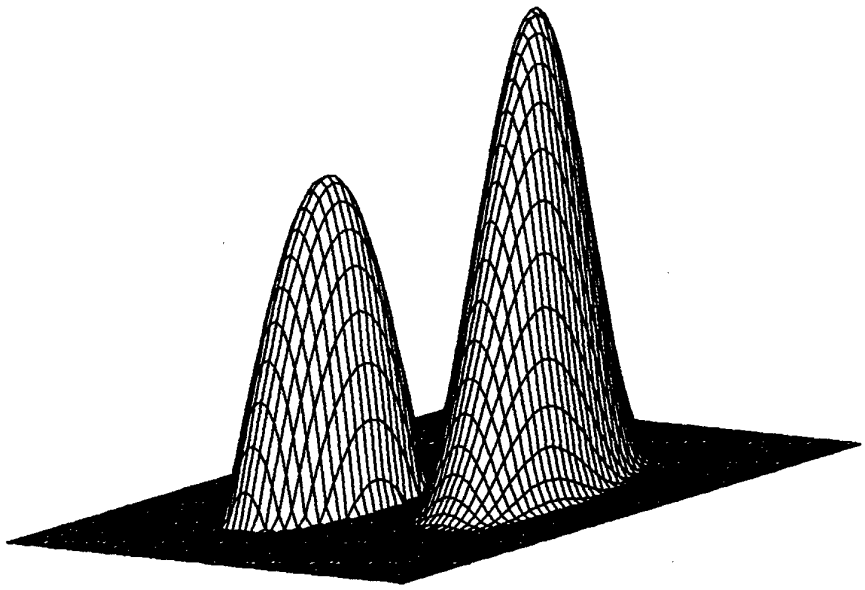

Fig. 10

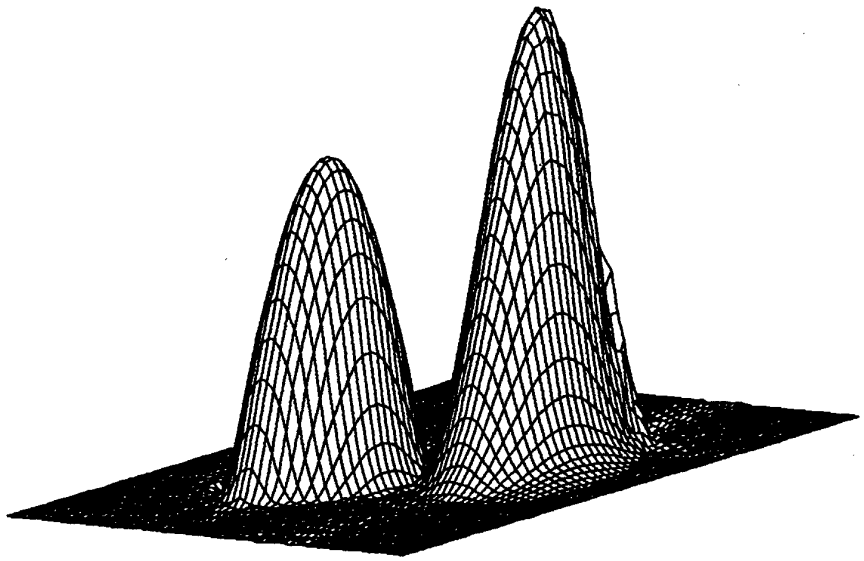

Fig. 11

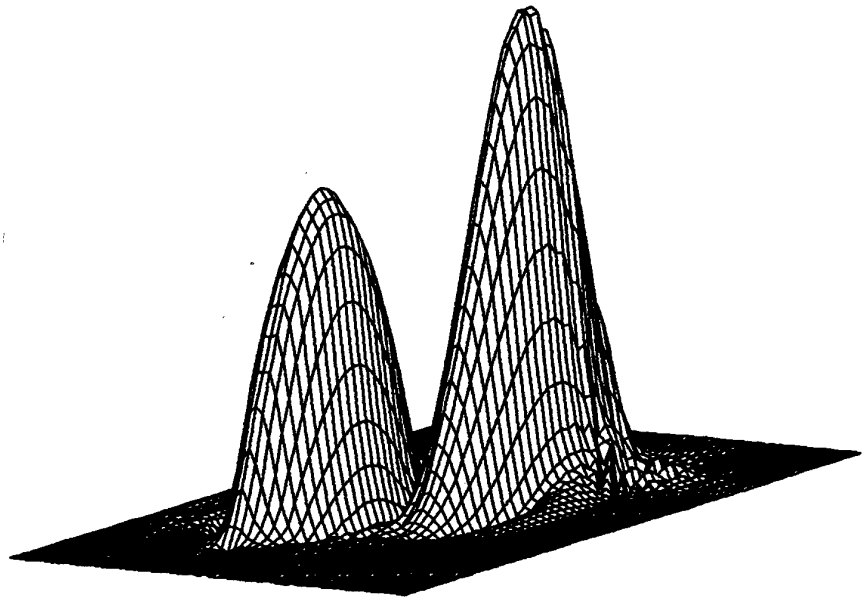

Fig. 12

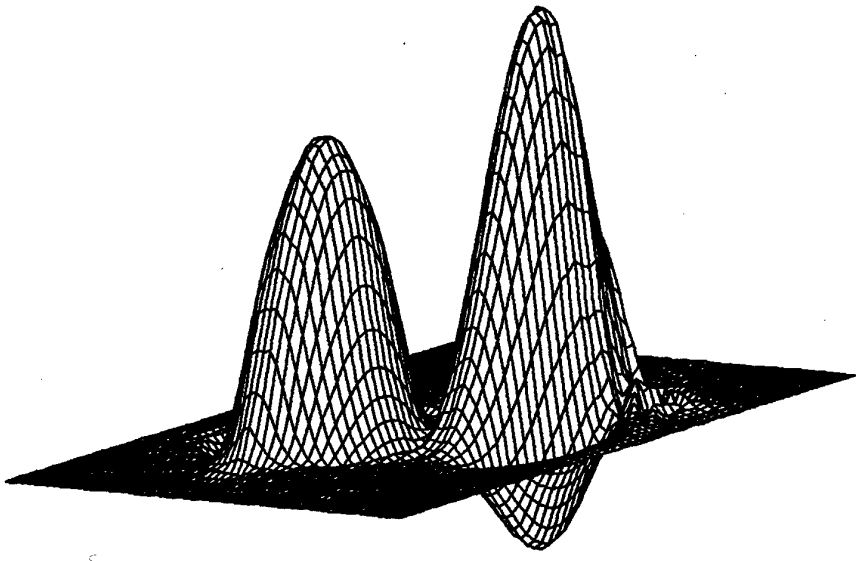

Fig. 13

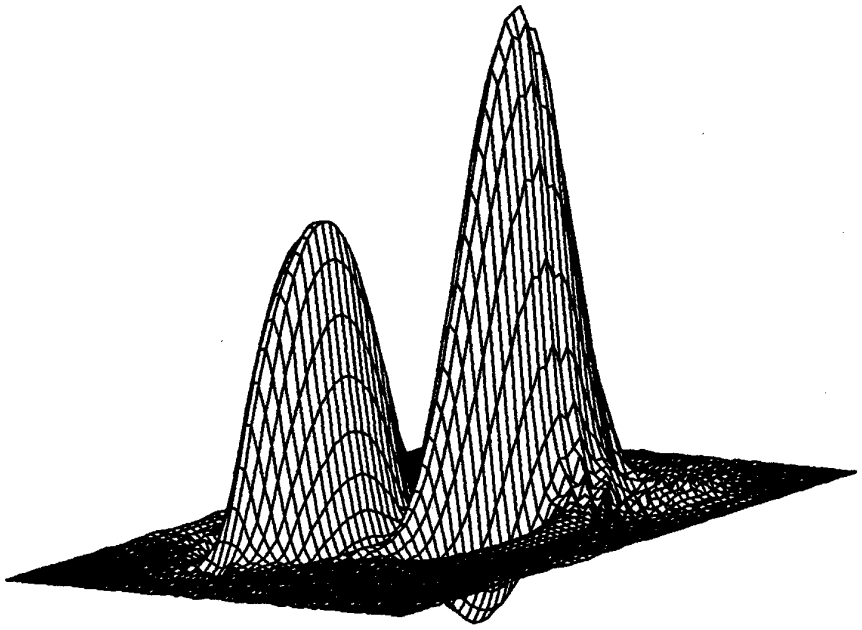

Fig. 14

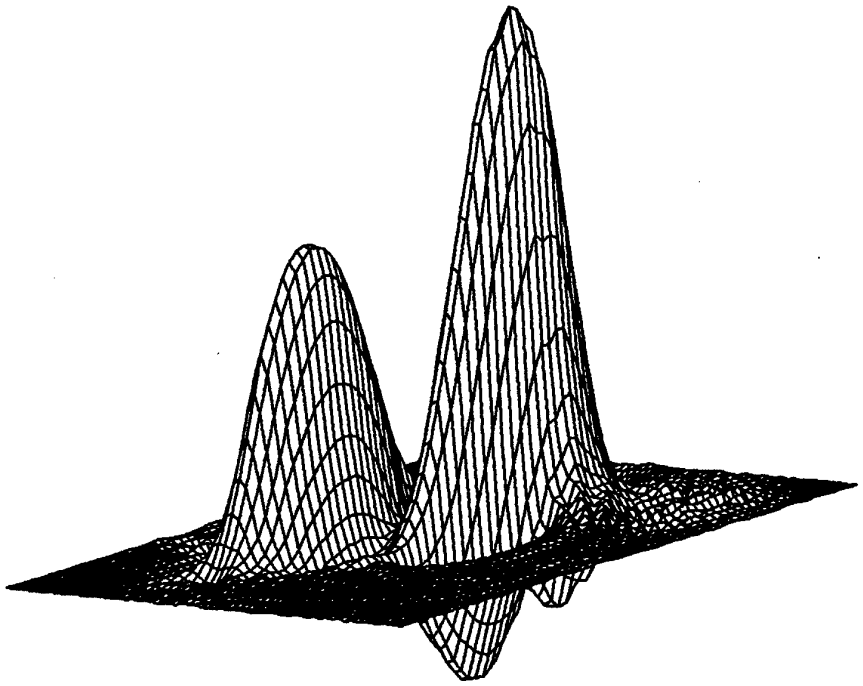

Fig. 15

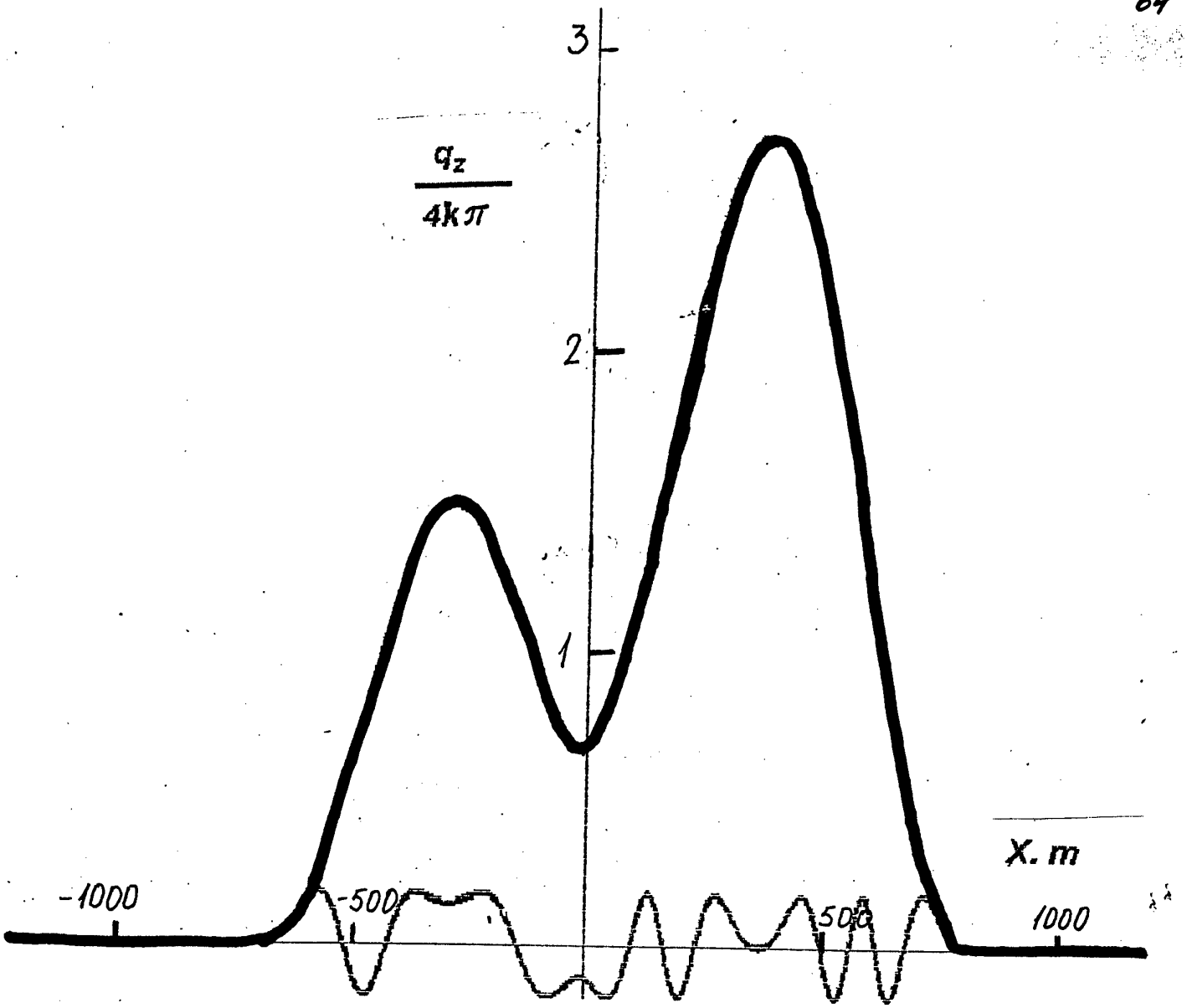

Fig. 16

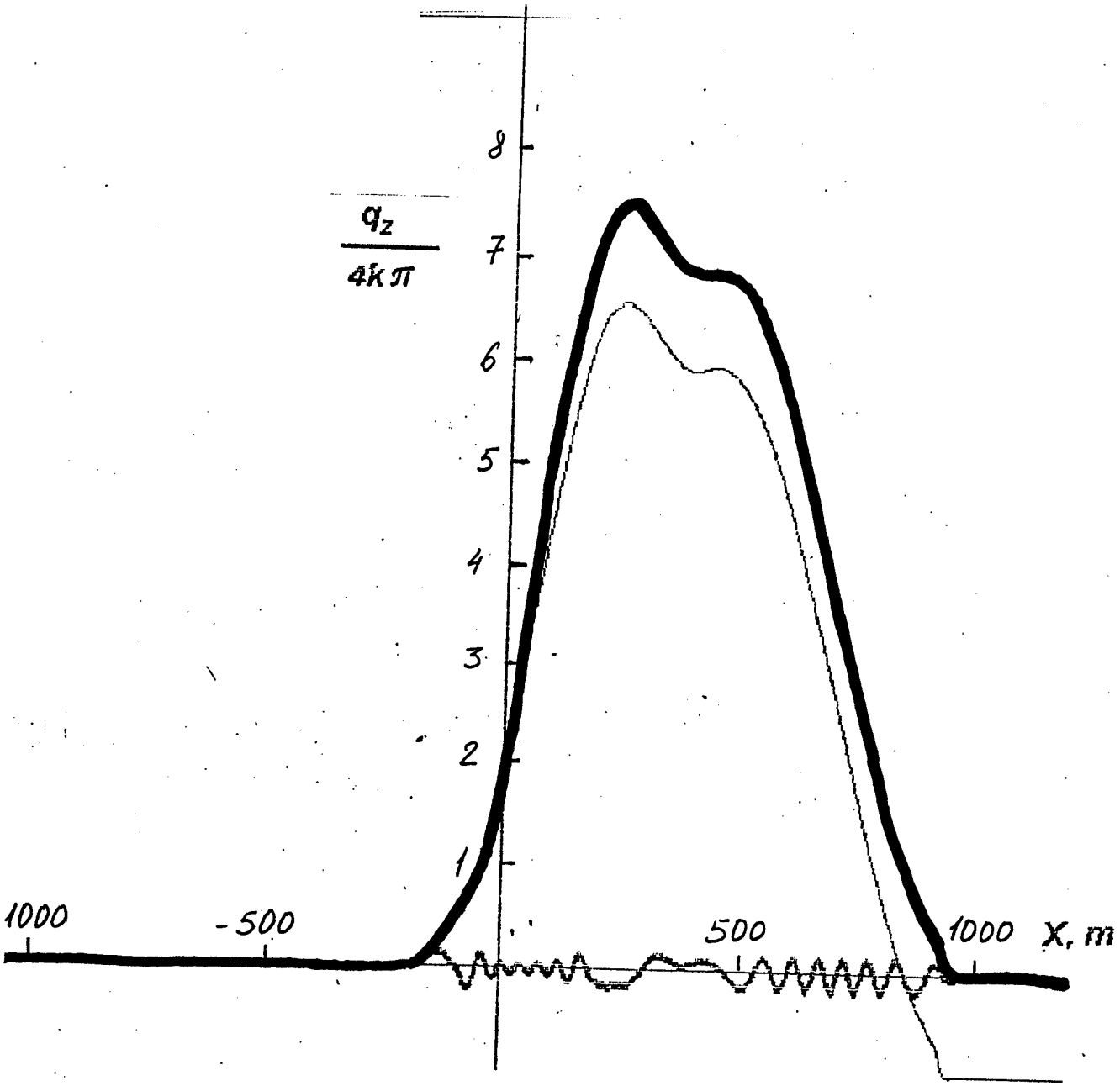

Fig. 17

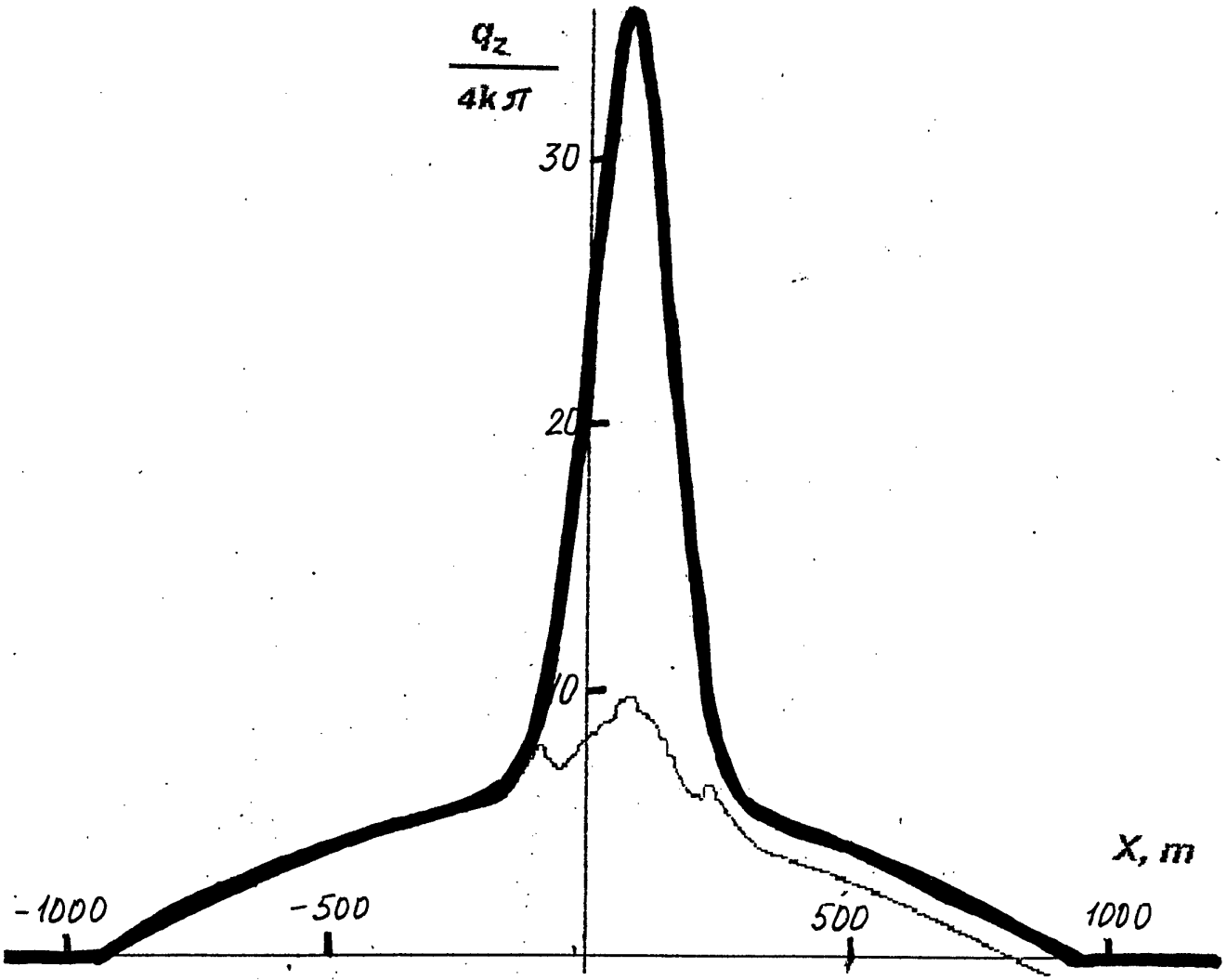

Fig. 18

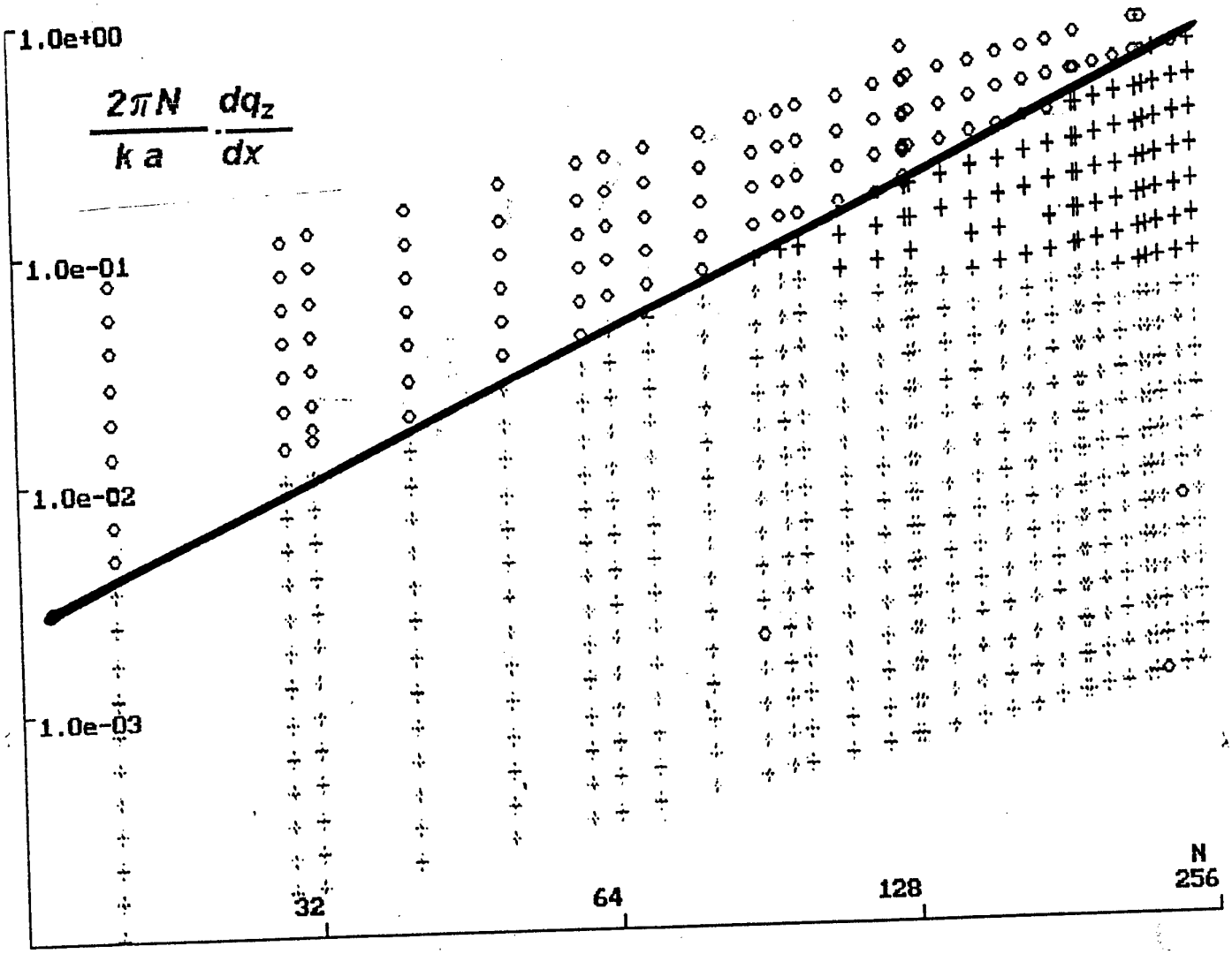

Fig. 19

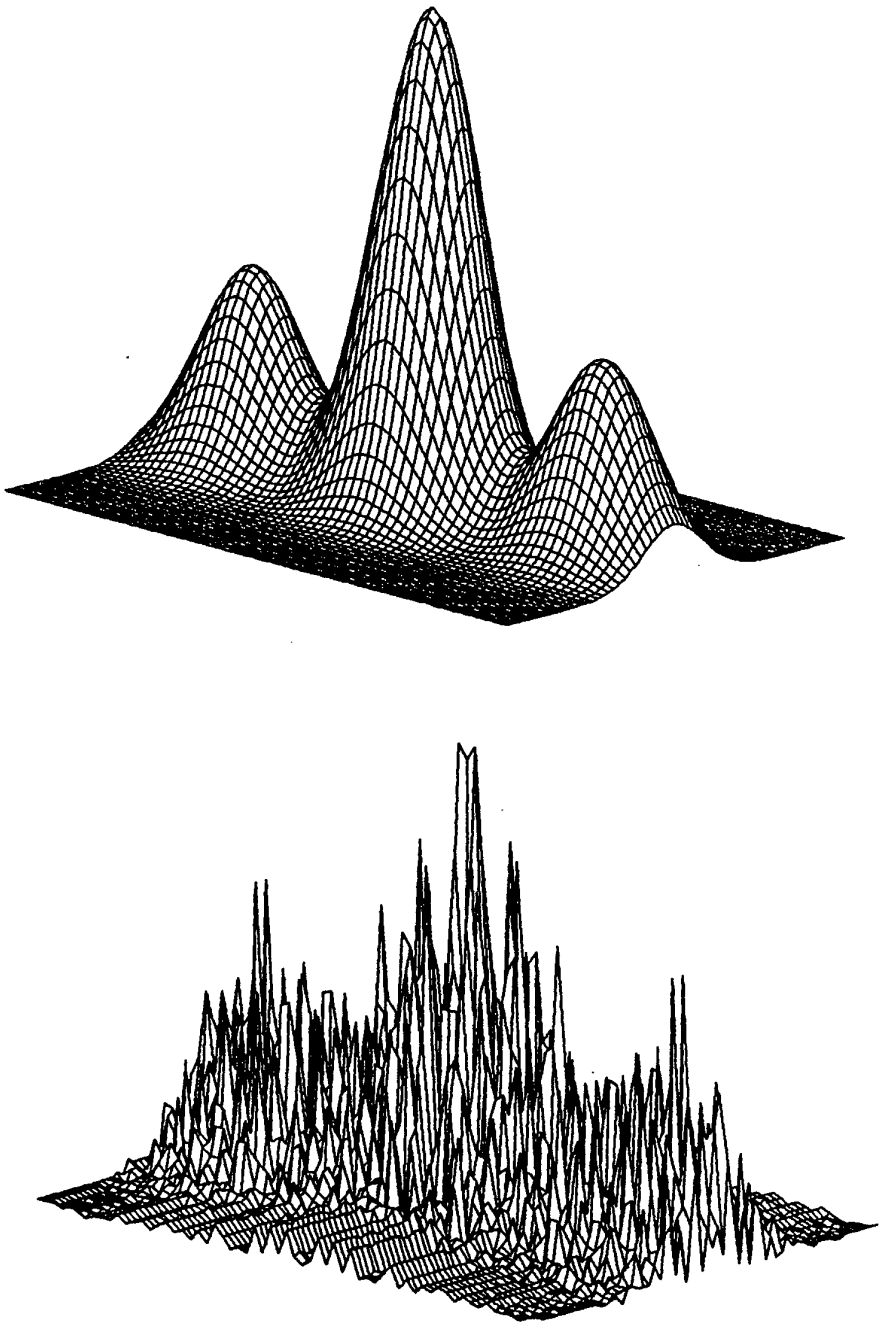

Fig. 20

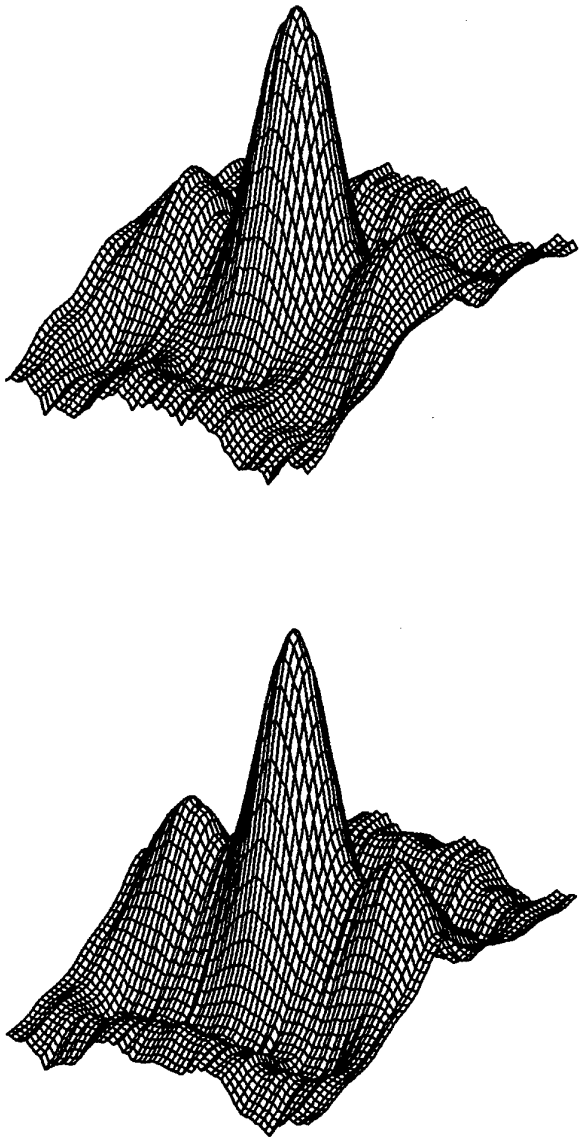

Fig 21

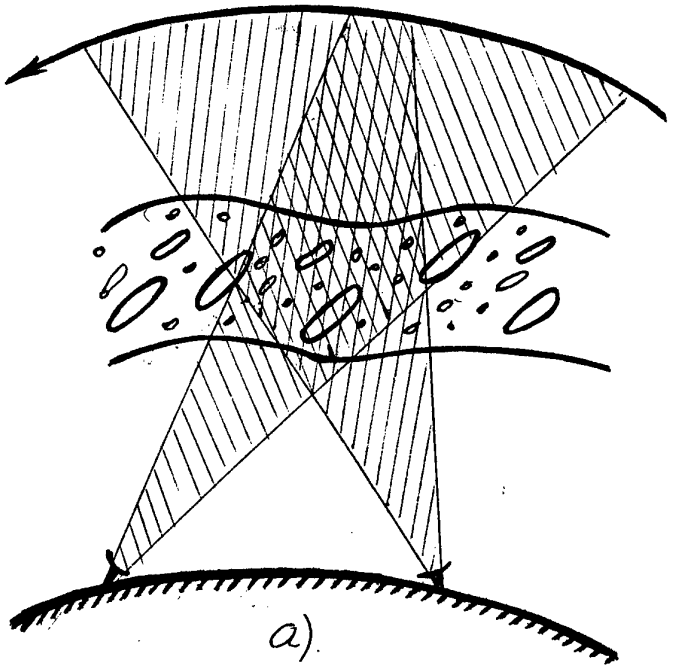

a)

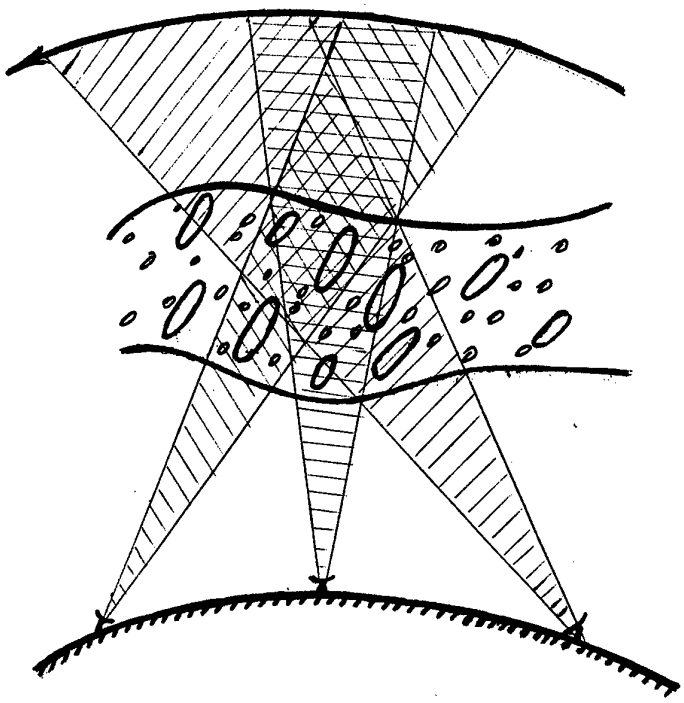

Fig. 22

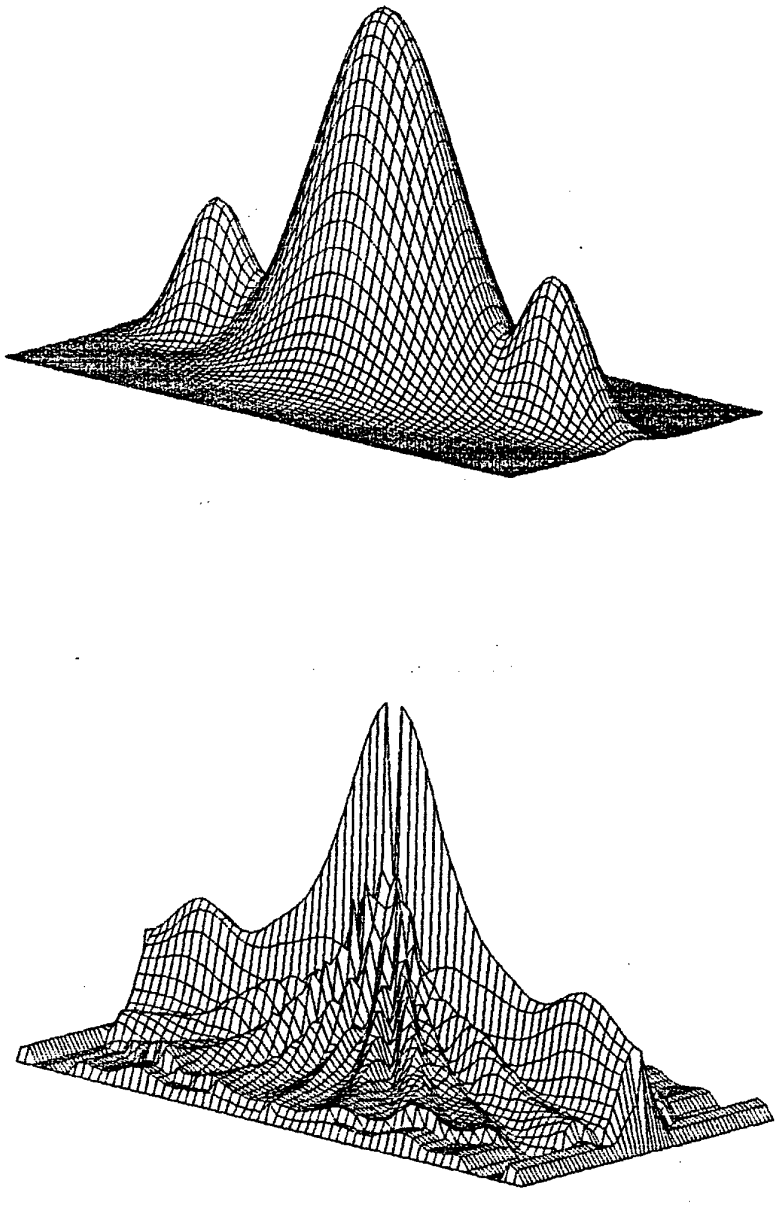

Fig. 23

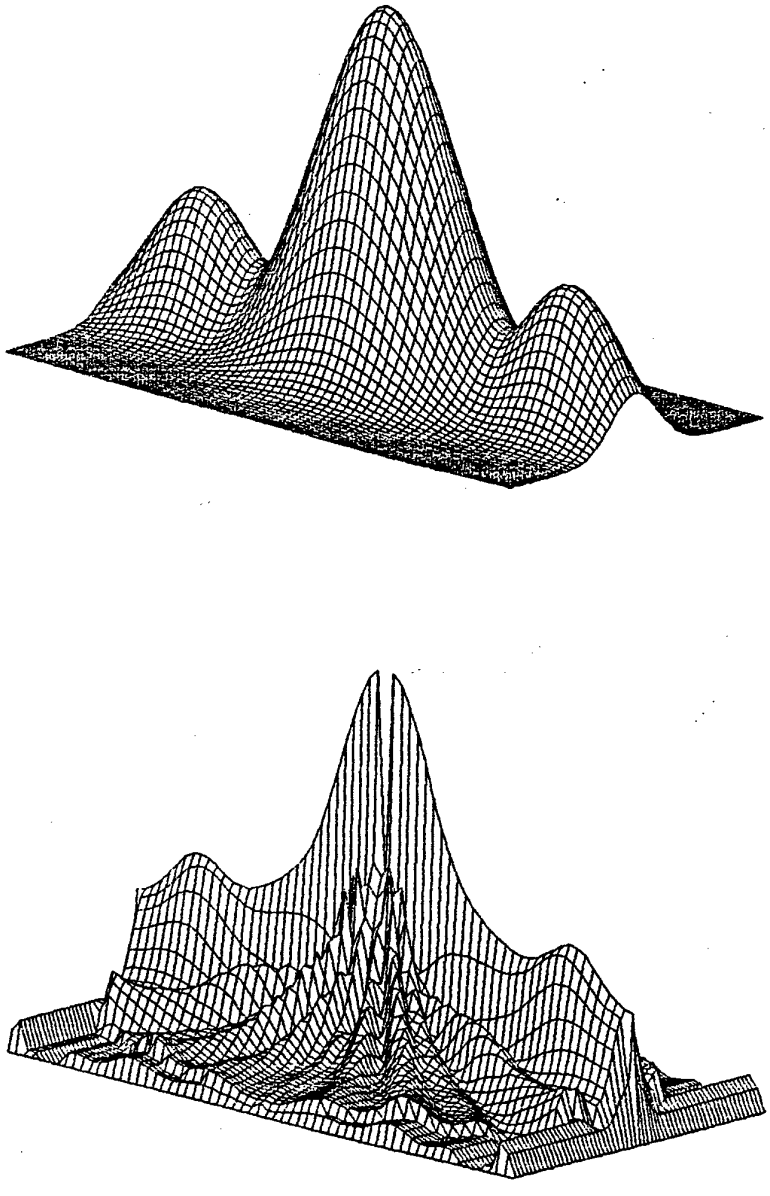

Fig. 24

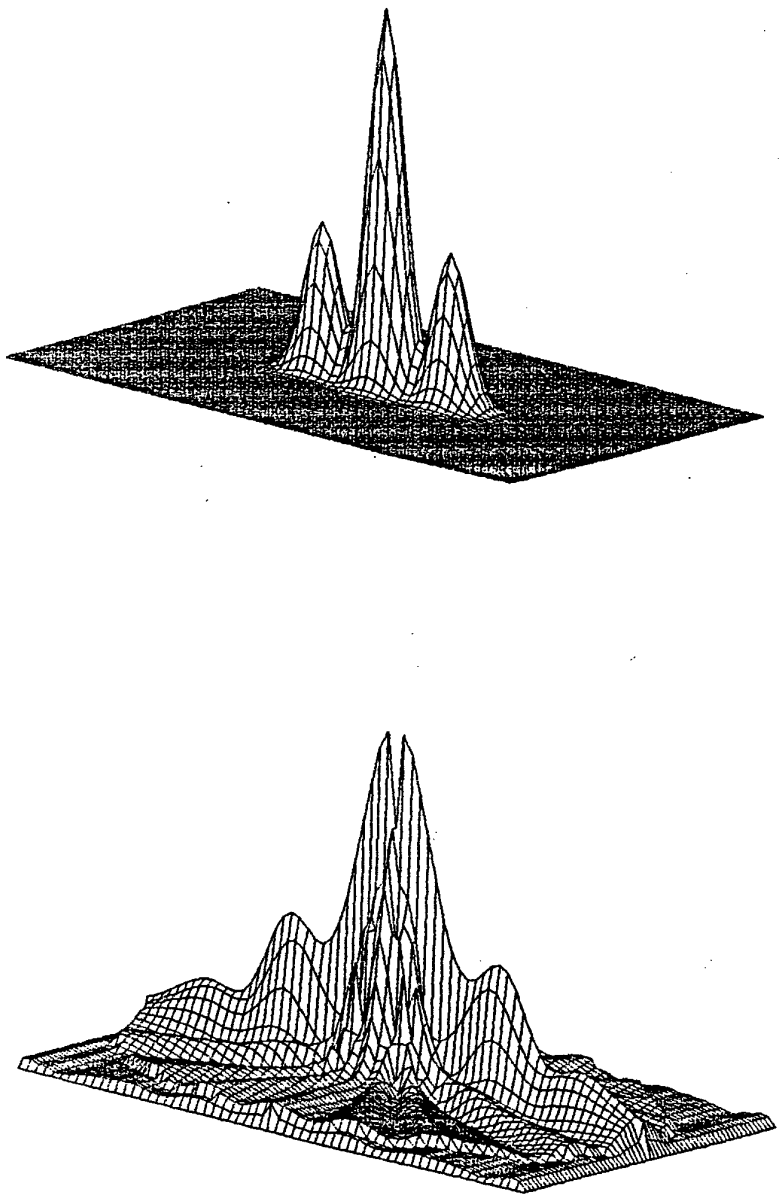

Fig. 25

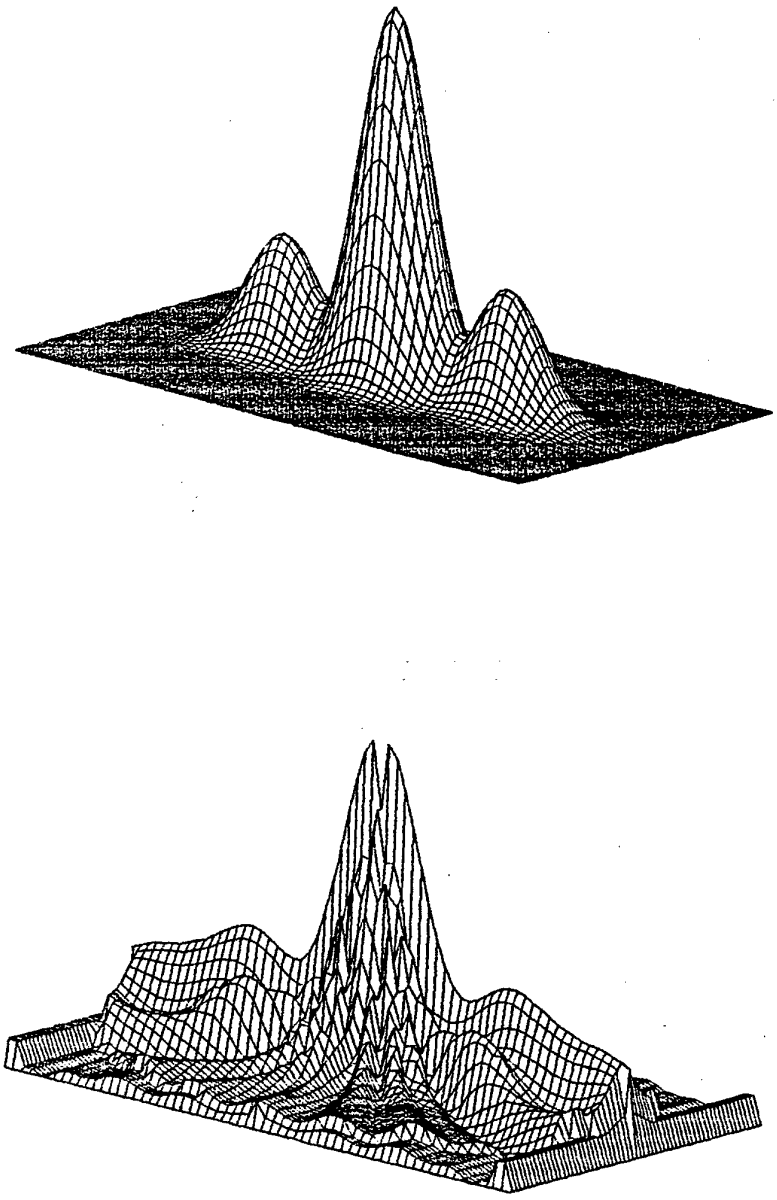

Fig. 26

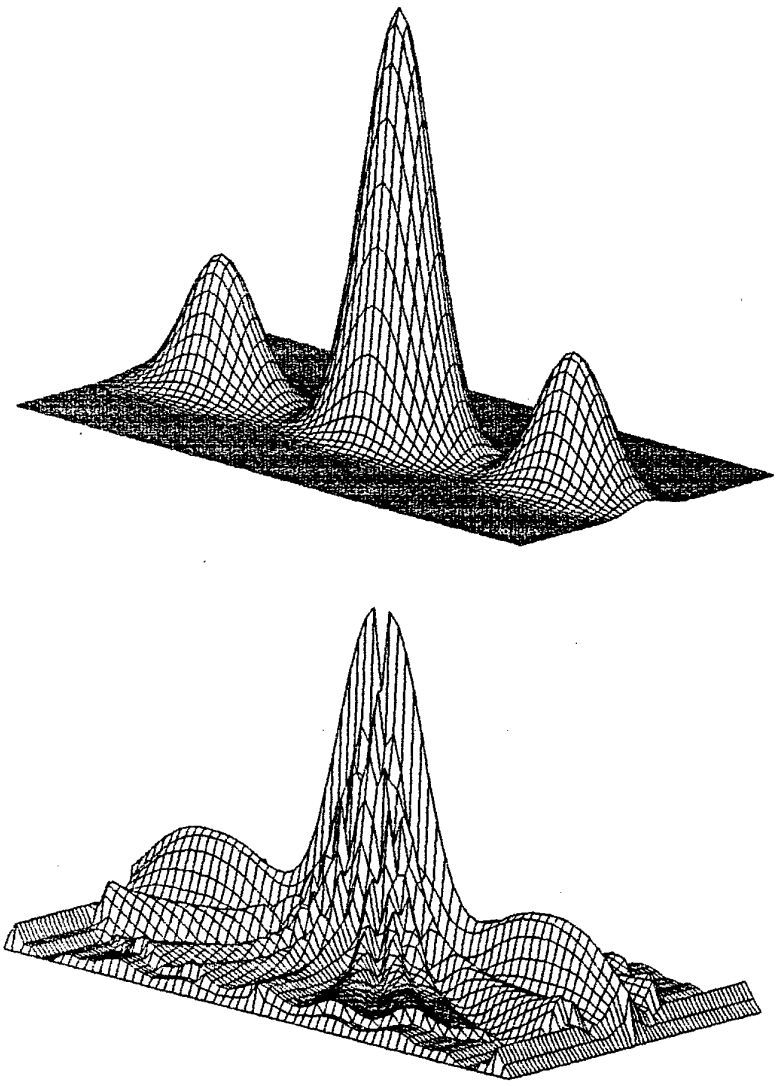

Fig. 27

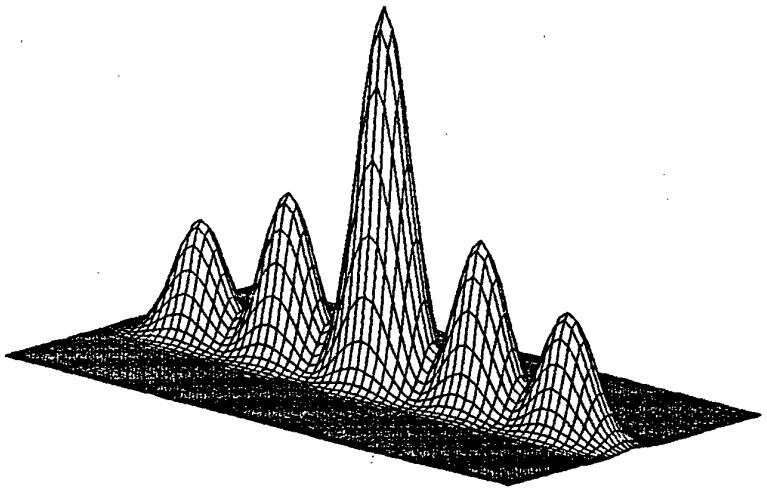

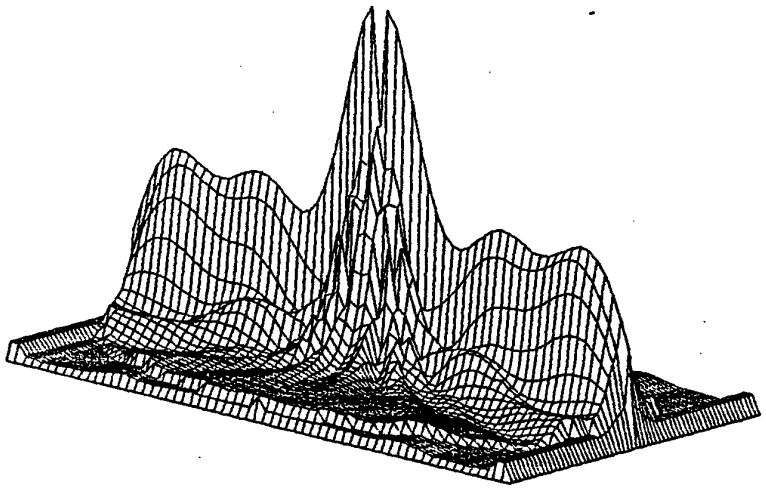

Fig 28

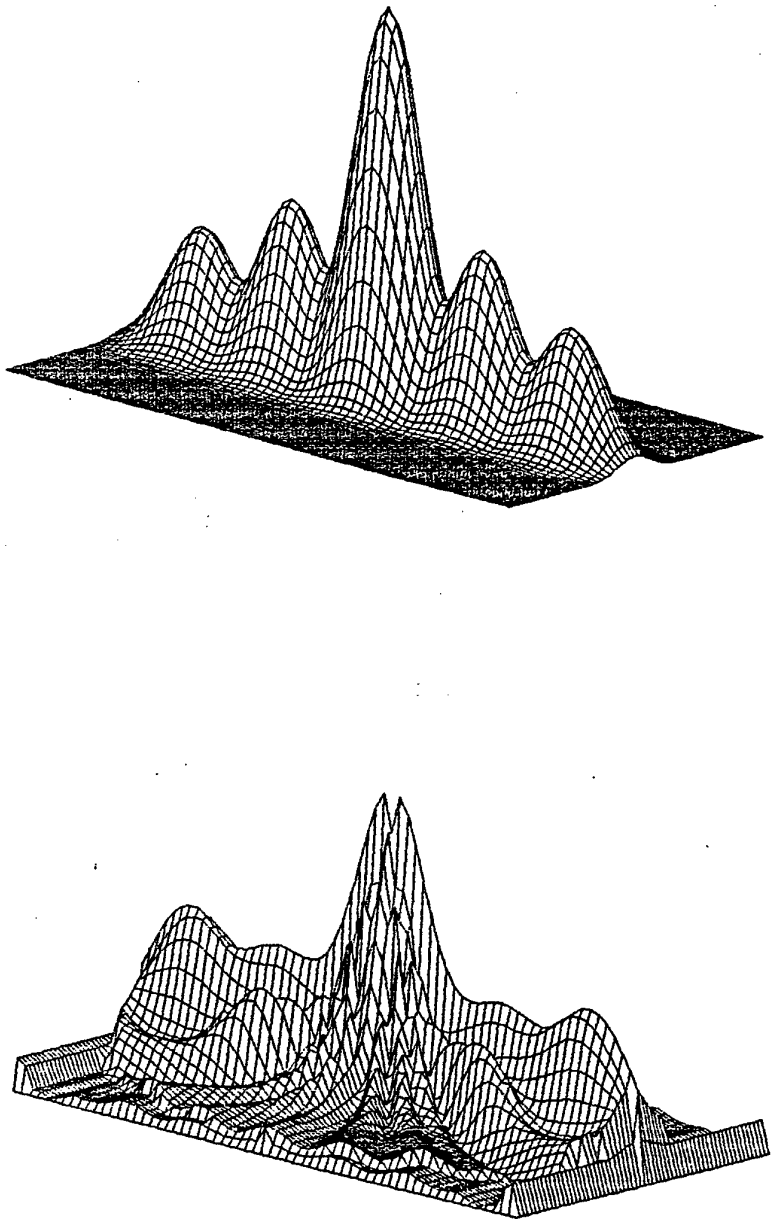

Fig. 29

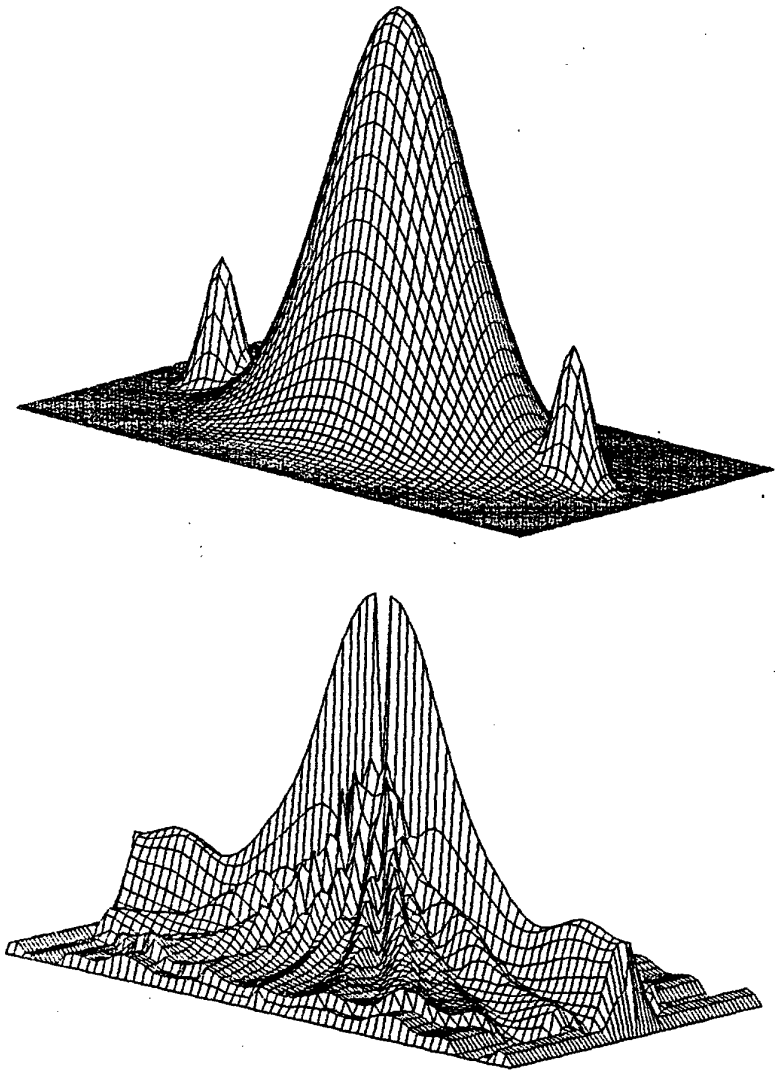

Fig. 30

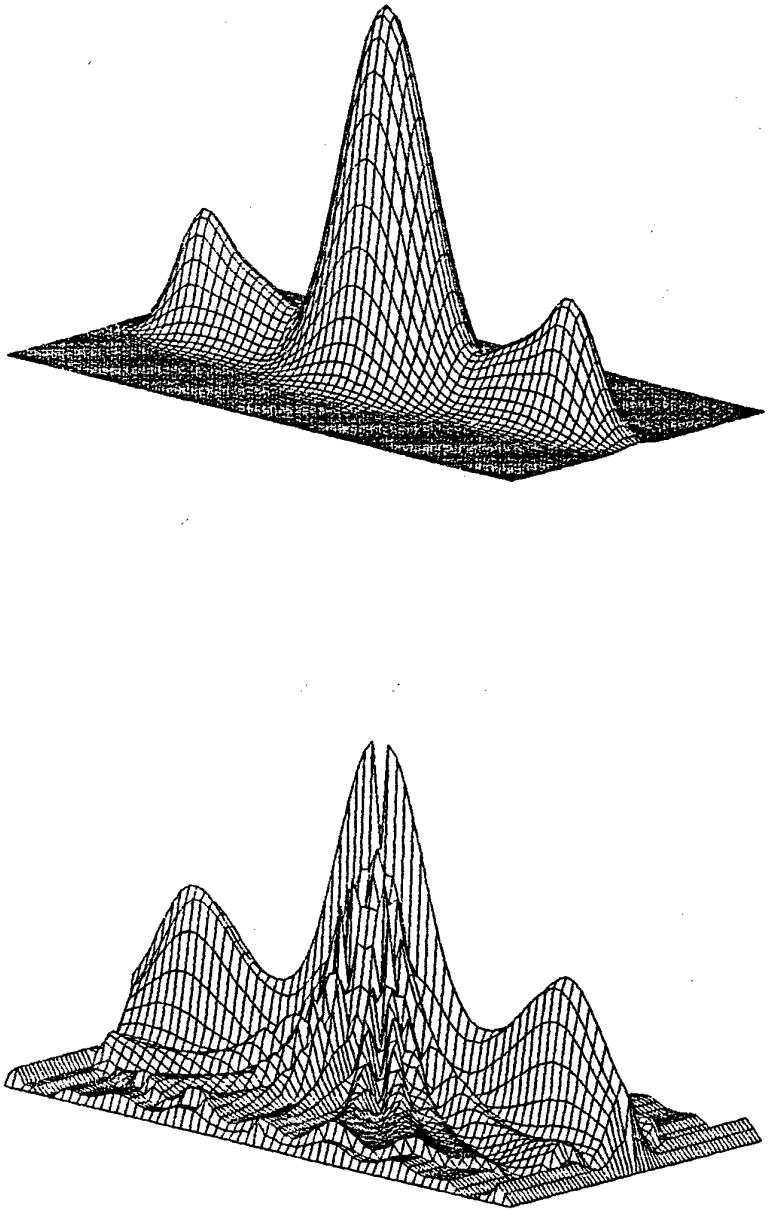

Fig. 31

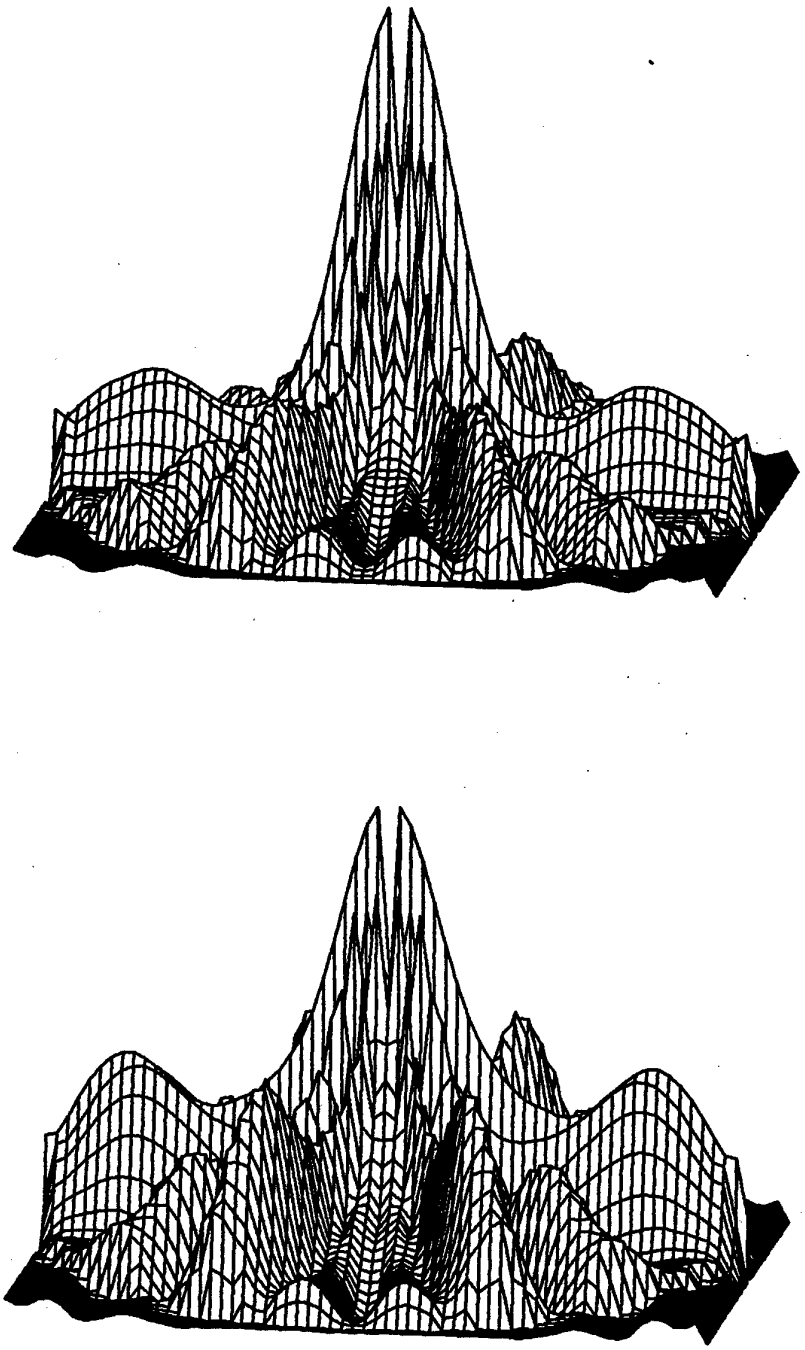

Fig. 32

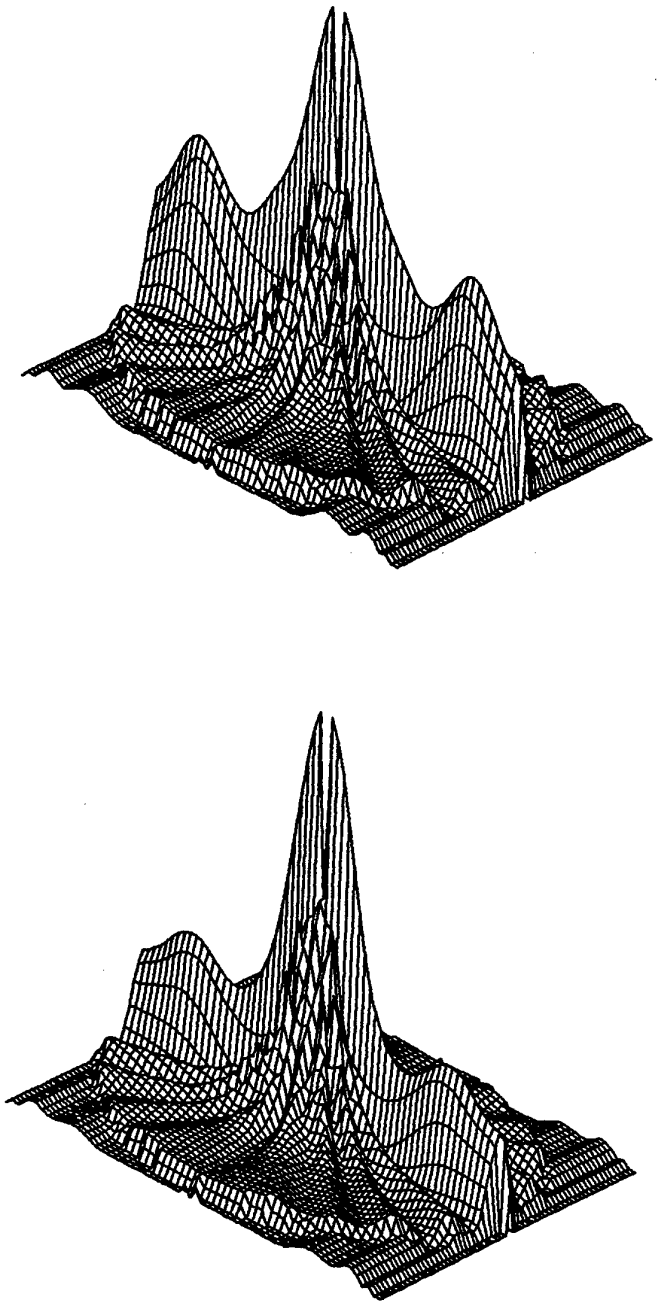

Fig. 33